PANAGIOTIS TATOULIS

SCHOOL OF MECHANICAL ENGINEERING

Feasibility study of a novel system for the production of advanced biofuels in Greece: Thermodynamic and technoeconomic assessment

Section: Thermal Egnineering

Supervisor: Sotirios Karellas, Professor NTUA

September 2024, Athens

ΠΑΝΑΓΙΩΤΗΣ ΤΑΤΟΥΛΗΣ

Διερεύνηση βιωσιμότητας ενός πρότυπου συστήματος παραγωγής προηγμένων βιοκαυσίμων στην Ελλάδα: Θερμοδυναμική και Τεχνο-οικονομική αξιολόγηση

ΣΧΟΛΗ ΜΗΧΑΝΟΛΟΓΩΝ ΜΗΧΑΝΙΚΩΝ

Τομέας: Θερμότητας

Επιβλέπων: Σωτήριος Καρέλλας, Καθηγητής ΕΜΠ

Σεπτέμβριος 2024, Αθήνα

--- Blank Page ---

Solemn declaration for plagiarism and copyright theft:

I have read and understood the rules regarding plagiarism and the proper citation of sources included in the guide for writing Diploma Thesis. I declare that, to the best of my knowledge, the content of this Diploma Thesis is the product of my own work and that all sources used have been cited.

The opinions and conclusions contained in this Diploma Thesis are those of the author and should not be construed as representing the official positions of the School of Mechanical Engineering or the National Technical University of Athens.

Panagiotis Tatoulis

Abstract

Advanced biofuels will play a central role in the decarbonization of the aviation and maritime sectors. Stimulated from the prospect of enhancing the energy security of Greece by domestically producing advanced biofuels, the goal of this thesis is to investigate the feasibility of a commercial scale biofuel plant in Greece. A framework is presented to identify a suitable candidate region to develop a case study for biomass utilization. The followed approach involved setting an initial basis, by assessing the current policy landscape surrounding biofuels, and determine policy trends of the EU and the Greek state. It was thus possible to align the region and feedstock selection with the established trends and evaluate the supply security for a biofuels production plant in the region. The chosen region is Peloponnese, and the results of supply security analysis indicate that 70kt_{DM} of biomass can be available, corresponding to 41 MW_{th} plant scale, under competitive market conditions and biomass availability constraints. More than 50% of biomass supply will be olive tree prunings with an expected average price of 70.3 €/t_{DM} at 20% share of total market available potential.

Considering the available biomass types and quantities, a preliminary level analysis of a proposed biomass processing plant is then conducted. This part of the thesis develops and analyses a processing scheme for the conversion of biomass feedstocks to advanced biofuels. It makes use of the novel chemical looping gasification (CLG) technology, and the OLGA process coupled with activated carbon beds for tar removal to produce a clean and high-quality syngas. This configuration upstream the fuel synthesis step makes possible to alleviate the plant of the expensive and energy intensive air separation unit (ASU) used for oxygen production. Also, a suitable catalyst for the employed Fischer-Tropsch synthesis (FTs) process catalysing both CO and CO_2 reactions is used, to examine the possible cost benefits of not including an Acid Gas Removal (AGR) unit for CO_2 removal. However, this led to high external H_2 demand, impacting operational costs. The process is modelled in Aspen Plus™ software using literature and experimental data. The results reveal the high efficiency of CLG which operates close to an 80% cold gas efficiency. Also, compared to other FTs, an increase is observed in carbon utilization towards FT-crude that reaches 58% stemming from the utilization of carbon content in CO_2. An overall plant efficiency close to 36% is achieved without including excess heat utilization.

The technoeconomic assessment of the proposed processing plant completes the case study. The results show a break-even selling price (BESP) of FT-crude at 3 €/kg with a Total Capital Investment of 176 M€. The high BESP is a result from the high green H_2 demand and priced at 3.5 €/kg_{H_2} making it the greatest contributor to operating costs.

The insights gained from the Peloponnese region case study, highlight its favorable prospects to harbor a bio-based industry. The technoeconomic assessment of the proposed plant reveals the sections of the process scheme that steep cost reductions can be achieved, thus lowering the BESP of produced FT-crude to a competitive range.

Περίληψη

Τα προηγμένα βιοκαύσιμα θα έχουν κεντρικό ρόλο στην απανθρακοποίηση της αεροπορίας και της ναυτιλίας. Η διπλωματική αυτή διερευνά τη βιωσιμότητα μίας εμπορικής κλίμακας μονάδας παραγωγής βιοκαυσίμων στην Ελλάδα με στόχο την ενίσχυση της ενεργειακής ασφάλειας. Αρχικά, παρουσιάζεται ένα πλαίσιο για την εύρεση κατάλληλης περιοχής για την ανάπτυξη μελέτης περίπτωσης για αξιοποίηση βιομάζας. Η ακολουθούμενη προσέγγιση ξεκίνησε με τη μελέτη του τρέχοντος τοπίου πολιτικών σχετικά με τα βιοκαύσιμα, και τον καθορισμό των τάσεων στην Ευρωπαϊκή Ένωση και το Ελληνικό κράτος. Έτσι, κατέστη εφικτή η ευθυγράμμιση της πρώτης ύλης με τις καθορισμένες τάσεις. Έπειτα αξιολογήθηκε η ασφάλεια προμήθειας βιομάζας σε μία μονάδα παραγωγής βιοκαυσίμων στην Πελοπόννησο που επιλέχθηκε ως η περιοχή της μελέτης περίπτωσης. Η ανάλυση έδειξε ότι 70 kt ξηρής βιομάζας θα είναι διαθέσιμοι υπό ανταγωνιστικές συνθήκες αγοράς και περιορισμούς στη διαθέσιμη βιομάζα. Η ποσότητα αυτή αντιστοιχεί σε μονάδα θερμικής κλίμακας 41 MW και περισσότερο από το 50% της προμηθευόμενης βιομάζας θα είναι κλαδοδέματα ελιάς. Η μέση τιμή προμηθευόμενης βιομάζας εκτιμήθηκε στα 70.31 €/t ξηρής βιομάζας με μερίδιο αγοράς 20% από την κινητοποιημένη βιομάζα.

Λαμβάνοντας υπόψιν τους διαθέσιμους τύπους και ποσότητες βιομάζας, διεξάγεται μία προκαταρκτικού επιπέδου ανάλυση της προτεινόμενης μονάδας. Στο τμήμα αυτό, αναπτύσσεται και αξιολογείται ένα σχήμα μετατροπής της βιομάζας σε προηγμένα βιοκαύσιμα. Χρησιμοποιείται μία πρότυπη τεχνολογία αεριοποίησης με χημική ανακύκλωση ώστε να παραχθεί υψηλής ποιότητας αέριο σύνθεσης και η πλύση αερίου με βιοέλαια συζευγμένη με στρώματα ενεργού άνθρακα. Έτσι, δεν χρειάζεται η ακριβή και ενεργοβόρα μονάδα διαχωρισμού αέρα για παραγωγή οξυγόνου. Ακόμα, στη Fischer-Tropsch σύνθεση χρησιμοποιείται καταλύτης που καταλύει αντιδράσεις για το CO και το CO_2 ώστε να εξεταστεί το πιθανό οικονομικό όφελος από τη μη χρήση μονάδας αφαίρεσης όξινων αερίων για την αφαίρεση CO_2. Αυτό οδήγησε σε υψηλή αναγκαία ποσότητα H_2, επηρεάζοντας τα έξοδα λειτουργίας. Οι διεργασίες μοντελοποιήθηκαν με το λογισμικό Aspen Plus™ με χρήση πειραματικών δεδομένων. Τα αποτελέσματα έδειξαν υψηλό βαθμό απόδοσης χημικής ενέργειας της μονάδας αεριοποίησης, κοντά στο 80%. Επίσης, σε σχέση με άλλες FT σύνθεση διεργασίες, παρατηρήθηκε αυξημένη αξιοποίηση άνθρακα προς το προϊόν, FT-crude, περίπου στο 58%. Η απόδοση ολόκληρης της μονάδας είναι κοντά στο 36%, χωρίς να ληφθεί υπόψιν η αξιοποίηση της περίσσειας θερμότητας.

Η τεχνοοικονομική ανάλυση της προτεινόμενης μονάδας ολοκληρώνει τη μελέτη με την τιμή κόστους του FT-crude να είναι 3€/kg με κεφάλαιο επένδυσης 176 εκ. €. Η υψηλή τιμή κόστους οφείλεται στην κατανάλωση πράσινου H_2 στην τιμή των 3.5 €/kg.

Η μελέτη περίπτωσης ανέδειξε τις ευνοϊκές προοπτικές της Πελοποννήσου να φιλοξενήσει βιομηχανία βασισμένη στη βιομάζα. Η τεχνοοικονομική ανάλυση της προτεινόμενης μονάδας φανέρωσε τμήματα της διεργασίας με έντονη μείωση κόστους μέσω των οποίων μπορεί να γίνει ανταγωνιστικό το παραγόμενο FT-crude.

Table of Contents

List of Figures

List of Tables

Nomenclature

Abbreviation	Explanation
IATA	International Air Transport Association
AGR	Acid Gas Removal
AP	Area production
AR	Air Reactor
ASF	Andrew-Schultz-Flurry
ASU	Air Separation Unit
BESP	break-even selling price
BTX	Benzene, Toluene, Xylene
CAP	Common Agricultural Policy
CEPCI	Chemical Engineering Plant Cost Index
CGE	Cold Gas Efficiency
CGESC	Cold Gas Efficiency incl. Syngas Cleaning
CLC	Corine land cover
CLG	Chemical Looping Gasification
CU	Carbon Utilization
DFBG	Dual Fluidized Bed Gasification
ECE	Energy Conversion Efficiency
ECN	Energy research Centre of the Netherlands
ELSTAT	Hellenic Statistical Authority
ER	Equivalence Ratio
EU	European Union
FCI	fixed capital investment
FORES	Forest Residue
FORESBROAD	Forest Residue from Broadleaved species
FORESCO	Forest Residue from Conifers
FORESMIXED	Forest Residue from Mixed stands
FR	Fuel Reactor
FT	Fischer-Tropsch
FTE	Yearly Fischer-Tropsch product energy
FTs	Fischer-Tropsch synthesis
GHGs	Greenhouse Gases
HC	Hydrocarbon
HEFA	Hydroprocessed Esters and Fatty Acids
HRSG	Heat Recovery Steam Generation
HTFT	High Temperature Fischer – Tropsch
HWCU	Heavy-wax Carbon Utilization
ICAO	International Civil Aviation Organisation
IRR	Internal Rate of Return
JFCU	Jet Fuel Carbon Utilization
KPIs	Key Performance Indicators
LCA	Life Cycle Analysis
LHV	Lower Heating Value
LTFT	Low Temperature Fischer – Tropsch

Abbreviation	Explanation
MCE	Mass Conversion Efficiency
MTFT	Medium Temperature Fischer – Tropsch
NACU	Naphtha Carbon Utilization
NECP	National Energy and Climate Plan
OC	Oxygen Carrier
OP	Orchard Prunings
OPE	Overall Plant Efficiency
OPEX	Operational Expenditure
OTC	Oxygen Transport Capacity
OTP	Olive Tree Prunings
PSA	pressure swing adsorption
RDF	Refuse Derived Fuel
RED III	Renewable Energy Directive III
RFNBO	Renewable Fuel of Non-Biological Origin
RPR	Residue to Product Ratio
RR	Recirculation Ratio
RSR	Residue to Surface Ratio
RSRmod	Modified Residue to Surface Ratio
rWGS	reverse Water Gas Shift
S/B	Steam to biomass ratio
SAFs	Sustainable Aviation Fuels
SMP	System Marginal Price
SO	Strategic Objective
SRF	Solid Recovered Fuel
TCI	Total cost of investment
TPEC	total purchased equipment cost
UCO	Used Cooking Oil
VP	Vineyard Prunings
WC	working capital
WGS	Water Gas Shift

Subscript	Explanation
app	approach
AR	Air Reactor
bio	Biomass
bio-in	Inlet biomass
bio-out	Outlet biomass
BTX	Benzene, Toluene, Xylene
cat	catalyst
cond	Condenser
cool	Cooler
d.b.	Dry basis
DM	Dry Matter
el,cons	Electricity consumed
el,prod	Electricity produced
FR	Fuel Reactor
int. cool	Intermediate cooler
prod	Product
reactor	Reactor
ref	reference
RR	Recirculated FT gases
w.b.	Wet basis

Symbol	Explanation	Unit
$C_{transport\ w.b}$	Cost of transport	€/$t_{w.b}$
R	Mean earth radius	km
Tapp	Temperature approach	^{o}C
W_n	Weight fraction of compound with n carbon atoms	-
Greek Symbols		
α	Chain growth probability	-
θ	CLG stable operation parameter	-
ϕ	Latitude	degrees
ω	Longitude	degrees

1. Introduction

Since the industrial revolution, the use of fossil fuel derived energy has expanded into everyday life and life quality is connected to the use of fossil fuels to a great extent. That is the main reason why, the decision to decarbonize many sectors and move away from fossil fuels has many challenges for the humanity. After Kyoto Protocol, the Paris Agreement is the most recent landmark for action against climate change in which a target has been set, to limit global temperature rise to well below 2 degrees Celsius and to act in pursuit of the 1.5 degrees Celsius target [1]. To achieve the climate goals and for quality of life not to suffer due to the major economic shocks caused by the transition towards very expensive sustainable solutions, the use of biomass derived energy (bioenergy) is essential. Biomass can be used in many sectors, but a promising pathway is its upgrading into materials and biofuels for transportation or other sectors. In particular, hard to decarbonize sectors like the long-distance and heavy-duty parts of the transportation sector will have to be supported by the use of drop-in biofuels or synthetic fuels.

Indicatively, shown in Figure 1 is the strategy of the International Air Transport Association (IATA) to align aviation with the Paris Agreement goals. In a report from Eurocontrol [2] it is explained that revolutionary types of aircrafts are not expected to represent a large share of flights in 2050.

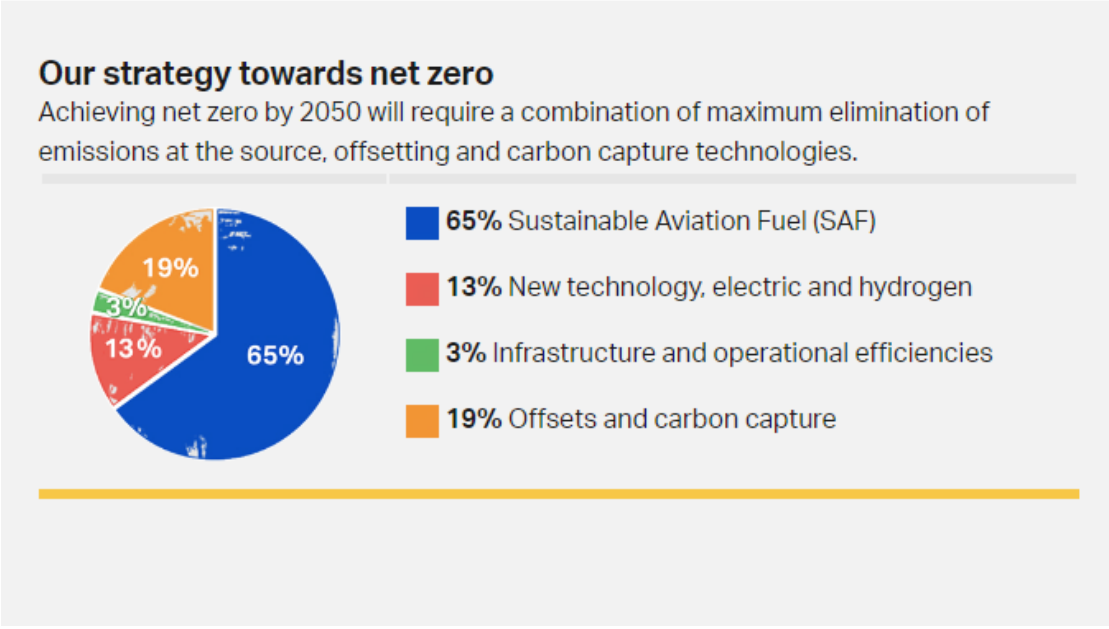

Figure 1: IATA strategy on aviation net zero by 2050 [3].

Biomass is used as feedstock to produce biofuels with properties close to the fossil derived fuels. In some cases, biofuels can substitute the respective fossil fuel while in other cases a blending of both is performed.

The principle behind the use of biomass as a source to directly produce energy e.g., combustion, or to process and transform it into a useful form such as biomaterials or an energy carrier e.g., biofuels, is to make use of solar energy and some nutrients to grow biomass. During this process, in an ideal scenario, no greenhouse gases (GHGs) are produced, but only recycled from existing GHGs in the environment. Biofuels can be produced from many biomass types because of the many different processes that exist. Biomass has many alternative uses with most important, its use as a food source. Therefore, there exist policy limitations for the types of biomass and the amounts that can be diverted to produce biofuels. Additional criteria have been set in policies with their aim being to limit the use of biomass which' use will: [4]

- Directly divert food sources from the feed chain.
- Divert land use that would else be used to produce feed crops.
- Expand agricultural land into high carbon sink stock areas.

Food security is a pillar for the well-being of a society and driving up food prices would cause unwanted disturbances in people's lives, so a limit and possibly, a gradual phase out of these feedstock types is prudent. In addition, the expansion of agricultural land into areas with high carbon stock will work counter to the goal of quickly lowering carbon emissions in the atmosphere. Carbon released from an expansion in carbon sinks will not be rebalanced soon by the emission savings. This will also for now act against the plan of the European Union (EU) to increase carbon sinks as a way to limit GHGs in the environment for the near-term.

Different categories of biofuels in accordance with the feedstock type used for its production are created based on the general characteristics of the biomass. A good way to identify sustainable biomass sources is to evaluate waste streams of an existing and stable process chain [5]. Significant amount of sustainable technical potential exists on forest residues, wood processing chains and agricultural residues [4]. These biomass types fall under the category of 2nd generation biofuels because they are non-edible biomass, so they do not take part in the food versus fuel debate.

Using biomass to produce biofuels has been a central topic of discussion for the past years, especially regarding its role in decarbonizing certain sectors that heavily rely on fossil fuels. The transportation sector is faced with a two-part problem of fulfilling its basic role, connecting distant regions, while taking measures to decarbonize every part of it. The sector is broken down into 4 distinct subsectors, namely, railroad, heavy and light duty vehicles, maritime and aviation. From these, the maritime and aviation sectors face the most difficult challenges from the combination of disadvantages of batteries and hydrogen regarding energy density, and their long-distance travel needs. Electrification or use of hydrogen will increase the cost of travel in a way that will hinder interconnectivity between isolated regions and disrupt trade. The problem is that high cost of fuel and the severe modifications needed on the ships' and aircrafts'

design and engine will result in higher costs of cargo shipments and air travel. Most harms will be borne by more isolated and distanced places that will need to somehow adjust the higher fares and fees. All these issues are sufficiently dealt with at a low additional cost, with the use of biofuels. Biofuels are, in many cases, compatible with current conventional engines and alternatively they can be blended with fossil fuels yielding less specific GHGs, allowing for a gradual transition. The adoption of biofuels or synthetic fuels mostly concern aviation and maritime, therefore these sectors will set a baseline for the use of such fuels.

Biomass can be converted into energy or value-added products by many routes with the most common being the use of thermochemical and biochemical routes. The thermochemical routes include the combustion, gasification, pyrolysis and thermal liquefaction of biomass and the biochemical route includes the anaerobic digestion and fermentation of biomass. The choice between these well-established routes and other, less explored options, is one that has to be taken into account in parallel or after considering the available feedstocks and the targeted product. Each route has different advantages such as being feasible in small scale allowing their decentralized operation e.g., combustion for energy production, pyrolysis for pyrolysis oil production. Another criterion can be energy requirements or the environmental impact these processes have in terms of GHGs emission intensity and pollution.

In this thesis, a preliminary level analysis of a case study in Greece was carried out employing biomass as the primary feedstock for the production of advanced biofuels at commercial scale. The steps taken to develop the case study was first to study the regional laws and policies surrounding biomass and biofuels deriving trends and setting the basis for subsequent analysis in the case study. A suitable region is chosen to develop the case study based on an overview of Greece's regions. Feedstock selection and potential assessment incorporated multiple criteria, which are laid out in chapter 3, with a major contributor being the policy landscape surrounding their use. Resulting from chapter 3 are biomass cost-supply curves for a hypothetical plant location based on which plant capacity is chosen and data are extracted regarding fractions of supplied feedstock by biomass type and average cost of biomass supply. Building on the previous work, a novel processing scheme for advanced biofuel production is introduced and developed at process simulation level. It is designed with the goal to capitalize on cost reductions from eliminating the need of certain cost and energy intensive equipment for the production of oxygen and CO_2 removal.

Due to the available feedstock being woody biomass, the thermochemical route was chosen for biomass conversion. Syngas is produced using a promising chemical looping gasification (CLG) technology. Then, it undergoes gas cleaning in a specially designed syngas cleaning train, suitable for medium scale biomass processing plants. The clean syngas is led through a fuel synthesis step using Fischer-Tropsch synthesis (FTs) producing a blend of hydrocarbons (HCs) called FT-crude. It can be sold to refineries or

be upgraded on-site with the latter requiring large capital investment and large-scale applications to be possible. The refineries will separate fractions of the FT-crude, producing a variety of products depending on the FT-crude composition. The targeted composition of FT-crude for this case is to maximize production of the jet-fuel fraction (C_{10}-C_{16}) to facilitate the production of SAF blends in Greece. The fraction not suitable for jet fuel blending can be used for other transportation fuel blends. Therefore, the production of biofuels is the key goal with a little more emphasis on the needs for SAF as will be discussed later.

A case study in Greece is investigated as its small size, dispersed biomass potential and underdeveloped biomass supply chains, make it an ideal candidate to set a baseline for the future of biofuels production at a medium to low scale in countries that have not yet used their biomass potential. Navigating through the currently fluid policies and regulations in the EU area, during the infancy of a bioeconomy, to identify long-term available opportunities is essential, as a low-risk investment is more appealing to investors and policy related uncertainty is a serious deterrent.

2. Regulatory and policy landscape

Policy making has been the main tool of countries and associations to steer communities and industries in implementing sustainable and environmentally friendly technological solutions. The use of energy from biomass has provided for many years the greatest share of the renewable energy in EU and others. The regulations governing its use have been mild thus far, but formal policy is being set forth to incorporate more sustainability criteria for biomass usage and ensure the smooth operation of all markets because a stable policy environment will encourage investments.

Understanding long-term policy goals is very important in order to assess the risks of certain paths, and especially at the time of researching and writing this thesis that policy changes are being adopted. This part of the thesis is essential in order to evaluate the non-technical barriers and to understand how the legal and regulatory framework at national and European level is in favor or against to such ventures. For example, in recently adopted stance, the production of biofuels from biomass that is used in the food sector faces difficulties. Research regarding long-term policy goals and the way in which they will be achieved is not an easy task and involves many personal understandings. The research conducted to investigate the regulatory landscape regarding biomass use, especially in the EU biofuel and bioenergy sectors included:

- Study of relevant regulations and policies.
- Articles and panels where policymakers and relevant stakeholders issued opinions.
- Official EU press releases during the negotiations for policy setting between regulatory institutions.
- Communication documents and opinions on shaping these legislations.

The rise of bioeconomy and the increased research in how to convert biomass energy into products, has caused fierce competition. Access to sustainable biomass sources will be the deciding factor for the expansion of the biomass sector.

The EU has clearly set 5 objectives surrounding bioeconomy which are: [6]

- Ensuring food and nutrition security
- Managing natural resources availability
- Reducing dependence on non-renewable, unsustainable sources
- Mitigating and adapting to climate change
- Strengthening European competitiveness and creating jobs

These are pillars of a bridge between the current unsustainable state of the economy and the future in which the European way of living is headed.

A highlight of EU policymaking was the adoption of ReFuelEU aviation regulation which sets a clear path towards the decarbonization of the aviation sector, a very important sector for the EU. Because aviation will be a baseline setter for biofuel production and ReFuelEU aviation regulation is one of the most comprehensive regulations regarding decarbonization of a sector, a thorough breakdown of its key points will prove to be insightful regarding the opinions and the will of policymakers on how to tackle certain issues. It should be noted that the extraction of conclusions, other than those clearly stated, from a regulation point of view, is quite abstract and was done here to assess the general trends regarding the future of biofuels which will serve as a basis for the case study regarding biomass utilization prospects.

2.1 ReFuelEU Aviation Regulation (Regulation (EU) 2023/2405)

Regulation (EU) 2023/2405 is the attempt of EU's legislative institutions to support the smooth transition of aviation to a decarbonized and less GHG intensive future. The key takeaways from this regulation are first and foremost, quotas on the use of sustainable aviation fuels (SAFs). By SAFs this regulation refers to:

i) Synthetic aviation fuels
ii) Aviation biofuels
iii) Recycled carbon aviation fuels

Each of these are defined as in Regulation (EU) 2018/2001.

The regulation sets minimum shares of SAF in aviation fuel according to Table 1.

The quotas set are:

Table 1: Minimum shares of SAF in aviation fuel as stated in annex I of ReFuelEU aviation regulation.

Year	2025	2030	2035	2040	2045	2050
SAF	2%	6%	20%	34%	42%	70%
Synthetic	-	1.2%-2%[1]	5%	10%	15%	35%

Fuel suppliers have been given some flexibility for the period 2030-2035 for meeting the quota of synthetic aviation fuels by allowing them to complement the shortfall in the next reporting period, which again highlights the cautious approach of EU as the market is still underdeveloped.

[1] For the period from 1 January 2030 until 31 December 2031, an average share over the period of 1.2% of synthetic aviation fuels, of which each year a minimum share of 0.7% of synthetic aviation fuels. For the period from 1 January 2032 until 31 December 2034, an average share over the period of 2.0% of synthetic aviation fuels, of which each year a minimum share of 1.2% from 1 January 2032 until 31 December 2033 and of which a minimum share of 2.0 % from 1 January 2034 until 31 December 2034 of synthetic aviation fuels

Also, renewable hydrogen for aviation and low-carbon aviation fuels are counted towards the target for synthetic aviation fuel supplied to union airports by fuel suppliers as an extra source to help not fall behind the targets set.

The quotas have been set on fuel suppliers and are transferred to union airports, as defined in article 2(1) of this regulation, by the obligation set to Union airport managing bodies to take all actions necessary so that aircraft operators have access to fuels meeting the above targets. In addition, aircraft operators that meet criteria set out in article 5 of this directive will have to uplift at least 90% of the yearly aviation fuel required from a given union airport. This shows the approach of this regulation is to involve all relevant stakeholders.

Measures to ensure a level market and mitigate competitive disadvantages as a result of this regulation have been taken and additions will be made, if necessary, along the way. These are:

- Fuel tankering
  It will happen due to different fuel prices at different countries and airports because of higher SAF costs. Aircraft operators will uplift more fuel than necessary to complete the flight, which will lead to higher fuel consumption and partly counteract the benefits of using SAF. This issue is addressed by the commission through the obligation of 90% of necessary fuel for the route to destination to be uplifted from the Union airport of departure. Thus, international differences in price of SAF and in turn, of fuel, will not be a problem for the local SAF market as the amounts of SAF needed can be expected.
- Union airports with small traffic
  Airports with small traffic will be exempted from this regulation as few emissions come from these destinations and a disproportionate cost might affect the interconnectivity of the regions served by these airports. So, when assessing a SAF production plant it will be important to know which airports are or will be under the obligations set out in this directive.

These are some of the most important measures to ensure a level playing field in the aviation sector. Other measures have been taken also but are not mentioned.

Regarding SAF feedstock the main criteria and methods are set by Directive 2018/2001 (RED III), but the ReFuelEU Aviation regulation imposes some restrictions on which feedstock will count towards meeting the quotas set in Annex I and are in article 4(5) of this regulation. These are food and feed crops as defined in article 2, second paragraph, point (40) of RED III, intermediate crops, palm fatty acid distillate and palm and soy-derived materials, and soap stock and its derivatives. However, the feedstocks included in annex IX of RED III still count. Main concerns for feedstock selection criteria are GHGs savings on Life Cycle Analysis (LCA) basis and interference with other

important sectors such as the agriculture sector. An assessment dated 2019 highlighted the main considerations for possible feedstocks to be added to Annex IX of RED III. It is expected that the list of biomass feedstocks will expand [5].

Assessing the trends set by ReFuelEU aviation regulation

The pool of SAF is not centered specifically on aviation biofuels, rather it includes almost all available alternatives. However, it recognizes that the deployment of synthetic aviation fuels will be more difficult than biofuels with the quota regarding their uptake increases significantly only after 2045, so aviation biofuels will be mostly used for the first years. Stimulating measures will most likely be taken for both biofuels and synthetic aviation fuels. Moreover, the cautionary measures taken to ensure a smooth transition for the EU aviation sector seem to support stakeholders across the board without heavily imposing burdens on a specific stakeholder. Overall, this regulation is a logical stance and a good starting point for the development of the aviation sector and more strict than other schemes such as the CORSIA [7] set by the International Civil Aviation Organization (ICAO).

On a general note, because the price of fuel is an important part of the operating costs of airlines amounting to around 30% [8], it should not be expected that fossil jet fuel will be taxed heavily in the near-term. However, it will be investigated, if it becomes possible in the coming decades, with impact assessments on the cost of air travel.

Based on this comprehensive regulation it is expected that both biomass derived, and synthetic fuels will be used not only in aviation, but in every sector that will have problems with directly converting to the long-term solutions. These will include most likely the long-distance transportations that will be disproportionately burdened by extra costs from the use of hydrogen or batteries.

Other relevant policies to consider are:

- Renewable Energy Directive III [9].
- Current Common Agricultural Policy (CAP, Now 2023-27) and its application in Greece [10].
- Greece's current national energy and climate plant (NECP) (Greece's NECP 2023) [11].

2.2 Renewable Energy Directive III

This directive will be transposed into national laws with different goals set by member states, but they must adhere to the guidelines set in the directive. Some important points are:

- The cap in bioenergy produced from food and feed crops to 7%.
- Quotas on renewable fuels of non-biological origin (RFNBOs).
- Increasing goals for renewable energy in the transport sector.

- Increasing the use of feedstocks listed in Part A of Annex IX towards the production of advanced biofuels and biogas, for the transport sector.
- Transferring of GHGs savings from one goal to other goals.

The amendment of renewable energy directive II comes as part of the fit for 55 package which sets more optimistic goals for the energy transition and widens the included sectors. The mentioned key points of the amendment highlight the attempt of the adopted RED III to turn towards a wide use of biomass and bioenergy. It is therefore expected that necessary measures will be taken on a national and EU level to expand the biomass market. This Directive is important for the proper selection of the candidate feedstock types in Chapter 3.

2.3 Common agricultural policy 2023-27 (CAP 2023-27)

The CAP 2023-27 and in particular the CAP strategic plan of Greece [12] has a very wide agenda but the strategic objective (SO) especially relevant to the biomass and bioenergy sectors is SO4. The overview of national CAP strategic plans can be found in [13]. The goals recognized are to achieve CO_2 storage in the soil and biomass, increase and protect soil quality and sustainable nutrient management will be met by the setting of mandatory guidelines to farmers. Agricultural practices regarding farm ground coverage, specific intermediate crop cultivation and others will be followed to achieve better soil quality, prevent soil erosion and face other relevant issues. As a rule of thumb to navigate through this policy's restrictions, sustainability and protection of the farmland and the farmer are of highest priority.

2.4 Greece's NECP 2023

The NECP is very insightful on how the country, in this case Greece, aims to implement regulations and policies from the EU as well as setting its own. Some of the key takeaways from Greece's energy and climate plan are:

- The aim to utilize renewable energy for the production of renewable fuels.
- The blending of advanced biofuels with conventional fuels.
- The aim to facilitate cost reductions in technologies needed for the future goals such as energy storage and RFNBOs.
- It foresees that advanced biofuels will be 32% of transport fuels in 2050.
- It aims to take measures to produce advanced biofuels and biogas upgraded to biomethane and injected into the gas network.
- It sets a time goal of 2035 that in sectors and applications where electrification is difficult, RES will be used to produce hydrogen which will in turn be used to produce fuels. This will be coupled with CO_2 capture from biomass and other sources.
- The transport sector will be decarbonized from 2030 onwards by the use of biofuels and electricity with the current target in the sector by 2030 being 29%.

- The main source of biomass feedstocks for the production of advanced biofuels will be lignocellulosic.
- It emphasizes the production of biomethane.
- It highlights the air transport sector's need for public-private partnerships, incentives and targeted funding to accelerate the sustainable adoption of biofuels.
- SAF will need to be produced domestically to the possible extent.
- Emphasis on forest protection, woody energy crops and carbon sinks.
- Under foreseeable waste management strategies part of wastes can be used for secondary fuels production.
- It mentions that subsidization of RFNBOs' price and tax relief might be done.
- The goal of net carbon emissions to be zero by 2050 with the use of carbon sinks, from soil, forests and sea.

When all of the key points addressed by Greece's NECP are considered, it is evident that a part of the country's decarbonization will be based on biofuels and synthetic fuels. For this case study that biomass is of interest, it is believed based on Greece's plan that the main prerequisites for a biomass market and application exist, as the plan reveals that biomass utilization is an essential part of Greece's plan.

2.5 Conclusions

Policy has a central role to support and guide investment to sustainable paths. The main goal for which the use biomass will be essential is decarbonizing sectors heavily dependent on fossil fuels with not yet feasible alternatives to the use of biofuels. Biomass utilization will be based on hierarchical use, focusing on carbon sequestration and long-term sustainability while avoiding conflicts with other sectors like the feed sector.

The ReFuelEU aviation regulation paves the way for similar policies in other sectors. Clear quotas for the future, while providing some flexibility to the underdeveloped market and distributing responsibility across stakeholders. Similar targets have been set in the past, e.g., gasoline and diesel blends, but not to the extent that this regulation has done.

From RED III and its application in Greece mainly through Greece's NECP it is clear that for biomass, many applications are sought for, which leaves it upon local conditions and stakeholders to determine which application is most needed and feasible. This does increase uncertainty towards biomass availability for transportation biofuels production. Therefore, it is deemed necessary to identify which available biomass types will be available and their potential in terms of quantity as their competing uses will play a significant role depending on local and national factors. The brief overview done for the main policies surrounding biomass use and biofuel goals, serves as a basis for the following case study.

3. Feedstock supply security

Biomass processing plants like the one proposed by this thesis are capital intensive and investors require low risk when deciding to invest in one. Especially, in the case the plant uses second generation biomass as feedstock then, available biomass quantity, quality and cost are considered to be main factors for the risk-assessment. Therefore, in this chapter, feedstock selection and the assessment of feedstock security in terms of quantity and cost is performed.

3.1 Feedstock selection criteria

The selection of proper feedstock can be difficult as there are many criteria to be factored in the final choice. To reach at a proper decision, a list of the main criteria for feedstock selection, in this case biomass source, are summarized in Table 2 in two wide categories, fuel characteristics and general aspects.

Table 2: Feedstock selection criteria.

Fuel Characteristics	General aspects
Energy content	Policy
Moisture	Sustainability criteria
Composition	Availability
Ash-content-composition	Pre-treatment need
Compatibility	Seasonality
	Storage – transportation needs

On the technical side, favorable characteristics of biomass are a high energy content, low moisture content, composition with low chlorine, sulfur and nitrogen content and lastly, low ash content and an ash composition not high in alkali metals to prevent from sintering or bed agglomeration issues [14]. Different biomass sources will generally have different elemental composition in addition to other differences e.g., particle size distribution. This variability leads to different behavior in the processing technologies used, and in the case of using multiple feedstocks this should be considered. When aiming for multiple feedstocks, the most crucial aspect to consider is the smooth operation of the processing technology with the different feedstocks despite differences in the products of intermediate stages throughout the process. Thus, despite some biomass types having better characteristics, other biomass types can be used as feedstock for biofuels production, if they are compatible with the employed processing technology. Compatibility can be facilitated on both ends, by using biomass sources that are similar in their behavior throughout processing or using versatile processing technology.

Feedstock selection involves additional important criteria, here referred to as general criteria. Firstly, the feedstock used will need to adhere to policy restrictions. These restrictions either prohibit their use or limit the extent to which they can be used (e.g., by limits in their use for certain bioenergy purposes). Also, if the use of this feedstock is in line with policy measures it strengthens the claim that the feedstock will become available in high quantity through policy support. Moreover, the sustainability criteria for biomass sources are a complex issue to deal with because it is not yet clear what is actually sustainable, and especially when considering that sustainability thresholds set in areas can change due to climate change. Generally, they include GHGs emission savings, indirect land use change, soil erosion risk, carbon stock increase and maintaining soil fertility and organic matter. With rising concern about environmental consequences of biomass exploitation, it can be difficult to navigate relevant policies because they are under development and for the past few years changing, adopting stricter rules to ensure the sustainability of the use of each biomass source. The next step is to assess the availability of the biomass source, and of course policy and sustainability criteria will affect the result. As mentioned before, the compatibility of the processing technology is an important factor and for this reason certain pre-treatment is usually necessary before the biomass is further processed e.g., pelletizing or chipping. Additionally, the seasonality of biomass can be a logistical struggle and is followed by increased costs due to greater size storage needs when a large amount from the annual needs is supplied in a short time span. Also, as a result of time passage, with long duration storage, biomass may lose some percentage of organic matter, and the extent depends on the measures taken to minimize it. Therefore, a variety of biomass sources should be used to mitigate the seasonality effects, if any exist. Lastly, storage and transportation need to be considered because they can entail additional costs or risks when special measures need to be taken for the safe and according to guidelines storage and transportation of biomass.

3.1.1 Feedstock selection

In Greece, many biomass sources are currently used for the production of energy, biogas or biodiesel. The operating plants are usually small-scale plants because there is no stable supply chain of biomass sources and feasible utilization of biomass sources is rare leading to low supplier engagement and low market available biomass potential. These factors can be largely attributed to Greece's economic crisis during 2010-2018 preventing the purchase of new equipment which would allow stakeholders to capitalize on the opportunities in the biomass sector with a more efficient and cheap collection of biomass making it a feasible investment. In conjunction to this, only in recent years the efforts of the state and initiatives have been able to reach stakeholders and initiate change in the biomass sector. Currently, small-scale plants make sense because the industry relies on local biomass supply chain.

3.1.1.1 Available biomass sources in Greece

In the project AGROinLOG [15] a long list of bioenergy and biofuels products derived from agricultural feedstocks has been created (see Annex A, [16]), the sector of their products' end use, the investment cost and scale of production-processing plant. In annex B an overview of biobased chemicals and materials is provided and in annex C a long list of logistical components. These provide a good basis not only for the feedstock selection, but also for the understanding of different paths regarding biomass utilization and the necessary steps.

Additional possible biomass sources were provided from the S2Biom project [17] that created a database and a visualization tool for, mostly lignocellulosic, biomass supply potential. Since it was calculated in 2013 to 2016, the project made projections for 2020 and 2030 which can also provide a preliminary biomass potential overview for different sources.

Other feedstocks considered were vegetable oils, used cooking oils, animal fats, animal manure, and the organic fraction of municipal waste.

3.1.1.2 Region selection

For the overview of Greece's regions regarding biomass supply potential, mainly the S2Biom tool [17] was used as it has data on many of the main biomass types found in Greece. For other possible biomass sources, available data from literature and stakeholders were used. It seems that Greece's regions, Thessaly, Peloponnese, Macedonia, Thrace and Crete have enough biomass potential to support some bio-economy investments. From these, it was decided to further study the Peloponnese region.

Region choice

In this thesis the prospect of a sustainable biomass supply chain in the Peloponnese region of Greece was studied. Other regions such as Thessaly and Central Macedonia were also candidates for study, but their biomass potential utilization has already been studied to some extent [18], [19]. Most importantly, a biomass-based industry already exists in these regions, and it is upon the local stakeholders to utilize the available potential and expand the market by establishing a supply chain. It is not clear if in 10 years, which is the expected time that large scale utilization of the technologies developed in the later chapters, there will be space in the market of these regions for a medium to large scale biomass processing plant. A lot of untapped potential exists in Peloponnese and has been studied in [20] and the projects [21], [22], [17], [23], [24]. Their findings are based on data that occur from the analysis of large regions and this thesis will attempt to break down the biomass supply potential in a deeper level. The use of data that do not factor in regional differences, introduces more uncertainty in the results and the prospect of utilizing biomass in the Peloponnese region is still uncertain despite the assessments showing promising results. Therefore, it was

decided that a valuable contribution of this thesis would be to further study this region. Irrespectively of the results from later chapters studying a specific biomass use, the work in this chapter will hopefully facilitate further biomass utilization in the region. The results from this chapter will be an estimate of the available biomass potential in municipality level for the Peloponnese region.

The region of Peloponnese studied is a geographical region comprised of 7 regional units, namely Achaia, Argolida, Arkadia, Ileia, Korinthia, Lakonia, Messinia. Hurdle to the development of a biomass supply chain in that region is on the one hand its topography being highly mountainous and on the other hand the road network being underdeveloped. These factors together increase the complexity of transportation as well as the travel distance. In Figure 2 the Peloponnese region and its mountainous topography are depicted.

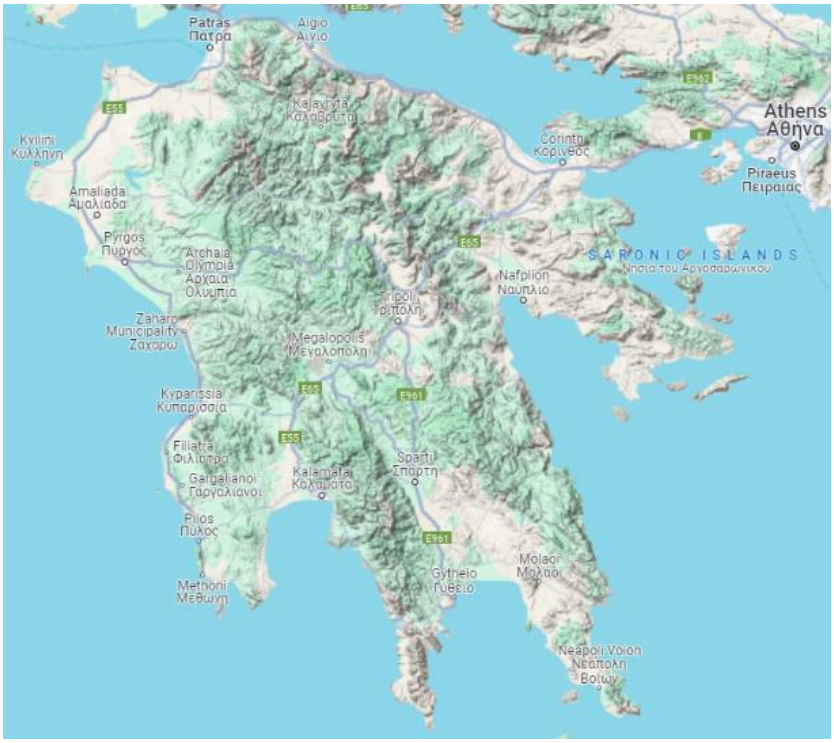

Figure 2: Peloponnese region and its mountainous topography [25].

3.1.1.3 Biomass source selection

The examination of possible biomass sources in the Peloponnese region revealed that the main biomass potential is in the agricultural and forestry sector. These sectors have large untapped potential and have biomass types which fit the biomass selection criteria set out in section 3.1. The Peloponnese region showed great potential in the following biomass types:

- Olive Tree Pruning (OTP)
- Orchard Pruning (OP)
- Vineyard Pruning (VP)

- Forest residue from conifers (FORESCO)
- Forest residue from broadleaved species (FORESBROAD)
- Forest residue from mixed stands (FORESMIXED)

The prunings of olive trees, orchards and vineyards become available as a result of normal practices in the sectors regarding the maintenance of these cultivations. They consist of mostly branches and some leaves and only in some cases they are further utilized and are otherwise burned on field. Other options are for the large diameter prunings, above 5cm, to be used as firewood or for prunings to be passed through mulchers or chippers and spread on the field, left to decompose, so the soil will reabsorb some of the elements [26].

Forest residues are categorized based on the tree category they come from and for the purposes of this analysis the land cover of the area is considered as mostly being covered by conifers or broadleaved species or mixed stands, meaning that no category of tree is more prevalent in the area. This categorization of forest residue occurred during a later stage of the analysis as will be explained. Forest residue come naturally as fallen matter or result from human activities. In the context of this thesis, they include logging residue from final fellings and thinnings, so, branches, treetops and stumps.

Assessment of additional biomass sources

For this assessment despite there being adequate potential for straw/stubbles residue to be used as a complementary feedstock when available, they were not considered further as the current regulatory framework allows for little certainty on the amounts that can be extracted from the field and under Greece's CAP strategic plan 2023-27, their mobilization is strongly encouraged towards other uses. The agricultural residue potential for Peloponnese including straw/stubbles, has been studied to some extent, in [17], [27], [20], [21], [22], but this analysis will focus on woody biomass potential.

A special mention should be done for Used Cooking Oil (UCO) and organic fraction of municipal and industrial waste. UCO is a waste stream efficiently converted to aviation biofuels through the Hydroprocessed Esters and Fatty Acids (HEFA) route. Despite this, UCO is included in part B of annex IX of RED III, availability is limited, and currently, in Greece, UCO is used to produce biodiesel. A single company, Verd S.A. controls approximately 50% of the market potential and directs it to biodiesel [28]. Until now, the market potential involves mostly businesses, i.e., restaurants, hotels, and not households, but in the last years the company has partnered with many businesses to establish a network, collecting cooking oil from households [29]. Thus, UCO has limited prospects as feedstock for any processing plant. The organic waste from industrial and household sources was rejected because current management plans are mostly focused on other uses such as biogas and compost production. The available potential after considering competing uses will not be sufficient for any large-scale processing

plant and becomes even more difficult if the potential needs to be collected by multiple dispersed locations in the region [30].

3.1.1.4 Feedstock selection criteria fulfilment

The biomass types selected from those available in the region have great potential for the development of bio-based industries. It is expected from the assessment of the available potential that each biomass type alone can be sufficient for the operation of a processing plant in the region, except maybe forest residue that have some difficulties in both predicting the available potential and mobilizing this potential at a feasible cost. Secondly, assuming suitable operating parameters, the chosen feedstocks are interchangeable in the proposed processing plant. Composition of VP and OTP were found in [31] from local samples and for OP the phyllis2 database was used [32]. The composition of the chosen feedstocks can be found in Table 3, and forest residue (FORES) have been described by one composition as they can differ even between different parts of the tree, e.g., branches vs bark and between different species of the same category, e.g., fir vs pine for conifers [33]. Thus, composition of FORES is a range, and the stated composition is an approximation and within this range and was from [33]. The composition of OP, VP and OTP is also a range but a narrower than forest residues as the latter includes many parts of trees and tree species. The composition of feedstock in a real industrial scenario will be tested after receiving it, so this is a sufficient estimation level.

Table 3: Feedstock composition.

	OP	VP	OTP	FORES
Proximate analysis (% d.b.)				
Moisture	-	39.8	25.2	56.8
Fixed Carbon	14.67	20.6	17.1	16.9
Volatile Matter	80.95	74.5	78.4	79.9
Ash	4.38	4.9	4.5	3.2
Ultimate analysis (% d.b.)				
Ash	4.38	4.9	4.5	3.20
Carbon, C	46.45	47.3	50.43	51.01
Hydrogen, H	5.29	6.5	6.79	5.23
Nitrogen, N	1.03	0.69	1.27	0.68
Sulphur, S	0.09	0.04	0.12	0.10
Chlorine, Cl	-	0.06	0.07	0.03
Oxygen, O	42.76	40.51	41.32	39.75
LHV (MJ/kg d.b.)	16.93	17.16	17.56	18.96

All selected feedstocks fulfil the feedstock selection criteria and together, it is likely they can support a medium-scale processing plant.

In terms of OTP, VP and OP fulfilling the feedstock selection criteria, their heating value is satisfactory if the moisture is not too high and usually it is not. Moisture content is initially, after harvest, around 40%, and if left at the field for a few days, without raining, moisture can reach, in average, 27.5% as shown in [26] before the transportation stage, therefore lowering transportation costs [34], [35], [36]. Composition is favorable with high carbon content, high volatiles and low Cl, N, S, Ash content. Ash composition will not be a problem as they have low ash content, less than 5%, and ash composition will not create problems during the processes as K, Na content is low and generally woody residues have been known to not cause ash composition related issues. Moreover, to address the general criteria, regarding policy, pruning mobilization will have the support from policy measures as the current practice of burning this residue on the field in open fires will not continue for long. Wasting the energy content of OTP when it could enhance energy security of Greece is an issue that should and probably will be dealt with the following years, either from the state or centrally from the European Union. For example, there was an attempt from the European commission to subsidize the purchase of chipping equipment for OTP which shows activity towards these biomass residue [37]. Furthermore, prunings fulfil sustainability criteria since pruning is part of normal practices in olive groves, vineyards and orchards, and is conducted once or twice per annum or biannually. Pruning potential is a residue stream that should be directed back into production of added value products and is not associated with any sustainability risks. In terms of availability there is enough biomass potential in the region, but this will be further analyzed in the following sections. It was expected from the beginning of this study that OTP can support a commercial scale biomass processing plant. However, the potential of the other biomass types remained unclear, and especially the readily available potential. As for pre-treatment, initially, natural drying will be employed in either the processing plant or in intermediate storage facilities, if the transportation distance significantly increases transportation cost. Additionally, the feedstock will be chipped and after further drying in a mechanical dryer to lower the moisture content to the range of 10-15% it will be fed into the gasifier. These stages are expected and do not pose any issues with special equipment or pre-treatment processes. Regarding seasonality, as was mentioned, pruning is done according to local practices at certain time periods within a calendar year which usually last for one to two months. However, the effects of the seasonality will be significantly mitigated due to the use of multiple feedstocks as shown in Table 4 illustrating the expected pruning time period of each. Lastly, transportation and storage needs might pose issues due to the low bulk density of prunings, but not to a significant extent.

Forest residues are slightly better than prunings in terms of heating value but have higher moisture content that will need to be lowered through natural or other drying methods. The composition is very favorable with low ash content and low Cl, N, S while the range of carbon content usually found in forest residues is high. Ash composition will not be a problem as they have low ash, less than 5%, and generally, woody residues have been known to not cause ash composition related issues. Moving on to general criteria, policy heavily supports forest management which will increase forest residue mobilization. More particularly the currently enforced program "Antinero III" in which "Antinero" means "instead of water" comes after the two previously implemented programs of smaller scale. Currently, the forests in Peloponnese as in many other regions of Greece, remain largely unmanaged leaving unutilized biomass potential and causing problems with forest wildfires as the forest residue left in the ground provide fuel for the fire to spread. Actions of the program among others, are to clean and manage forests, maintenance and improvements on the forest road network, maintenance of existing firebreaks [38]. These actions will stimulate forest residue mobilization especially in the Peloponnese region that has high forest cover and will have great opportunities in the biomass market. Furthermore, sustainability criteria are met for some regions and for others they are not. The extent of sustainability risks is uncertain, but considering the great potential of the region, the sustainably available potential will also be high. There are no special pre-treatment needs for forest residues. Seasonality of forest residue exists, but as previously explained, the use of multiple feedstocks mitigates its effects. Transportation and storage needs are similar to prunings.

Overall, prunings are a very favorable feedstock with very little associated issues and the forest residues have some sustainability concerns that can pose problems if not correctly tackled. All other criteria are met and only in terms of availability and cost, more insight will be gained in the following section.

Table 4 shows the usual harvesting periods for the biomass types selected. Harvested biomass becomes available and ready for processing later than the harvesting period due to the intermediate steps needed, but it provides a good overview of the seasonal issues. It should be noted that OP are harvested in a wide time frame because of the different varieties and harvesting periods depending on climatic conditions.

Table 4: Harvesting periods for each selected biomass type.

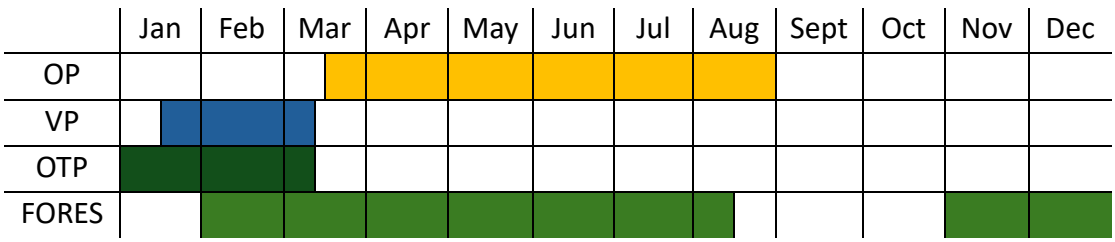

3.2 Feedstock supply sustainability

The feedstocks presented in section 3.1 show most promise in the region of Peloponnese and they can probably supply enough potential to a biomass market in the region. In this section two things are done. Firstly, the estimation of quantity of available biomass in several layers e.g., theoretical potential, technical potential and market available potential, including different factors at each layer. Then, a total cost is calculated at the gate of the processing plant. The methodology and results are separately presented.

3.2.1 Methodology

The methodology involves the quantity estimation at municipality level using a known method from the BEE project [39]. Coupled with estimates of the total cost at the processing plant gate, a sensitivity analysis is conducted varying the market share parameter to assess the behavior of supply-cost curves when different amount of the market available biomass potential is directed to competing uses. Figure 3 presents a block flow diagram of the methodology.

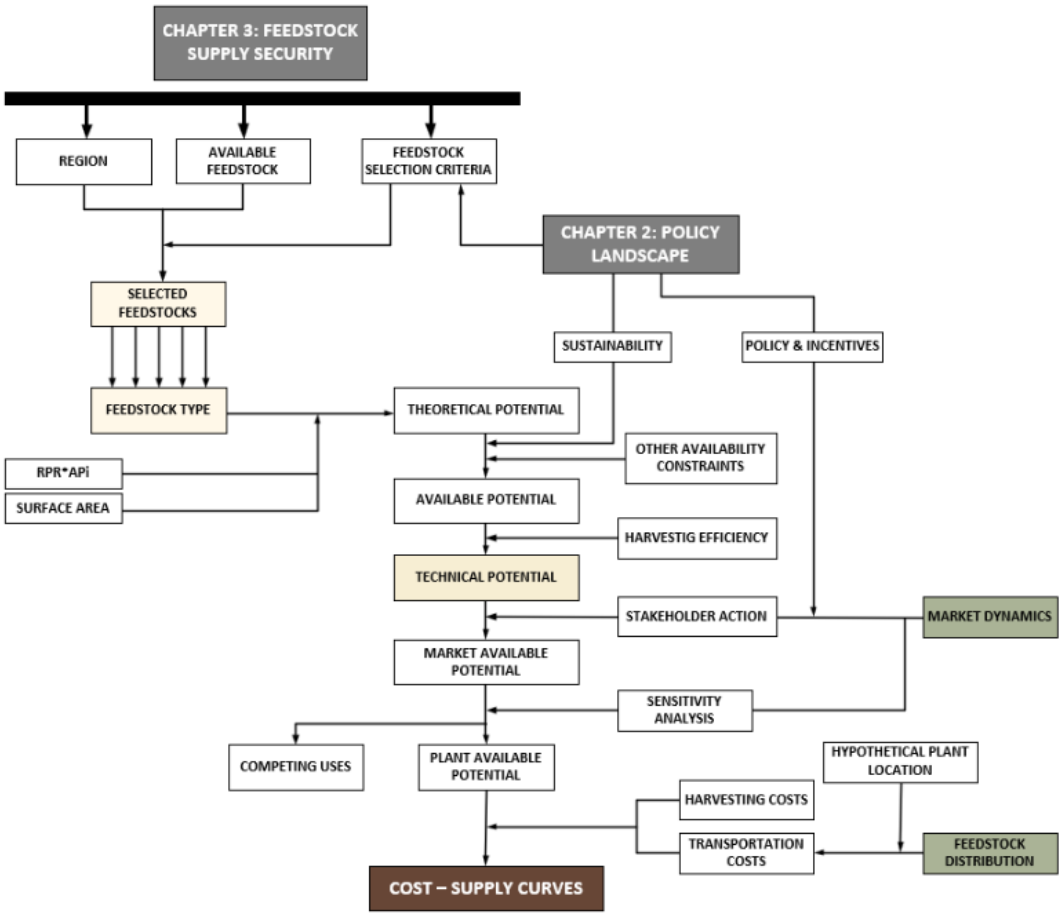

Figure 3: Block flow diagram of the methodology to derive cost - supply curves.

3.2.1.1 Surface area

Data regarding cultivated surface area are extracted from the platform BIORAISE created from the CHRISGAS project.[2] This project used geospatial data from the Corine Land Cover (CLC) 2012 product which offers an overview of 44 thematic classes of land cover in Europe. The surface area for each biomass type was extracted in municipality level which corresponds to the subregion choice in the platform. This was done for the municipalities in the 7 regional units excluding the municipality of Elafonisos, a small island. Surfaces for orchards, vineyards and olive groves were available and as for forest land cover, the surfaces were segregated for land areas covered by conifers, broadleaved species or mixed stands. Harvesting costs are different from each stand, which is the reason for the corresponding categorization of forest residues.

3.2.1.2 Theoretical potential estimation

The theoretical potential estimation is based on the methodology from the BEE project which has also been used in [17], [24], [23] and [27]. This methodology utilizes one of three available ratios, namely the residue to surface area ratio (RSR), residue to product ratio (RPR), and depending on the available data and the methodology followed, RPR can be coupled with area production (AP) to derive an estimate of RSR, from now on mentioned as RSR_{mod}. For the calculation of AP, data for area and production were extracted from the Hellenic Statistical Authority (ELSTAT) [40] for the year 2021. Production data were divided by cultivated surface area, both from ELSTAT to keep a coherent data source. RSR_{mod} is calculated according to Eq. 1. This method has been used in Biomasud and provides the area distribution of residue.

If for a region there are available data on cultivated area and production, RSR_{mod} is calculated and thus it can yield different ratios for different regions. The alternatives are to derive RSR from many locations which is difficult or assume a general RSR for a greater region.

Another, approach is to estimate the number of trees as their residue potential can be calculated based on per tree residue productivity values. A technical report from 2004 made by the Technical Chamber of Greece used this method for the pruning potential of the Peloponnese region but the data from this technical report were not used [36]. An estimation for residue per tree productivity can be found in [41].

[2] The first version of BIORAISE was developed in the EU VI Framework Program 'CHRISGAS' for Spain (except of Canaries), Portugal (except of Azores and Madeira), France, Italy and Greece and was updated in 2012, in the framework of the H2020 Project BIOMASUD

$$RSR_{mod} = RPR \cdot AP \quad \text{Eq. 1}$$

Where:

RSR_{mod} = Modified residue to surface ratio

RPR = Residue to product ratio from Table 9 (t_{DM}/t_{prod})

AP = Area productivity in (t_{prod}/ha)

The theoretical potential is calculated according to Eq. 2.

$$(Theoretical\ potential)_{i,j} = R_{i,j} \cdot Area_{i,j} \quad \text{Eq. 2}$$

Where:

Theoretical potential = Theoretical potential of biomass in (t_{DM})

R= RSR or RSR_{mod} in (t_{DM} /ha)

Area= Cultivated surface area (ha)

Indice i is for municipality and j for biomass type

Generally, pruning productivity depends on various factors such as climate, variety of crop, age of trees and tree density, pruning intensity [42]. An extensive literature review has been conducted in this study to find the estimates of RSR and RPR values most relevant to Greece and to the Peloponnese region. Table 5 shows RSR values found in the literature and on-field measurements available from projects and those most relevant to the Peloponnese region of study are reported. Table 6 shows RPR values found in the literature and those most relevant to the Peloponnese region of study are reported. Especially, for OTP there were available values from on-field data all over Greece and two locations of Peloponnese from the Up_Running project [43] which reinforces the estimations from the methodology with a range of reliable values. The reported RSR and RPR values refer only to pruning potential of Orchards, Vineyards and Olive groves and not the forest residue potential. For the forest residue potential estimation data from the Biomasud project were used which were incorporated in the updated BIORAISE platform of the CHRISGAS project. The Biomasud and CHRISGAS projects have used various data sources about forest residue productivities and these values were selected for this analysis.

Table 5: Residue to surface ratio (RSR) literature review.

RSR (t_{DM} /ha)					
Biomass source	Residue	Value	Min	Max	Reference
Orchards	Prunings	1.8	1	5.64	[44]
	Prunings	1.68	0.6	5.14	[45]
	Prunings		1.6	1.8	[46]
	Prunings		4.84	7.18	[47]
Vineyards	Prunings	1.15	0.11	2.57	[44]
	Prunings	1.3	0.11	2.66	[45]
	Prunings		1.1	1.5	[46]
	Prunings		4.42	12.01	[47]
Olive tree	Prunings	2.8			[43]
	Prunings		2.11	16.12	[43]
	Prunings	1.9	0.35	5.46	[44]
	Prunings	1.29	0.35	5.74	[45]
	Prunings	1.3			[46]
	Prunings		1.3	1.45	[47]
	Prunings		2.44	5.53	[48]

Table 6: Residue to product ratio (RPR) literature review.

RPR ($t_{DM}/t_{product}$)					
Biomass source	Residue	Value	Min	Max	Reference
Orchards	Prunings	2.3	2	2.9	[49]
	Prunings	0.35			[50]
Vineyards	Wood	0.65	0.5	0.83	[49]
	Prunings	0.5			[50]
	Prunings	0.72			[27]
Olive tree	Prunings	1.02			[43]
	Prunings		0.6	3	[43]
	Prunings	1.55	0.5	2.6	[49]
	Prunings	0.637			[27]
	Prunings	0.5			[50]
	Prunings		0.26	2.2	[48]

3.2.1.3 Available potential

The available potential is considered here to be the theoretical potential, but with applied the sustainability and other constraints, such as the accessibility to the resource. For the case of Peloponnese such factors apply heavily on the forest residue. For the pruning potential it was assumed by the Biomasud project that there are no availability constraints, and all pruning potential will become available. The main factors determining pruning availability are the slope and the structure of farms which can be a hurdle for harvesting and loading. Also, farmers might choose to use some of the prunings as firewood or to chip them and spread them on the field. The BIORAISE platform offers a visualization tool for both the farms and the terrain which was used and from the overlap of orchards, vineyards or olive groves with the areas of rough terrain. A factor taking into account all these has been used, although it could be assumed that almost if not all prunings can be part of the available potential. The value of this factor for this analysis is 0.8. For the forest residue potential, the CHRISGAS and Biomasud projects have incorporated restrictive conditions in forest residue availability, namely slope, soil erosion risk and the soil organic carbon content which lower the availability of forest residue, and these values were selected.

3.2.1.4 Technical potential

Technical potential is calculated from the available potential when harvesting efficiency is considered. They represent the percentage of biomass loss because the harvesting method used is not collecting all available biomass. Harvesting efficiencies derived from the Biomasud project set a baseline for harvesting efficiency but since their sources are a bit older, a slightly improved harvesting efficiency is used for Orchard and Vineyard prunings while the harvesting efficiency for Olive tree prunings is assumed to be significantly lower to take into account terrain complexity leading to lower harvesting efficiency of equipment. Also, the approach towards this feedstock security assessment is to be conservative and set a reliable baseline. The technical potential is calculated according to Eq. 3.

$$(Technical\ potential)_{i,j} = (Theoretical\ potential)_{i,j} \cdot (Harvesting\ efficiency)_j \qquad Eq.\ 3$$

Where:

Technical potential = Technical potential of biomass in (t_{DM})

Theoretical potential = Theoretical potential of biomass in (t_{DM})

Harvesting efficiency = Values from Table 13

Indices i is for municipality and j for biomass type

3.2.1.5 Market available potential

Market available potential is derived from the technical potential incorporating market dynamics such as stakeholder engagement and incentives that will lead to biomass mobilization. A different mobilization rate was assumed for woody agriculture residues and forest residues which will be harder for the region to mobilize its potential as it requires equipment and labor not yet acquired. In the following 5-10 years it is expected that significant steps will be taken towards biomass mobilization and utilization in Greece and the Peloponnese. Calculation is done according to Eq. 4.

$$(Market\ available\ potential)_{i,j} = (Technical\ potential)_{i,j} \cdot (Mobilization\ rate)_j \qquad Eq.\ 4$$

Where:

Market available potential = Market available potential of biomass in (t_{DM})

Technical potential = Technical potential of biomass in (t_{DM})

Mobilization rate = Values from Table 15

Indices i is for municipality and j for biomass type

3.2.1.6 Plant available potential

Plant available potential is based on the market available potential considering the share of the market that the consumer will be able to capture. This factor is important to take into account because not all of the cheaper or for other reasons, desired biomass will be available for the consumer. As this factor cannot be estimated, it was varied in a sensitivity analysis to see whether it had a significant impact to the cost of feedstock for the processing plant.

$$(\text{Plant available potential})_{i,j} = (Market\ available\ potential)_{i,j} \cdot (Market\ share)_j \qquad Eq.\ 5$$

Where:

Plant available potential = Plant available potential of biomass in (t_{DM})

Market available potential = Market available potential of biomass in (t_{DM})

Market share = Value subject to sensitivity analysis

Indices i is for municipality and j for biomass type

3.2.1.7 Feedstock distribution

The last step of the methodology is to find an estimated location of each biomass type in each municipality. It was assumed that biomass potential is evenly distributed across the cultivated surface area within each municipality and a center of mass was found using a visualization tool included in the BIORAISE platform. The coordinates of the center of mass represent the distributed feedstock, so feedstock distribution is 222 nodes in this case. These nodes will later be used to calculate the mean travel distance to the storage facility and the processing plant.

3.2.1.8 Harvesting cost

Literature data for harvesting costs are not conclusive and many sources need to be examined for a more representative cost estimate. For relevance maximization, data from the most relevant to the Peloponnese region case studies and projects were used. Differences between cost estimates can be explained by many factors such as, average residue density and harvesting method and steps used for the study. Other factors are, regional differences in labor costs, and geomorphology affecting fuel consumption and productivity of the equipment and workers. Lastly, the equipment used during harvest is usually different and thus operational costs are not the same. This factor is especially relevant for the Greek agricultural and forest sectors which due to Greece's economic crisis have outdated equipment. A review on pruning harvest is available in [51]. Pruning harvesting costs have two broad steps that need to be included, namely collecting and loading. The costs reported can also include some treatment of the residue such as chipping which is sometimes integrated with the harvesting stage. Forest residue harvesting costs include felling, bundling, hauling and baling operations. Different steps and equipment can be used during pruning and forest residue collection and loading depending on the specific needs and available methods. The costs can vary significantly because the nature of residue harvesting varies significantly between cases. During this analysis the variability in harvesting costs was considered and an estimate was provided that included the special features of the Peloponnese region and learning curves reducing harvesting cost. Not having purchased harvesting equipment is both a hurdle and an advantage because technology improved and the more modern equipment, will perform better during harvesting operations and particularly under more difficult circumstances.

3.2.1.9 Transportation cost

The means of transportation used, and travel distance are the two main factors to be considered when determining transportation costs. For biomass transportation, trucks are the only available option in the Peloponnese region. Costs associated with the use of truck transportation can be broken down to the main constituents, fixed and variable costs which include truck value depreciation, maintenance, labor, fuel, and profit. The estimation of these costs is bypassed with a commonly used value for transportation cost via trucks. This cost is expressed in currency, per distance, per freight weight e.g., euro, per kilometer and tonne respectively. An indicative value for transport cost by trucks can be found from public works auctions. This value provides an estimate of the maximum cost of transport because based on this the participants to the auction provide a discounted value at which they price transportation. Because prunings and forest residues are less dense than other goods usually transported they have special prices.

It is clear that weight and travel distance will be the two variables of this analysis since the adopted price includes everything else. Transportation costs can be very high if the

travel distance gets high. For example, when a transportation cost of 0.13 €/tonne/km is set, the travel distance is 100km and the moisture content is 40%, the corresponding transport cost is 21.7 €/t_{DM} which added to the cost of harvest can be a hefty increase in feedstock cost.

The transportation cost value represents the cost of load weight transport and as biomass is transported with moisture, Eq. 6 calculates the cost of transport with dimensions of $C_{transport\ w.b.}$ being €/$t_{w,b.}$. Then it is converted to dry basis.

$$C_{transport\ w.b.} = (Transportation\ cost) \cdot (Travel\ distance) \qquad Eq.\ 6$$

Where:

$C_{transport\ w.b.}$ = Cost of transport in €/$t_{w.b.}$

Transportation cost is the price set for transport in €/tonne/km

Travel distance = Distance traveled in km

The established feedstock distribution is considered as nodes and depending on the processing plant location, their distance will be constant thus, the $C_{transport\ w.b.}$ from this node will be constant. The calculation was done using a hypothetical plant location close to Korinthos. Korinthos is a favorable location in close proximity to a refinery that can buy the crude product of the processing plant proposed by this thesis. Additionally, it has an industrial zone and locations near the sea. For the final calculations the precisely calculated distance by Google maps [25] was used to calculate transportation costs with the preferred route being the closest one and easiest one in terms of road complexity so in some cases the long way around a mountain is chosen instead of the not so safe and easy mountain road. For the initial calculation when the plant location and some pre-treatment facilities was not finalized, the haversine formula was used to calculate the great circle distance between two points of the surface of a sphere and considering earth as a sphere with a radius of 6371 km it can produce a good approximation of the travel distance. A manually calculated correcting factor of 1.9 was used to account for the complex terrain of Peloponnese since it can in certain cases significantly increase the actual travel distance.

The travel distance d is calculated by the haversine formula shown in Eq. 7.

$$d = 2R \cdot \arcsin\left(\sqrt{\sin^2\frac{\varphi_2 - \varphi_1}{2} + cos\varphi_1 \cdot cos\varphi_2 \cdot \sin^2\frac{\omega_2 - \omega_1}{2}}\right) \qquad Eq.\ 7$$

Where:

ϕ_1, ϕ_2 are the latitude of point 1 and point 2 in radian

ω_1, ω_2 are the longitude of point 1 and point 2 in radian

R is the mean earth radius equal to 6371 km

Moisture content

Moisture content is at its highest when biomass is firstly harvested and according to the following analysis, the values presented in Table 7 are assumed for each biomass category. For prunings, an initial moisture content of 35-40% is common but can be lowered, when left for a few days at the field, as shown for the OTP in [26] that reached an average of 27.5% moisture content. This will additionally get rid of leaves therefore achieving better biomass composition. As data were available for OTP having lower than 30% moisture content a value of 30% is used and a conservative value of 35% for the other pruning residue. The assumed moisture content represents the moisture content at which the prunings will be transported. Forest residues can have 40-60% moisture and an average of 50% is assumed because they will be transported after being left near the harvesting location for a few days [34].

Table 7: Initial moisture content of each biomass category.

Moisture content (% t_{DM} /t_{WM})					
OP	VP	OTP	FORESCO	FORESBROAD	FORESMIXED
35%	35%	30%	50%	50%	50%

Pre-treatment facilities used

The use of pre-treatment facilities will improve the feedstock energy density and bulk density and will lower transportation costs and thus the biomass cost from distant biomass sources. Two cases were evaluated, with and without intermediate pre-treatment facilities which for the case were considered to be two central facilities that collected the prunings and forest residue from multiple municipalities when it was better than transporting the biomass straight to the processing plant. The one was in the Megalopolis municipality and the other in the Aigialeia municipality. The facility in Megalopolis can be seen also as a possible plant location due to its central position. The pre-treatment facility will include natural drying and chippers when chipping was not integrated during harvesting, effectively reducing the moisture content to around 20% and the density will increase. The new moisture content will be used for biomass transport to the processing plant. Ideally, the pre-treatment would be close to the harvesting location in a decentralized way.

3.2.1.10 Total cost at the gate of processing plant

The cost of feedstock at the gate of the processing plant is the sum of harvesting and transportation costs and can be expressed in either wet or dry basis. In this analysis, it is calculated in dry basis for easier comparison to literature data. Feedstock cost can be less or higher depending on market dynamics, but the sum of harvesting and transportation costs represents the break-even price and thus the cost of feedstock.

3.2.1.11 Cost-Supply curve

The cost-supply curve is constructed by sorting the resulting case available potential for each municipality with its corresponding total cost at the gate of the processing plant. It is assumed that the processing plant will be supplied by the cheapest biomass first. The average cost of feedstock for the processing plant will increase for each next biomass unit supplied. Plant capacity is then chosen.

3.2.2 Results

3.2.2.1 Cultivated surface area

Data on cultivated surface area are from the BIORAISE platform for the municipalities of 7 regional units for each biomass type. These results are presented in Table 8. For some biomass types the potential surface areas seem small, but this is not enough cause to exclude them as long as the very small cultivations or forests are part of larger potential surface areas.

Table 8: Potential surfaces extracted from BIORAISE platform.

	Potential Surfaces (ha)					
	OP	**VP**	**OTP**	**FORESCO**	**FORESBROAD**	**FORESMIXED**
ARGOLIDA						
ARGOS - MYKINES	10509.7	292.3	10690.8	2184.1		857.1
EPIDAVROS	708.3		5558.6	988.9	511.7	
ERMIONIDA	193.9		6520.7	890.8	17.2	89.1
NAFPLIO	5385.8		2652.9	317.0		
ARKADIA						
VOREIA KYNOURIA	88.6		5669.2	2982.7	1857.4	1187.0
GORTYNIA			3183.0	13455.6	1293.9	4553.8
MEGALOPOLI			337.2	2659.8	4145.1	1039.4
NOTIA KYNOURIA			1354.4	6234.0	1095.7	585.3
TRIPOLI		440.3	794.1	14724.8	889.2	1928.4
ACHAIA						
AIGIALEIA	4154.4	4376.4	6837.2	9615.8	294.1	910.3
DYTIKI ACHAIA	562.8	697.4	5287.3	827.8	681.8	214.3
ERYMANTHOS	25.0	38.5	1927.1	2501.1	20.6	229.4
KALAVRYTA		1560.9	47.0	14708.8	2468.2	1540.9
PATRA	971.9	86.1	3627.2	714.7	176.2	986.0
KORINTHIA						
VELO - VOCHA	1572.5	5236.0	2298.2	494.2		2.4
KORINTHOS	2154.6	2186.3	9351.1	8083.6		
LOUTRAKI - AGIOI THEODOROI	116.6		788.1	8243.8		
NEMEA	2.2	4399.1	3755.1	307.9	41.0	
XYLOKASTRO - EVROSTINI	1183.1	3159.6	4392.2	5608.5	144.2	6.0
SIKYON	2061.7	3866.3	2029.6	9953.2	576.4	151.4

LAKONIA						
ANATOLIKI MANI	78.0		12644.0	79.3	157.5	916.9
EVROTAS	2357.3		14048.7	1434.0		210.2
MONEMVASIA	602.2		14379.5	1013.3		467.5
SPARTI	2942.4	138.6	15807.5	12597.2	2879.5	1431.6
MESSINIA						
DYTIKI MANI	229.1		3255.9	2886.0	291.7	684.5
KALAMATA	227.5		5541.5	1843.3	6493.0	1178.1
MESSINI			13859.4		43.8	2288.3
OICHALIA			8821.0		2518.9	1011.4
PYLOS - NESTOROS		25.1	13253.6		879.6	1645.7
TRIFYLIA		79.7	15491.8	33.5	731.2	3234.8
ILEIA						
ANDRAVIDA - KYLLINI	405.3		1714.2	571.3	393.0	
ANDRITSAINA - KRESTENA	380.0	27.3	9326.2	160.6	257.3	1267.6
ARCHAIA OLYMPIA	116.1		3363.1	1715.3	2040.9	4289.2
ZACHARO			7565.5			355.7
ILIDA		1420.1	2400.8	55.0	577.8	81.5
PINEIOS	416.4	310.4	935.0	71.7	76.4	
PYRGOS	403.0	1547.5	6499.2	139.5	109.8	101.2

3.2.2.2 Technical potential

The technical potential was estimated for the municipalities of 7 regional units for each biomass type based on the theoretical and available potential. The theoretical potential was calculated, from the RSR_{mod} derived by AP and RPR values for prunings, while for the forest residue potential the RSR from Biomasud was used.

The RSR_{mod} values for some regions were outside the RSR range set by literature values. Therefore, based on data from on-field measurements and literature, values outside the expected RSR range were set to the upper or lower limit of the range. As a result, the summarized values used and presented in Table 11 have been filtered from the values that would not be very likely to be realistic. The used RPR and AP values, are shown in Table 9,Table 10 respectively. The above approach is necessary because the RPR and AP values can be unreliable if for example the productivity of the specific year's data does not represent the average.

Table 9: RPR values used for the analysis.

RPR (t_{DM}/t_{prod})		
OP	VP	OTP
0.35	0.5	0.8

Table 10: Production per surface area AP calculated from ELSTAT data.

	AP (t_{prod}/ha)			
	OP	**VP**	**OTP**	**Source**
ARGOLIDA	23.86	6.56	3.42	ELSTAT
ARKADIA	4.22	6.73	3.51	ELSTAT
ACHAIA	18.46	12.00	3.83	ELSTAT
KORINTHIA	7.26	9.68	0.77	ELSTAT
LAKONIA	16.33	7.68	4.33	ELSTAT
MESSINIA	8.70	15.20	6.64	ELSTAT
ILEIA	7.41	5.67	9.63	ELSTAT

Table 11: RSR_{mod} and RSR values used for the analysis.

	RSR (t_{DM}/ha)					
	OP	**VP**	**OTP**	**FORESCO**	**FORESBROAD**	**FORESMIXED**
ARGOLIDA						
ARGOS - MYKINES	5.60	3.28	2.73	0.76		0.95
EPIDAVROS	5.60	3.28	2.73	0.94	1.30	
ERMIONIDA	5.60	3.28	2.73	0.85	1.48	1.03
NAFPLIO	5.60	3.28	2.73	0.85		
ARKADIA						
VOREIA KYNOURIA	1.60	3.37	2.81	0.79	1.17	0.78
GORTYNIA	1.60	3.37	2.81	0.84	1.63	1.01
MEGALOPOLI	1.60	3.37	2.81	0.99	1.49	0.99
NOTIA KYNOURIA	1.60	3.37	2.81	0.83	1.21	0.82
TRIPOLI	1.60	3.37	2.81	0.83	1.42	1.15
ACHAIA						
AIGIALEIA	5.60	4.40	3.06	0.92	1.48	1.18
DYTIKI ACHAIA	5.60	4.40	3.06	1.08	1.61	1.31
ERYMANTHOS	5.60	4.40	3.06	0.89	1.48	1.11
KALAVRYTA	5.60	4.40	3.06	0.86	1.41	1.03
PATRA	5.60	4.40	3.06	0.86	1.48	1.21
KORINTHIA						
VELO - VOCHA	2.54	4.40	1.30	0.85		1.03
KORINTHOS	2.54	4.40	1.30	0.90		
LOUTRAKI - AGIOI THEODOROI	2.54	4.40	1.30	0.91		
NEMEA	2.54	4.40	1.30	0.85	1.48	
XYLOKASTRO - EVROSTINI	2.54	4.40	1.30	0.77	1.48	1.03
SIKYON	2.54	4.40	1.30	0.83	1.31	0.92
LAKONIA						
ANATOLIKI MANI	5.60	3.84	3.46	0.85	1.48	1.04
EVROTAS	5.60	3.84	3.46	0.78		1.15
MONEMVASIA	5.60	3.84	3.46	1.05		1.14

SPARTI	5.60	3.84	3.46	0.87	1.46	0.93
MESSINIA						
DYTIKI MANI	3.05	4.40	4.20	0.91	1.48	0.98
KALAMATA	3.05	4.40	4.20	0.89	1.50	1.09
MESSINI	3.05	4.40	4.20		1.48	1.03
OICHALIA	3.05	4.40	4.20		1.56	1.00
PYLOS - NESTOROS	3.05	4.40	4.20		1.70	1.07
TRIFYLIA	3.05	4.40	4.20	0.85	1.56	1.13
ILEIA						
ANDRAVIDA - KYLLINI	2.59	2.83	4.20	1.07	1.53	
ANDRITSAINA - KRESTENA	2.59	2.83	4.20	0.97	1.45	1.12
ARCHAIA OLYMPIA	2.59	2.83	4.20	0.87	1.45	1.27
ZACHARO	2.59	2.83	4.20			1.15
ILIDA	2.59	2.83	4.20	0.93	1.54	1.18
PINEIOS	2.59	2.83	4.20	0.93	1.48	
PYRGOS	2.59	2.83	4.20	1.53	1.48	1.18

The RSR_{mod} for prunings is the same for each regional unit because of the data available from ELSTAT being on a regional unit scale. The results seem to be in-line with factors known to affect pruning productivity per surface area. Regarding olive tree pruning productivity per surface area, the koroneiki olive tree specie is known for high pruning productivity and the regional unit known to have this specie in the Peloponnese is Messinia [34]. The available RSR data for the Lakonia regional unit indicate a range of 2-3.6 from 2 data points and a much larger range when on-field measurements from other locations in Greece where included. Data show a greater production for the Messinia and Ileia regional units, but a conservative cap was set for their RSR_{mod} a little above the Lakonia region and well within Greece's range. Moreover, the regional units known for their large-scale citrus trees cultivation have the highest pruning productivity per surface area for orchards, so probably an intensive cultivation can explain the higher surface area pruning productivity values. This factor does not fully explain the vineyard pruning productivity per surface area differences between regional units and more data are needed to find the root cause of these differences and the RSR_{mod} for vineyard prunings is capped to the lowest value used by the Biomasud project. Factors that could affect these results are local conditions, irrigated or rainfed cultivation, intensive cultivation or not and the targeted product of the cultivation which all affect pruning and product productivity. The values of Table 11 are well within the ranges of literature. The available potential is calculated with the availability factors presented in Table 12. From the available potential, the calculation of the technical potential follows with the consideration of harvesting efficiencies. The baseline for harvesting efficiencies set by the Biomasud project and the used values are presented in Table 13. The values used are in line with other literature data [52], [53].

Table 12: Availability constraints for each biomass type.

	Availability					
	OP	**VP**	**OTP**	**FORESCO**	**FORESBROAD**	**FORESMIXED**
ARGOLIDA						
ARGOS - MYKINES	0.8	0.8	0.8	0.571		0.512
EPIDAVROS	0.8	0.8	0.8	0.507	0.595	
ERMIONIDA	0.8	0.8	0.8	0.624	0.500	0.493
NAFPLIO	0.8	0.8	0.8	0.569		
ARKADIA						
VOREIA KYNOURIA	0.8	0.8	0.8	0.500	0.476	0.493
GORTYNIA	0.8	0.8	0.8	0.518	0.537	0.514
MEGALOPOLI	0.8	0.8	0.8	0.554	0.606	0.526
NOTIA KYNOURIA	0.8	0.8	0.8	0.530	0.500	0.387
TRIPOLI	0.8	0.8	0.8	0.518	0.499	0.555
ACHAIA						
AIGIALEIA	0.8	0.8	0.8	0.525	0.509	0.607
DYTIKI ACHAIA	0.8	0.8	0.8	0.918	0.266	0.219
ERYMANTHOS	0.8	0.8	0.8	0.593	0.346	0.579
KALAVRYTA	0.8	0.8	0.8	0.570	0.531	0.495
PATRA	0.8	0.8	0.8	0.496	0.518	0.500
KORINTHIA						
VELO - VOCHA	0.8	0.8	0.8	0.354		0.000
KORINTHOS	0.8	0.8	0.8	0.556		
LOUTRAKI - AGIOI THEODOROI	0.8	0.8	0.8	0.528		
NEMEA	0.8	0.8	0.8	0.353	0.476	
XYLOKASTRO - EVROSTINI	0.8	0.8	0.8	0.543	0.541	0.000
SIKYON	0.8	0.8	0.8	0.571	0.447	0.489
LAKONIA						
ANATOLIKI MANI	0.8	0.8	0.8	0.520	0.441	0.542
EVROTAS	0.8	0.8	0.8	0.580		0.496
MONEMVASIA	0.8	0.8	0.8	0.647		0.590
SPARTI	0.8	0.8	0.8	0.547	0.486	0.581
MESSINIA						
DYTIKI MANI	0.8	0.8	0.8	0.745	0.622	0.519
KALAMATA	0.8	0.8	0.8	0.592	0.528	0.573
MESSINI	0.8	0.8	0.8		0.500	0.458
OICHALIA	0.8	0.8	0.8		0.482	0.472
PYLOS - NESTOROS	0.8	0.8	0.8		0.549	0.532
TRIFYLIA	0.8	0.8	0.8	0.242	0.345	0.508

ILEIA						
ANDRAVIDA - KYLLINI	0.8	0.8	0.8	0.965	0.585	
ANDRITSAINA - KRESTENA	0.8	0.8	0.8	0.480	0.541	0.479
ARCHAIA OLYMPIA	0.8	0.8	0.8	0.706	0.654	0.520
ZACHARO	0.8	0.8	0.8			0.571
ILIDA	0.8	0.8	0.8	0.500	0.606	1.000
PINEIOS	0.8	0.8	0.8	1.000	0.605	
PYRGOS	0.8	0.8	0.8	0.616	0.500	0.568

Table 13: Harvesting efficiencies for each biomass type.

	Harvesting Efficiency (%)					
	OP	**VP**	**OTP**	**FORESCO**	**FORESBROAD**	**FORESMIXED**
Values from biomasud	75	70	94	60	60	60
Values used in this thesis	80	80	80	60	60	60

Together, the availability and harvesting efficiency factors amount to 36% of prunings to be used in alternative ways or being lost in the process which is thought to be high and should be considered in a specific region's pruning potential evaluation because these factors will vary locally. The technical potential is presented in Table 14.

Table 14: Calculated technical potential for each municipality of Peloponnese.

	Technical potential (t_{DM})					
	OP	**VP**	**OTP**	**FORESCO**	**FORESBROAD**	**FORESMIXED**
ARGOLIDA						
ARGOS - MYKINES	37667	613	18706	572		249
EPIDAVROS	2539		9726	284	237	
ERMIONIDA	695		11409	284	8	27
NAFPLIO	19303		4642	92		
ARKADIA						
VOREIA KYNOURIA	91		10193	704	622	274
GORTYNIA			5723	3496	678	1421
MEGALOPOLI			606	871	2239	326
NOTIA KYNOURIA			2435	1644	398	112
TRIPOLI		949	1428	3792	377	741
ACHAIA						
AIGIALEIA	14890	12324	13404	2786	133	392
DYTIKI ACHAIA	2017	1964	10365	494	175	37
ERYMANTHOS	90	108	3778	788	6	89
KALAVRYTA		4396	92	4334	1108	473
PATRA	3483	242	7111	183	81	357

KORINTHIA						
VELO - VOCHA	2557	14745	1912	89		0
KORINTHOS	3503	6157	7780	2421		
LOUTRAKI - AGIOI THEODOROI	190		656	2377		
NEMEA	4	12388	3124	55	17	
XYLOKASTRO - EVROSTINI	1924	8898	3654	1406	69	0
SIKYON	3352	10887	1689	2831	203	41
LAKONIA						
ANATOLIKI MANI	280		28013	21	62	310
EVROTAS	8449		31125	390		72
MONEMVASIA	2158		31858	412		188
SPARTI	10546	341	35022	3584	1223	464
MESSINIA						
DYTIKI MANI	447		8752	1171	161	210
KALAMATA	443		14896	586	3092	443
MESSINI			37254		20	648
OICHALIA			23711		1139	286
PYLOS - NESTOROS		71	35626		493	560
TRIFYLIA		224	41642	4	236	1118
ILEIA						
ANDRAVIDA - KYLLINI	673		4608	355	211	
ANDRITSAINA - KRESTENA	631	50	25069	45	121	409
ARCHAIA OLYMPIA	193		9040	636	1158	1696
ZACHARO			20336			140
ILIDA		2576	6453	15	324	58
PINEIOS	691	563	2513	40	41	
PYRGOS	669	2807	17470	79	49	41

As can be seen from Table 14 a large technical biomass potential exists in the whole Peloponnese region and locally some regional units and municipalities can support some biomass-based industries. Technical potential distribution is illustrated in Figure 4. The results until this part show great opportunities for the region and it is upon the local stakeholders to take actions and the state to support these actions.

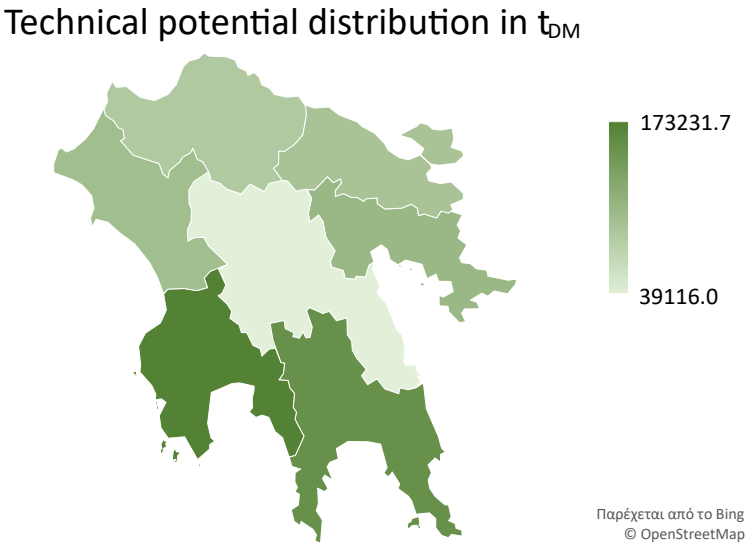

Figure 4: Technical potential distribution in the Peloponnese regional units.

Shown in Figure 5 is the technical potential calculated in this thesis compared to other available data of assessments conducted for the same biomass types in the Peloponnese region. The results vary significantly in certain biomass types which supports the initial hypothesis of this thesis, that the use of data not region specific introduces variability in the results. An example of this is in the S2Biom tool that most likely underestimates the OTP potential as the RSR value used for OTP is 1.3 while the range of RSR for OTP in the Peloponnese region from two on-field measurements available in [43] is 2-3.6 and even more is expected for the Messinia and Ileia regional units. The best way to maximize accuracy is to obtain on-field measurements, over many years and account for the factors that lead to different productivities. A way for safer investment in the pruning gathering and management and not as costly as large-scale assessments would be to focus on a smaller region and accurately estimate its potential securing the availability of resources for a biomass-based industry and expand to other biomass suppliers, steadily gathering relevant data and finally making better estimates for the entirety of the region.

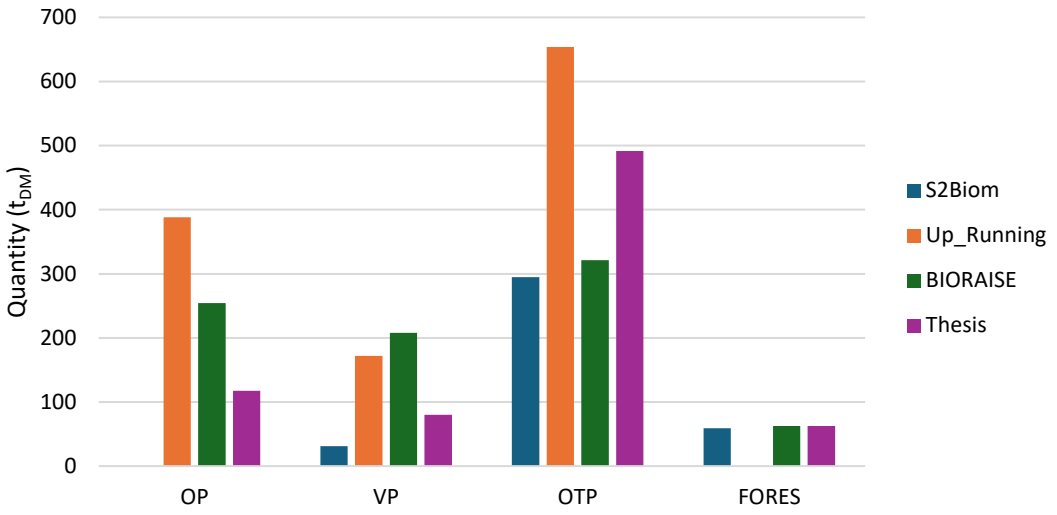

Figure 5: Cumulative technical potential of Peloponnese comparison of this analysis and literature [17], [54], [47].

Regarding the results of the analysis conducted in this thesis in terms of the technical potential, they are quite different, but within the margins of other assessments. For OTP which are the prominent biomass source in the region, the data vary a lot, but since region-specific data were used to filter out overestimates stemming from either the RPR value or the year's production data from ELSTAT, it is a well-supported estimate. Vineyard and orchard prunings are lower than other literature estimates, but still, they have enough potential to be used in the biomass market. Data regarding forest residues are available from only two sources and they are close in the estimate of their technical potential. Taking into account the abovementioned arguments it's safe to say that these results can be viewed with a significant degree of confidence and can be a benchmark for future work in developing a biomass industry in Peloponnese.

3.2.2.3 Market available potential estimation

The time frame considered for this estimation is 5-10 years and the assumed values of biomass mobilization percentage for this time frame are presented in Table 15. Prunings are the most promising in terms of mobilization as a supply chain can easily be formed around them. It is as simple as having the equipment and labor to get the prunings at roadside and loading them in trucks for transportation. The mobilization rate is assumed here to be 50% for prunings and 20% for forest residue. This will be heavily influenced by the policy measures the Greek state will enforce. If for example it is deemed necessary the following years to enforce a ban on burning the prunings, the farmers will mobilize close to 100% of the technical potential. The same is for forest management used to prevent forest wildfires in Greece which have become an issue. A ramp-up of the forest residue mobilization is unlikely in the next 5-10 years, but the future is uncertain. The mobilization of 20% of the technical potential is possible within this time frame if the current plans are successful and possibly become more intense the coming years, which seems to be the case due to both EU and Greece's policy striving for forest management.

Table 15: Mobilization rate of each biomass type in 10-year time.

Mobilization rate (%)					
OP	**VP**	**OTP**	**FORESCO**	**FORESBROAD**	**FORESMIXED**
50	50	50	20	20	20

3.2.2.4 Feedstock distribution

Figure 6 shows the center of mass for each of the biomass types for each municipality. The coordinates are presented in annex I for each municipality and biomass source in longitude and latitude format of WGS84.

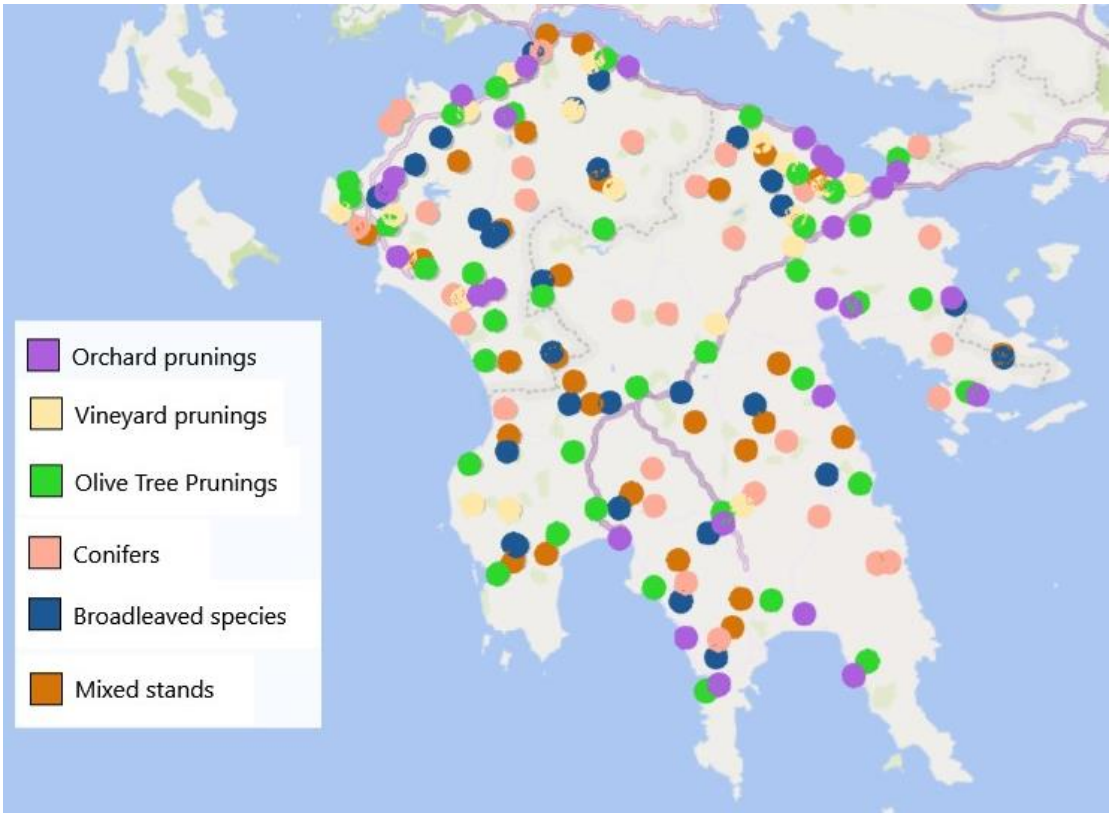

Figure 6: Center of mass nodes used for feedstock distribution.

3.2.2.5 Harvesting cost estimation

Table 16 shows the costs that were included in the harvesting cost estimation. Harvesting of prunings is studied in many regions and especially those of VP and OTP have been studied in Greece as well [18], [26]. For orchard prunings no study for Greece was found, so a conservative estimate was used. For the forest residue, in addition to literature data, two sources from state pricing were used, because forest residue harvesting in the region is probably not the same with others. The region's intricacies regarding the terrain and the underdeveloped road network were considered important enough for a more relevant pricing than the available ones from the literature to be used. The two state pricing sources are one state funded logging activities pricing catalogue and state pricing of forest products.

Table 16: Harvesting cost literature data.

Harvesting cost (€/t_{DM})						
OP	**VP**	**OTP**	**FORESCO**	**FORESBROAD**	**FORESMIXED**	**Reference**
30.53	37.79	37.79	51.38	66.35	61.43	[23]
50	47	38				[55]
						[50]
	55-65					[56]
	55.55	68.63				[57]
		46-62.3				[26]
			67.83	56.00		[58]
			87.80	80.57		[59]
			53.26	45.79	48.39	[47]
	50	50	70	70	70	[18]
		40				[42]

A conservative approach was followed for harvesting costs estimation and an average cost from literature was used because the lowest cost estimates are probably not attainable in a difficult case study such as the Peloponnese region. Even if they were attained in certain locations, the scale of the plant requires great amounts of biomass which will be harvested under more difficult conditions and counterbalance the differences. The higher cost estimates are unrealistic as well, because in the scenario of a biomass supply chain, learning effects start to act, reducing harvesting costs through higher productivity and efficiency. For harvesting of orchard prunings, which are mainly citrus trees, the highest value and close to that for OTP harvesting was used. For vineyard prunings a value close to OP and OTP and within the literature range was chosen. For OTP, because data were available from several studies, the projection of harvesting cost was used from [26] when learning effects are included. Harvesting cost of forest residue is difficult to estimate in the region, but according to data from the BIORAISE platform that incorporated cost increase due to the slope of local terrain and those from state pricing a good estimate is given. From the cost comparison of the two main sources, it was observed that state pricing was in line with the highest costs given by the BIORAISE platform and in line with prices for CHP plants reported in [60] and with the value of 65 €/t_{DM} for pine forest residue in East Europe and the range of 25-80 €/t_{DM} reported in [61].

The estimated values for harvesting costs are shown in Table 17.

Table 17: Harvesting costs used in the analysis and derived from literature data.

Harvesting cost (€/t_{DM})					
OP	**VP**	**OTP**	**FORESCO**	**FORESBROAD**	**FORESMIXED**
50	50	46	67	56	61

3.2.2.6 Transportation cost estimation

In the project AGROinLOG the value 0.13 €/tonne/km was used and chosen for this thesis, in-line with other values reported in literature for truck transportation and the assumed value in the CLARA project of 0.10 €/tonne/km for pine forest residue pellets considering the lower density of prunings [61]. The methodology used for feedstock distribution might cause an underestimation of the transportation distance within the same municipality. This is because the center of mass for the biomass source might be close to the destination. The minimum value set for travel distance was 20km because even if the actual average distance is lower than that, in reality a higher price for close distance transportation is set thus increasing the cost of transport. Biomass transport is done either directly to the processing plant or it is first transported to one of the two pre-treatment facilities and then to the processing plant. The coordinates of the hypothetical sites for the plant and the pre-treatment facilities are given in Table 18 in WGS84 format.

Table 18: Coordinates of the processing plant and intermediate pre-treatment facilities.

	Longitude	**Latitude**
Processing Plant	23.024717	37.92559
Lakonia Pre-treatment facility	22.147386	37.38535
Achaia Pre-treatment facility	22.077765	38.23688

3.2.2.7 Case available potential estimation and Cost-supply curve

From the market available potential, a part will go to competing uses while the rest will be available for the processing plant. From the case available potential, cost-supply curves are constructed for the two considered cases, with or without the intermediate biomass pre-treatment facilities.

Several market share cases are considered for each of the two cases. These values are in Table 19 - Table 22 and are the same for both cases to allow for direct comparisons. The title of each market share case is for the maximum market share attained in a regional unit. It was assumed that higher market share is attainable in the closer regional units.

Table 19: Case with a maximum market share of 20%.

Market share (20%)						
	OP	**VP**	**OTP**	**FORESCO**	**FORESBROAD**	**FORESMIXED**
ARGOLIDA	0.2	0.2	0.2	0.2	0.2	0.2
ARKADIA	0.2	0.2	0.2	0.2	0.2	0.2
ACHAIA	0.2	0.2	0.2	0.2	0.2	0.2
KORINTHIA	0.2	0.2	0.2	0.2	0.2	0.2
LAKONIA	0.2	0.2	0.2	0.2	0.2	0.2
MESSINIA	0.2	0.2	0.2	0.2	0.2	0.2
ILEIA	0.2	0.2	0.2	0.2	0.2	0.2

Table 20: Case with a maximum market share of 30%.

Market share (30%)						
	OP	**VP**	**OTP**	**FORESCO**	**FORESBROAD**	**FORESMIXED**
ARGOLIDA	0.30	0.30	0.30	0.30	0.30	0.30
ARKADIA	0.25	0.25	0.25	0.25	0.25	0.25
ACHAIA	0.25	0.25	0.25	0.25	0.25	0.25
KORINTHIA	0.30	0.30	0.30	0.30	0.30	0.30
LAKONIA	0.15	0.15	0.15	0.15	0.15	0.15
MESSINIA	0.15	0.15	0.15	0.15	0.15	0.15
ILEIA	0.15	0.15	0.15	0.15	0.15	0.15

Table 21: Case with a maximum market share of 40%.

Market share (40%)						
	OP	**VP**	**OTP**	**FORESCO**	**FORESBROAD**	**FORESMIXED**
ARGOLIDA	0.40	0.40	0.40	0.40	0.40	0.40
ARKADIA	0.35	0.35	0.35	0.35	0.35	0.35
ACHAIA	0.35	0.35	0.35	0.35	0.35	0.35
KORINTHIA	0.40	0.40	0.40	0.40	0.40	0.40
LAKONIA	0.20	0.20	0.20	0.20	0.20	0.20
MESSINIA	0.15	0.15	0.15	0.15	0.15	0.15
ILEIA	0.15	0.15	0.15	0.15	0.15	0.15

Table 22: Case with a maximum market share of 50%.

Market share (50%)						
	OP	**VP**	**OTP**	**FORESCO**	**FORESBROAD**	**FORESMIXED**
ARGOLIDA	0.50	0.50	0.50	0.50	0.50	0.50
ARKADIA	0.45	0.45	0.45	0.45	0.45	0.45
ACHAIA	0.45	0.45	0.45	0.45	0.45	0.45
KORINTHIA	0.50	0.50	0.50	0.50	0.50	0.50
LAKONIA	0.30	0.30	0.30	0.30	0.30	0.30
MESSINIA	0.30	0.30	0.30	0.30	0.30	0.30
ILEIA	0.15	0.15	0.15	0.15	0.15	0.15

The cost-supply curves are shown in Figure 7, Figure 8 for cases 1 and 2, with and without an intermediate pre-treatment facility, respectively. The different curves for each case, represent the forementioned market shares. The name of each curve corresponds to the previously specified market share cases.

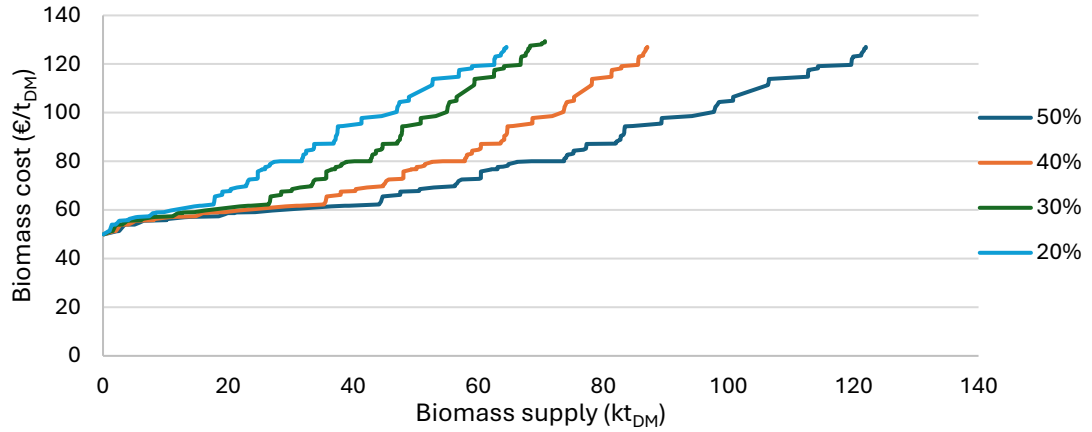

Figure 7: Cost-supply curve for case 1 and its corresponding market share cases.

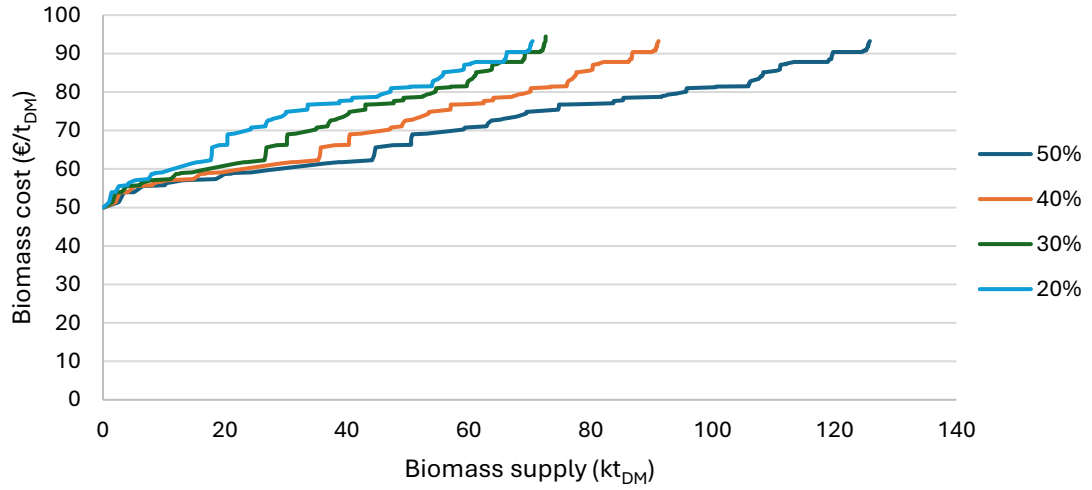

Figure 8: Cost-supply curve for case 2 and its corresponding market share cases.

The cost-supply curves when an intermediate pre-treatment facility is not considered seem to be more stable at 20-40kt of biomass supply with a steady, sharp cost increase from then on. In other words, for higher capacity biomass plants there would need to exist significant benefits, since increasing capacity will mean higher average cost of biomass. The case with a higher local market share shows that a 50kt$_{DM}$ supply is possible at around the same cost that of a 30kt$_{DM}$ supply case when a lower local market share is assumed. This shows the importance of aiming for the increase of local market share when developing a business plan as this biomass will be more economical and can significantly lower the average price of supplied biomass.

In the second case, two intermediate pre-treatment facilities are used to gather the distant biomass sources at a lower cost due to transportation cost decrease. The cost-supply curves are in this case less sharp and the average cost of biomass supply decreases. The supply of 70kt$_{DM}$ of biomass is now reasonable even under the harshest conditions and a 100kt$_{DM}$ biomass supply in this case is likely to be economically feasible allowing for economy of scale to take effect. An intermediate pre-treatment facility will allow for more biomass to be procured at approximately the same average price since the graph of the cost-supply curve is less steep than the cost-supply curve when a pre-treatment facility is not considered. The variability of the average cost of biomass supply can show how vulnerable the processing plant is in terms of feedstock cost. The average biomass supply cost is calculated for the case of 70kt annual biomass supply and shown in Table 23.

Table 23: Average cost of supply of 70kt biomass annually.

Supply 70kt$_{DM}$ of biomass

			Average cost (€/t$_{DM}$)	
Market share case	**Total market share**	**Market share utilization**	**Without**	**With**
20%	20%	98%	89.46	74.06
30%	20.6%	95%	80.66	**70.31***
40%	25.8%	76%	68.37	65.99
50%	35.6%	55%	64.66	62.75

*Chosen as the base price for biomass in the technoeconomic assessment.

Table 23 and Figure 9 show the importance of having intermediate pre-treatment facilities as they can significantly lower long-distance transportation costs and therefore the average cost of biomass supply decreases. Also, it shows that the average cost is not greatly affected from intermediate processing facilities, if a large local market share is achieved, further establishing the importance of the business plan to revolve around this target.

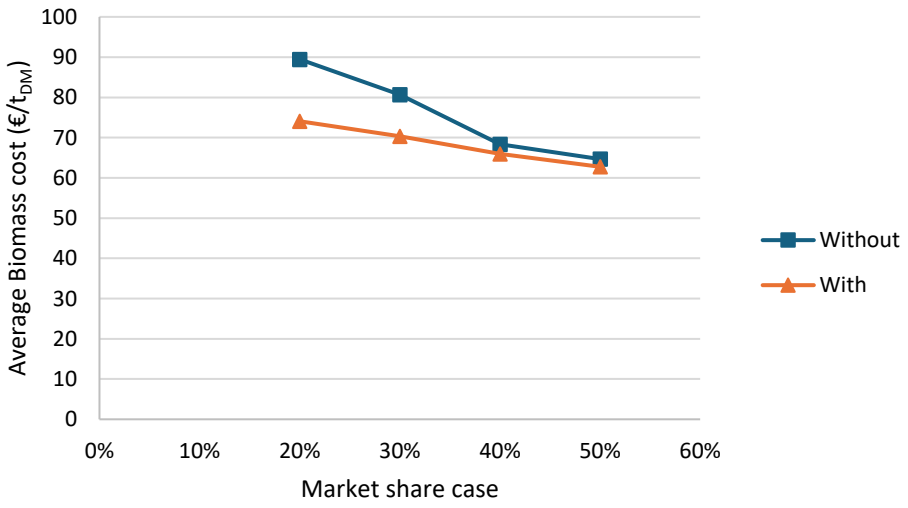

Figure 9: Average cost of 70kt DM biomass with and without intermediate processing facilities.

System marginal price

The system marginal price (SMP) is largely used in electricity pricing, but its concept can also be used to know the worst-case biomass market scenario. This method has not been encountered in the literature, so it is developed for the first time, to the knowledge of the author, for the biomass sector.

Similar to electricity production it is assumed that the price of biomass will be the break-even price for its harvesting and transportation. This will be true until biomass becomes a commodity with high demand, and farmers or other suppliers will try to sell it above the break-even cost. In a negotiation scenario, the consumer, in this case the plant, will negotiate with the biomass suppliers on the biomass supply cost. The suppliers will seek to maximize their profit. In a market setting, the biomass suppliers will try to sell to the one that will buy from them at the highest price. As a result, the cost-supply curve for the consumer negotiating will be shifted towards the more expensive biomass sources when the cheaper sources are sold to another consumer.

Assuming the market share that the plant is able to secure will fill the knowledge gap about the demand from competitors, their location and the break-even biomass price of biomass for their use, that would be needed to calculate the SMP. The market share scenarios were built upon the assumption that locally, because the transportation costs are lower, the plant will be able to pay a slightly higher price to the biomass supplier compared to a competitor at a greater distance. Basically, the SMP in a real application, is calculated based on market dynamics and the market share attained by the consumer is a result of market dynamics. A sensitivity analysis in which regional unit's market share is assumed will reveal the different SMP of biomass supply under various market dynamics.

In Table 24 the SMP is shown for the two cases, with and without intermediate processing facilities. When local market share is low, thus transport distance increases, a great decrease in the system marginal price is observed when intermediate pre-treatment facilities are used. Their benefit is lower when a larger local market share is achieved, because SMP depends on the cost of the last unit of biomass that needs to be transported to the processing plant. The last unit will be cheaper at a higher local market share under the same biomass supply demand.

Table 24: System marginal price for the supply of 70kt biomass annually.

	SMP (€/t_{DM})	
Market share case (%)	**Without**	**With**
20%	130.94	90.65
30%	128.08	90.40
40%	97.80	80.07
50%	80.09	74.87

3.3 Discussion and considerations

Bioenergy will play a significant role in Greece's plan to achieve energy security and the green transition. Many biomass sources will be utilized towards these goals and each region should emphasize its efforts to support its most promising biomass sources. Biomass source selection can be a complicated process, but a framework has been used to comparatively assess different feedstocks that provides the basic criteria that should be considered. The Peloponnese region has rich biomass potential in prunings and forest residues. Sustainable management of resources is an important concept for all sectors, but especially for the biomass sector because otherwise biodiversity and the region's ecosystems will be affected. All selected feedstocks fulfil the feedstock selection criteria and are thus suitable to be used in the bio-based industry. These sources can be used complementary to one another allowing for greater processing plant flexibility which increases investment security. Together, they can support small to medium scale processing plants and even large scale, if a central location in the Peloponnese is chosen and a high market share achieved.

The development of stable supply chains utilizing these easy to mobilize biomass sources is a good first step as it, will help stakeholders that are already involved in the bioeconomy, to mobilize other, of lower quantity biomass sources. It is important to understand why the stakeholders have yet to take sufficient action to achieve large-scale utilization of biomass in the region. The cumulative technical potential in Peloponnese, under harsh availability and sustainability conditions, is 752.3 kt_{DM} and well distributed in the regional units. If more biomass sources are included such as industrial and household waste, or other agricultural residue, it is clear that a biomass-based industry is feasible in terms of quantities.

As already mentioned, the rough terrain and the underdeveloped road network hinder long-distance travel as the associated costs will be too high. Also, the economic crisis led to outdated equipment and lack of capital to invest in new equipment. Nowadays, high interest rates and inflation made it more difficult for loans to be given to the stakeholders, a situation that is expected to continue for the coming years. To battle this, financial tools should become available to the stakeholders that want to invest in new equipment or somehow give them access to better equipment. It would be of great benefit if large cooperatives can be formed because then, collaboration becomes easier between stakeholders, and they can be better informed for best practices and opportunities. Also, small farmers can form groups to share large machinery, when possible, reducing individual capital cost for equipment. All these actions will help the stakeholders be ready when the opportunity to utilize the biomass potential is presented.

The biomass potential distribution reveals the prospect of some municipalities being able to easily sustain small to medium scale biomass industries in their region. The

biomass potential is dispersed, so decentralized pre-treatment facilities can significantly reduce the cost of transport making long-distance transportation feasible and thus large-scale processing plants can be developed. Special focus should be given in Messinia and Lakonia regional units as they have very large technical potential, mostly coming from OTP. A more centralized, in relation to the biomass sources, location inside Arkadia might be a better solution to the problem of biomass potential being distributed across regional units. It would, under conditions, even allow for large-scale biomass processing plants at low costs.

The product of the processing plant proposed by this thesis will be given to a refinery for further processing. The Korinthia regional unit was chosen as the location of the plant because “Motor Oil Hellas” operates a refinery in the same area and there is an industrial zone able to house such a processing plant with access to the sea and near large cities providing the necessary personnel. Feedstock availability in the region, even under harsh competition, is sufficient for a medium-to-large scale plant at an expected average price ranging from 62.75 to 74.06 €/t_{DM} and if a system marginal price approach is assumed the price range is 74.87 to 90.65 €/t_{DM}. Thesefore, prices in the range of 3.6 to 5.5€/GJ with an average LHV d.b. of 17.5 MJ/kg. This analysis on biomass potential distribution and feedstock security in the Peloponnese region provides a clearer picture on the prospects for the region to harbor a biomass industry. When this feedstock distribution is coupled to the cost estimates, it makes possible for the significant risk regarding the price range at which the biomass will become available to be evaluated. The results of the analysis conducted in this chapter can be used as a basis to develop a process scheme for advanced biofuels production and perform the technoeconomic analysis for the proposed processing plant. The average cost of biomass supply for the plant’s hypothetical location and 70kt_{DM} capacity is 70.31€/t_{DM}.

4. Process integration and simulation of the biorefinery plant

There are several routes for biomass conversion into useful energy (heat and power), biofuels, biomaterials or products. Significant progress has been made in the last decades towards biomass valorization into other than heat and power, but the main drawback of many processing schemes is that they require large scale plants in order to be economically viable. To acquire the necessary amounts of biomass for the yearly operation of large-scale plants, favorable conditions are needed, and it is possible only in few regions. As shown in chapter 3, the Peloponnese region is likely to be able to safely support a medium-scale bioprocessing plant with annual biomass supply around 70kt. Conversion routes with high capital investment are not feasible in this scale as the low operational cost will not be exploited to the necessary degree for profitable operation. Therefore, the main goal of this chapter is to propose a processing scheme suitable for small to medium-scale processing plants. The angle is to use promising, low-cost, feedstock flexible and demonstrated technologies. This way improving economics in medium scales and mitigating feedstock related risks.

The proposed processing scheme employs three promising technologies. In particular, biomass is gasified via a thermochemical route known as chemical looping gasification (CLG) producing a high-quality syngas. Syngas cleaning is done using low-cost technologies suitable for medium to small scales and more specifically, oil-based gas washing (OLGA) for heavy tar removal, that benefits the use of activated carbon beds for removing lighter tars, such as BTX. The third promising technology is Fischer-Tropsch synthesis (FTs) without upstream removal of CO_2 from the syngas. The employed Fischer-Tropsch (FT) reactor and catalyst favors the reactions for both CO and CO_2 therefore the removal of CO_2 via a cost and energy intensive Acid Gas Removal (AGR) unit is now undesirable and more carbon is available for utilization.

In this chapter it will be firstly explained how each step of the chosen processing scheme works and then the process modelling using Aspen Plus™[62] software. The results about the proposed processing scheme will be based on the developed model as will the technoeconomic analysis in the chapter 5.

The main goals of this chapter are summarized in the following:

- Develop and validate a simple model for chemical looping gasification.
- Configure a suitable route for the syngas cleaning step.
- Model syngas upgrading via Fischer-Tropsch synthesis.
- Evaluate each process step and the whole processing scheme by means of mass and energy balance calculations.

4.1 Brief description of the processing plant layout

The layout of the biomass processing plant is depicted in Figure 10. Biomass reaches the plant's gate either already dried and chipped in which case it goes to storage, or in raw form, in which case it is pilled awaiting an initial sorting and pre-treatment before being stored in the plant's storage facilities. The thermochemical conversion of biomass via gasification will be done in a fluidized bed which is capable of handling many feedstocks while yielding a high carbon conversion and overall process efficiency [63]. However, further pre-treatment is needed prior to the feedstock entering the gasifier, which aims to lower the moisture content and particle size distribution to facilitate the gasification process. Following is the gasification process, but it is discussed in more detail in the respective part of the chapter. In the gasifier, a high-quality syngas is produced and undergoes gas cleaning which aims to remove the particulate matter exiting the gasifier with the syngas and other unwanted compounds. Particulate matter is removed by a hot gas ceramic filter. Prior to the filter, the syngas is cooled down to filter temperature and after that, the syngas is further cooled down to OLGA process temperature which is employed for the removal of tars and BTX. The syngas exiting OLGA is cooled during the process thus exiting the OLGA unit slightly above water dew point. The removed tars are recovered and recirculated to the gasification unit. After the OLGA unit, syngas is further cooled to remove syngas moisture and is lead to four (two operating at a time) activated carbon beds for the complete heavy tar and BTX removal while H_2S is also removed. The prior syngas cooling brings the temperature down to the operating temperature of the carbon beds. Syngas is heated up to the hydrolysis reactor temperature which is used to convert HCN and COS to NH_3 and H_2S respectively. For the last cleaning steps, a two-stage water scrubber is used to remove NH_3, HCl. Then, a smaller activated carbon bed is used before the syngas is heated up to the temperature of the warm guard bed which consists of two beds. The first is a ZnO bed to ensure the final polishing, and the second bed has a deoxygenation catalyst for removal of O_2 present in the syngas from an air injection. The three beds act as a final polishing step for the syngas to meet the specifications of the FTs.

A heat recovery steam generation (HRSG) system is used to recuperate heat from the cooling down of process streams providing it to the process streams that need to be heated while producing medium pressure and high temperature steam to be expanded in turbines for electricity production. It is the aim of this system to recover enough heat for the plant to achieve self-sufficiency of both heat and electricity demand.

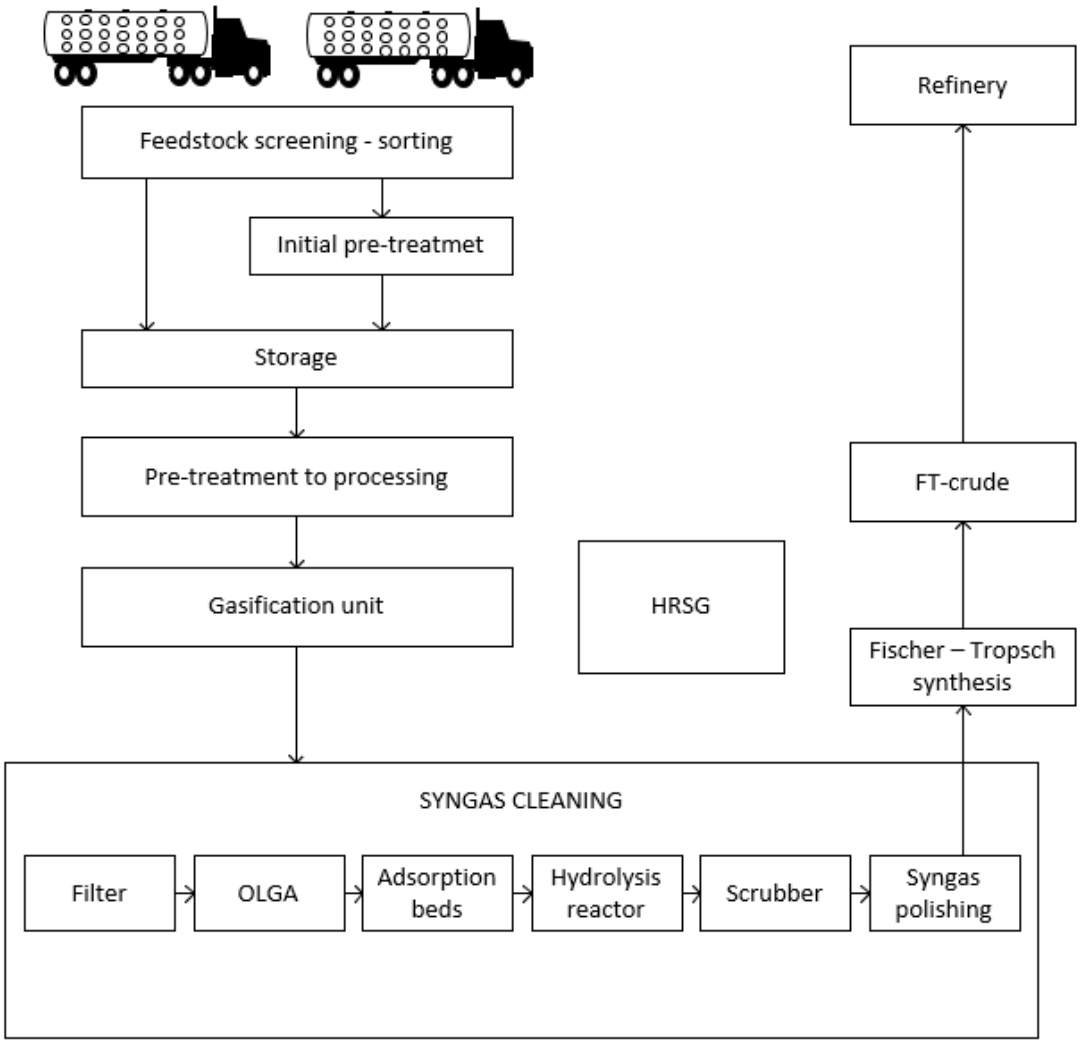

Figure 10: Biomass processing plant layout.

The proposed plant layout is suitable for the lignocellulosic biomass types investigated in chapter 3. However, it is capable of handling additional biomass types, even dirtier feedstocks such as wastes (SRF or RDF). The gasifier has operational flexibility when sufficient pre-treatment is done, and the downstream cleaning and fuel synthesis processes are able to handle the different syngas composition as long as certain specifications are met.

4.2 Process description

4.2.1 Initial Pre-treatment and storage

Biomass can arrive pre-treated from an intermediate pre-treatment facility in which case it will be ready for storage, or it can arrive with minimal to no pre-treatment, depending on the harvesting scheme employed, therefore requiring some additional steps before storage. The initial pre-treatment typically involves sorting, size reduction and drying of biomass which improves storage efficiency and prepares the biomass for further treatment, before entering the process. Investing in a good storage solution

lowers the associated storage costs, e.g., decrease space requirements and controls used to monitor storage conditions. Furthermore, it will enhance the efficiency and lower the cost of the downstream processes by feeding a higher quality feedstock. The initial pre-treatment can counterbalance the associated cost by the following steps being more efficient, e.g., more efficient drying process as a result of the smaller particle size. Size reduction can be done by chipping equipment to reduce particle size to less than 6cm and moisture content can reach 20% by natural air drying [64]. Moisture must not be too low because during storage, low moisture containing biomass can auto-ignite due to the biological activity, and control methods are needed to regulate the storage conditions.

4.2.2 Pre-treatment to processing

The additional pre-treatment needed to ensure smooth and efficient operation of the gasifier involves the further size reduction and drying [65]. Moisture removal is accomplished with a belt dryer to increase energy density of biomass and gasification efficiency however alternative and more efficient drying methods exist and can be used. Fuel particle size is limited by the feeding system to 7-10 cm [66] which is mostly covered by the initial pre-treatment chipping, however a grinder is used to achieve a desirable particle size of approximately less than 6mm. Alternative methods available are discussed in [67] that can reduce particle size up to 0.2 mm.

4.2.3 Feeding system

Biomass is fed into the gasifier operating at atmospheric pressure with a feeding screw. A sweep gas is used to inert feeding and the system operates at ambient pressure, thus the high amounts of pressurization gases, relative to feed input, are avoided. Power consumption of the feeding screw is 7 kJ/kg of dry biomass [68].

4.2.4 Chemical Looping Gasification

The gasification of biomass for syngas production can be carried out using various established technologies. The aim of a gasification system is to produce a high-calorific value syngas with few undesired compounds, that must be removed via gas cleaning to produce a syngas appropriate for a coupled downstream process technology that upgrades it to e.g., biofuels or biochemicals. To achieve a high-calorific value syngas, pure oxygen or steam have been used to gasify biomass without diluting the produced syngas with inert N_2 or to avoid excessive oxidation of the syngas. Another concept that has lately been established is the looping of bed material to the gasifier with the aim to transfer the necessary heat and or oxygen to sustain the overall endothermic gasification reactions [69]. The case in which only heat is transferred to the gasifier refers to dual fluidized bed gasification (DFBG) and if heat and oxygen are transferred via the circulating bed material, then it is CLG. The concept of CLG is similar to the established DFBG with the difference being that CLG uses as bed material a metal oxide undergoing reduction-oxidation (redox) cycles between two reactors providing both

heat and oxygen to the gasifier. The metal oxide in CLG is referred to as an oxygen carrier (OC). In DFBG, unconverted char from the fuel reactor (FR) is transferred to the oxidizer to be combusted, thus generating the necessary heat that the bed material e.g., sand, transfers to the FR, but leading to substantial CO_2 emissions [63]. During CLG, in the FR, biomass reacts with the oxidized OC, leading to partial oxidation of the biomass and reduction of the OC. The reduced OC is then transferred to the air reactor (AR), where it is re-oxidized with air, generating heat that is subsequently transferred back to the FR to sustain the endothermic gasification reactions. Some char from the fuel reactor can slip to the AR with the oxygen carrier and be combusted therefore some CO_2 emissions can occur from the AR. Increasing char conversion by increasing temperature and residence time minimizes the effect. Carbon slip is not considered to be an issue in the case of low fixed carbon containing biomass [63]. Additional CO_2 emissions occur from recirculation of combustible compounds to the AR.

The reactions of the OC taking place in the AR and FR are R. 1 and R. 2 respectively.

$$\text{AR: } 2Me_xO_{y-1} + O_2 \rightarrow 2Me_xO_y \qquad R.\ 1$$

$$\text{FR: } Fuel + Me_xO_y \rightarrow CO + H_2 + CO_2 + H_2O + CH_4 + C_zH_a + Tars + Me_xO_{y-1} \qquad R.\ 2$$

The loop of OC between AR and FR provides the necessary heat and oxygen for the gasification process without fuel and air mixing. Thus, N_2 dilution of the produced syngas is avoided that would lead to a low heating value of gas, 4-7 MJ/m_n^3 [70], or expensive and energy intensive equipment to separate oxygen from air in order to supply pure oxygen to the gasifier.

CLG has been demonstrated at many scales with the highest being a 1 MW_{th} pilot plant in [71] and the results are promising for future industrial applications. The pilot test showed great carbon conversion efficiency that could reach nearly 100% and very low gravimetric tar content, even less than 1 g/Nm^3. The operating conditions of CLG are very important in determining syngas composition as the oxidizing environment created in the FR by the OC circulation coupled with the heat transfer and the possible catalytic effects of the circulating bed material significantly affects tar yield and oxidation degree of the fuel.

The reactor types available for gasification vary in their operation, allowing feedstocks with different characteristics to be gasified. The main types of gasifiers are three, i.e., fixed bed reactor, entrained flow and fluidized bed reactor operating either at the superficial fluidization velocity or at higher superficial velocities, thus entering the bubbling, turbulent or fast regimes. For CLG, fluidized bed reactors have been predominantly used, because they show uniform temperature distribution, more effective mixing and higher heat and mass transfer enhancing gasification reactions

and being especially suitable for CLG. Fluidization of the AR and FR is done by air and steam or CO_2 respectively. A simple schematic is shown in Figure 11.

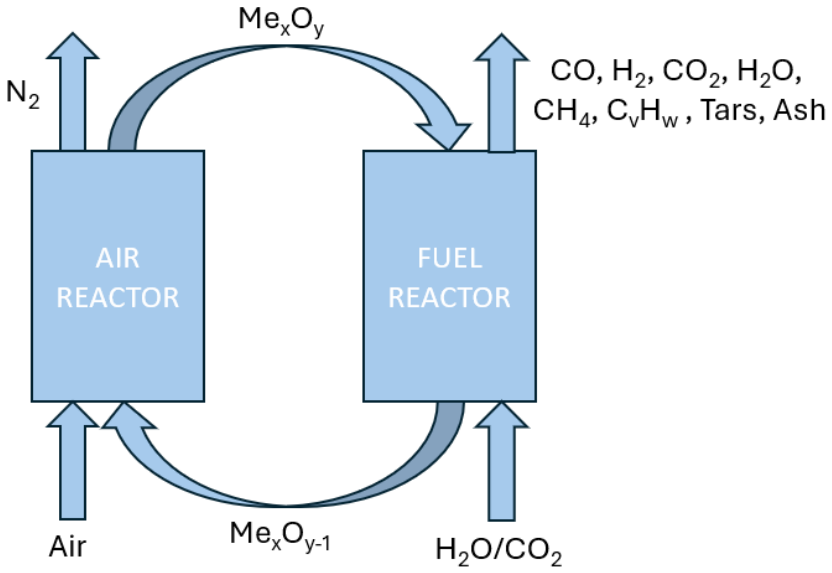

Figure 11: Simple schematic of CLG operation.

The configuration of a CLG unit comprises of two reactors, two cyclones for gas-solid separation and two loop seals in addition to a J-valve which are responsible for the control of solid circulation between the reactors. The seals and the J-valve are also fluidized using N_2 or CO_2. This configuration was used for the 1 MW_{th} scale pilot test [71] while other designs have also been used in smaller scale pilot tests.

The OC is circulated from the AR operating as a fast fluidized bed (riser), through a cyclone that separates oxygen depleted air and some off gases that come from the AR. The loop seal with the J-Valve control the OC that is directed to the FR. The temperature of the AR is sufficiently higher than in the FR to ensure enough heat transfer occurs between the AR and FR without excessively increasing the OC circulation. Partial oxidation of the fuel due to the lattice oxygen provided by the OC also occurs in the FR to further compensate the globally endothermic reactions of gasification and creating an oxidizing atmosphere facilitating the breakdown of tars. If uncontrolled the oxidizing atmosphere can lead to high extent of fuel oxidation. The FR can operate as a turbulent fluidized bed, similar to the pilot scale experiments or as a circulating fluidized bed.

Oxygen carriers

There are many options for OCs, differing in reactivity, oxygen transport capacity (OTC), but most importantly there are market and environmental considerations that follow each OC. In the CLG unit of this thesis, ilmenite will be used as an OC. An OC can have multiple uses in a CLG unit because it allows for example catalytic effects on tar cracking which is the case observed for ilmenite [63]. Some mineral elements in OCs

have been observed to catalyze gasification due to enhanced char and tar cracking [72] and OCs can reduce tar formation during CLG [73]. Many OCs have been studied in [73] and the use of Fe-based OCs seems to be a suitable choice for CLG units, if the technical disadvantages of agglomeration, low reactivity, low OTC and circulation rate are dealt with. Ilmenite has been used successfully as an OC in many pilot tests up to 1 MW_{th} and the forementioned issues have been dealt with. The advantages of Fe-based OCs compared to other available OCs i.e., being non-toxic and environmentally friendly while being cheap, make them a very suitable choice for the developed CLG unit.

Ilmenite is a natural mineral mainly composed of $FeTiO_3$ and is the reduced form of the OC with its oxidized form being pseudobrookite (Fe_2TiO_5) [74]. However, when ilmenite is used, it is not pure [75] and has an amount of hematite (Fe_2O_3) which will also take part in oxygen transfer. Hematite is the oxidized form and is reduced to magnetite (Fe_3O_4). Magnetite can be further reduced to FeO and Fe which would lead to higher OTC values, but due to thermodynamic limitation, it cannot be reduced further in this case [74], [76]. OTC is calculated according to Eq. 8 and is the ratio of the mass difference between the oxidized and reduced states and the mass of the oxidized state. The OTC of Fe-based OCs is relatively low and for the redox couples that are considered for ilmenite, i.e., Fe_2TiO_5/ $FeTiO_3$ and Fe_2O_3/ Fe_3O_4 it is 5% and 3.4% respectively.

$$OTC = \frac{m_{ox} - m_{red}}{m_{ox}} \qquad \textit{Eq. 8}$$

The low OTC will not be a problem in CLG applications as the limiting factor is adequate heat transfer which needs large amounts of OC circulation, so even at very low OTC values, sufficient oxygen will be transported to the FR. During continuous operation and make-up feeding of OC, the OTC of the OC is stabilized between 2.7-3.2% [77]. A question arises about how the catalytic effects of the OC change with the changing physical and chemical characteristics of the OC during CLG operation. Ilmenite is expected to have a lifetime greater than 300h and the OC will be replaced if attrition, agglomeration, deactivation or ash sluicing occurs [77]. OCs can either directly react with the fuel or release oxygen which is called oxygen uncoupling. The OCs that do oxygen uncoupling are not suitable for CLG [63].

The reduction reactions of pseudobrookite and hematite for the oxidation of main syngas species are R. 3 - R. 9.

$$4Fe_2TiO_5 + 4TiO_2 + CH_4 \rightarrow 8FeTiO_3 + CO_2 + 2H_2O \qquad \textit{R. 3}$$

$$Fe_2TiO_5 + TiO_2 + CO \rightarrow 2FeTiO_3 + CO_2 \qquad \textit{R. 4}$$

$$Fe_2TiO_5 + TiO_2 + H_2 \rightarrow 2FeTiO_3 + H_2O \qquad \textit{R. 5}$$

$$12Fe_2O_3 + CH_4 \rightarrow 8Fe_3O_4 + CO_2 + 2H_2O \qquad \textit{R. 6}$$

$$3Fe_2O_3 + CO \rightarrow 2Fe_3O_4 + CO_2 \quad \text{R. 7}$$

$$3Fe_2O_3 + H_2 \rightarrow 2Fe_3O_4 + H_2O \quad \text{R. 8}$$

$$4\,FeTiO_3 + O_2 \rightarrow 2Fe_2TiO_5 + 2TiO_2 \quad \text{R. 9}$$

The oxidation reactions of the reduced forms are R. 10 and R. 11 respectively.

$$4Fe_3O_4 + O_2 \rightarrow 6Fe_2O_3 \quad \text{R. 10}$$

$$\text{R. 11}$$

Issues to be addressed

Apart from the issues already addressed and having established that ilmenite has many advantages when compared to other available OCs, some other issues should be considered. In particular, carbon deposition and deactivation phenomena were not observed to be feedstock related during the large-scale pilot plant [77]. Also, the use of herbaceous or agricultural biomasses might pose ash melting issues so pre-treatment is needed for the use of these feedstocks. However, woody biomass is not expected to have these problems due to low ash content and sufficiently high ash melting points [77]. When using ilmenite as an OC it has been observed that the hematite fraction increases and the pseudobrookite fraction decreases with the redox cycles. It has been connected to the operating temperature, with temperatures below 800ºC favoring the formation of Fe_2O_3 and TiO_2 and temperatures higher than 900ºC pseudobrookite and TiO_2 are formed [78].

Parameter considerations

Biomass CLG process parameters have been summarized in [73]. The biomass specific characteristics play an important role in gas yield and composition. Operating temperature will impact the gasification reactions via the higher heating rate with an increase in temperature and based on the Le Chatelier's principle, because gasification is globally endothermic [69], an increase in gasification temperature will increase H_2 and CO content, more char will be converted to gaseous products and less tars will be formed. It is important to mention that hydrogen content at temperatures higher than around 860ºC will decrease. In [73] it is explained by an increase in reactivity of the OC with the combustible gases, but it can possibly be also due to the promotion of the endothermic reverse water gas shift (rWGS) reaction which converts H_2. An increase in steam to biomass ratio (S/B) will increase total gas yield and many aspects of the gasification process, but it will also lead to an increase in CO_2 content which is undesirable in many cases. Another factor investigated is the OC to Biomass Ratio, but it is not clear how it affects the gasification process. Usually, not all of the oxygen carrier is oxidized in the AR so using this as a metric dismisses the more relevant

effective equivalence ratio (ER) the FR operates at. Due to carbon slippage and therefore some combustion reactions happening in the AR, part of the oxygen that would be captured by the OC is instead reacted with the fuel. Also, under unsteady conditions of OC circulation and its redox cycles it can be seen that the effective ER in the FR will be higher when more reduction of OC occurs in the FR and lower when the reduction of the OC in the FR is decreased. This can be measured during operation and the OC circulation to be regulated. The oxidation of the OC in the AR can be regulated by e.g., recirculation of part of the oxygen depleted air and mixed with the fresh air to not affect the fluidized bed's operating regime while correcting the oxidation reactions in the FR. Generally, the process parameter control is an important issue to be solved because the interrelations of parameters do not allow for individual parameter control. These concepts and proposals on plant design are discussed in detail in [63]. The ratio of ER_{FR} and ER_{AR} can be a parameter indicating stable operation regarding oxygen transfer.

$$\Theta = \frac{ER_{FR}}{ER_{AR}} \qquad \textit{Eq. 9}$$

The bottom line for CLG application with biomass feedstock is that the use of ilmenite as an OC is suitable and the possible operation has been investigated in a large-scale pilot plant with promising results. It ensures the suitability of this process with multiple biomass feedstocks and the biomass types investigated in chapter 3 are suitable. Taking into account the gas cleaning step it is an additional benefit that CLG produced syngas with ilmenite as an OC and biomass as feedstock has very low tar content making this step easier.

4.2.5 Syngas cleaning

In this section the syngas cleaning process steps are described and the configuration of syngas cleaning used in this thesis is presented. The syngas cleaning process train is inspired by the GoBiGas plant [79] and the experimental work done on activated carbon beds and a gas ultra-cleaning process train [80]. The aforementioned sources are used to configure an effective gas cleaning train suitable for medium scale applications.

The raw syngas exiting the CLG unit contains particulate matter, tars, nitrogen and sulfur-based compounds and many other contaminants such as HCl and alkali compounds. The removal of these impurities is necessary if the syngas is used in a downstream FTs process. However, the order of the employed gas cleaning process steps can prove difficult, and a sacrifice in process efficiency and cost to achieve the desired gas cleaning is necessary.

The woody biomass feedstock is of the cleanest of biomass types with lower nitrogen, sulfur and chlorine concentrations. Taking into account the low tar production of biomass CLG it will be easier to avoid tar related problems which are a major source of equipment fouling and operational rigidity. Thus, the starting point of the gas cleaning process design is favorable in terms of effectiveness and cost. If syngas cleaning processes are not suitably designed and operated, significant plant availability issues arise due to equipment fouling eventually leading to plant shutdown. The primary methods to deal with the cause of the problems is to adjust the operating parameters of the upstream processes to mitigate the problems faced during syngas cleaning. If primary methods are exhausted then secondary methods will be used, during syngas cleaning.

The principles followed for the configuration of an effective syngas cleaning process for medium scale plants were the use of established, cheap, robust and flexible process steps. Plant availability should be maximized, especially when considering a medium-scale process plant, to improve plant economics. Also, heating up and cooling down of the syngas should be avoided as much as possible to maximize plant efficiency and lower costs. The durable and flexible process steps allow variability in the composition of produced syngas to be tolerated by coupled processes downstream syngas cleaning. The flexible gasification process is coupled to flexible syngas cleaning therefore allowing better plant economics when cheaper and compositionally different biomass becomes available. Besides, biomass exhibits variability even between the same biomass type, so gas cleaning equipment scaling is a complex issue. The use of steps optimally designed for specific contaminants, but multifunctional if needed, is one alternative way to oversizing which would lead to a high capital investment.

For the choice of suitable syngas cleaning process steps and their proper configuration it is important to understand issues and constraints imposed by the presence of the main impurities. The specifications of a typical Fischer-Tropsch synthesis catalyst are shown in Table 25 [81].

Table 25: Fischer-Tropsch synthesis feed composition specifications.

Impurity	Chemical species	Specification
Sulfur compounds	H_2S + COS + CS_2	<1ppm
Nitrogen compounds	NH_3 + HCN	<1ppm
Halogen acid compounds	HCl + HBr + HF	<10ppb
Alkaline metals	Na + K	<10ppb
Solids	Soot, dust, ash	Practically removed
Organic compounds	Tar	Below dew point
Organic hetero compound	S+N+O	<1ppm

A good understanding of the aforementioned implications can be attained from the literature and for brevity reasons they will not be reiterated here [82], [83]. The most relevant points are briefly summarized with some extensions. Firstly, particulate matter in the case of a CLG unit is composed mostly of inorganic compounds, residual solid carbon, spent OC and ash. A higher separation efficiency of the cyclone after the FR will lessen the load of the used filter. Tars are organic compounds with the produced tars being mainly aromatic hydrocarbons. They can be classified according to the formation path with the classes being primary, secondary and tertiary compounds or according to a classification proposed by Energy research Centre of the Netherlands (ECN) which is based on physical tar properties and ring numbers [84]. The main problem regarding tars is their condensability causing fouling and clogging of equipment leading to lower up-times for the plant. Therefore, the dew point of tars is a main condition for the avoidance of tar related issues [84]. The nitrogen contained in biomass is converted during gasification more than 60% to NH_3, a lesser part to HCN and very little to nitrogen oxides while the rest is converted to N_2. The sulfur contained in biomass is almost completely converted to H_2S, less to COS and very little part is converted to CS_2 and other sulfur containing compounds. Alkali compounds will not be a problem with the hot gas filter used. The only relevant halogen compound in CLG is HCl, because it is usually present in a measurable quantity, when the feedstock contains Cl, and passes through the hot gas filter.

A significant hinderance in the GoBiGas plant in terms of operation and economics was the use of activated carbon beds for BTX adsorption, while heavier tars were still present in measurable quantities, because the RME scrubber let much of the naphthalene and heavier tars to pass through and be adsorbed to the activated carbon beds. The adsorbed heavier tars made the carbon beds' full regeneration impossible under the plant's current strategy [85]. To battle this, a highly effective oil-based gas washing solution, named OLGA, is employed that removes almost all heavy tars and some of the lighter BTX compounds. This ensures the better operation of activated carbon beds, especially when their regeneration is done using steam at higher temperatures than the GoBiGas plant.

The work done in [80], [86] demonstrated the multifunctional capabilities of activated carbon beds regarding the adsorption of many compounds and especially, the complete removal of Benzene and H_2S already by the second activated carbon bed. This however is not always desirable and further work on the adsorption of multiple compounds should be done. A known way of dealing with COS and HCN as shown in their ultra-cleaning process is their hydrolysis and downstream removal. However, H_2S and NH_3 adsorption from the guard bed will lower its lifetime. Therefore, it is decided to use the COS and HCN hydrolysis reactor under an alumina catalyst. After the hydrolysis reactor, a two-stage scrubber follows and lastly, three beds. These are an activated carbon bed to prolong the lifetime of the guard bed that follows by adsorbing

part of the H_2S produced in the hydrolysis reactor and the part might having broken through the previous activated carbon beds. The third bed has a deoxygenation catalyst to remove oxygen from an air injection in the first activated carbon bed used for BTX removal. The evident and main difference to employed gas cleaning trains in other thermochemical pathways is that CO_2 removal is not done, thus additional measures are taken, dedicated to removal of compounds usually removed in the step of CO_2 removal.

Summarizing, final gas cleaning process consists of a hot gas filter, OLGA tar removal process, scrubbers, a hydrolysis reactor, activated carbon beds and a ZnO guard bed. In addition, multiple heat exchangers are necessary to recover heat when the syngas temperature needs to be lowered and to provide heat at heat demanding process steps. The purpose and operation of these components are explained in detail later in this section.

4.2.5.1 Hot gas filter

A ceramic hot gas filter was used in this configuration operating at 550°C [68]. For temperatures in the range of 500-600°C the filter showed stable operation while for temperatures above 600°C, filter blinding occurred. A sticky filter cake was created for temperatures above 600°C that caused incomplete regeneration of the filter [87]. Gas exiting the gasifier is cooled down from the gasifier temperature to the operating temperature of the filter via the HRSG. The operating temperature of the filter is appropriate to achieve condensation of alkali and heavy metal species [88], [89] and capture them in the filter. The rest of the particulate matter is also captured in the filter. Together, the captured compounds form the filter cake which is removed by a reverse pulse of nitrogen or other gases [90]. An important note on chlorine present in the syngas is its reaction with alkali metals that result in solid chlorides that are removed in the filter [87]. The chlorine passing through the filter is in the HCl compound [91].

4.2.5.2 OLGA tar removal

There exist many methods to deal with tars, however only few are capable of producing a syngas fulfilling the specifications of a downstream fuel synthesis process such as FTs. A simple technology is employed in this configuration due to the very low tar content produced by the gasifier which leads to expensive technologies losing their major benefits such as the catalytic cracking of tars. OLGA, named after the Dutch acronym for oil-based gas washing, effectively removes almost all heavy tar compounds and many of the lighter and more volatile tars. Tars heavier than naphthalene were almost completely removed during operation while 25% of Benzene and 50% of Toluene were also removed [92]. Therefore, additional measures should be taken for sufficient BTX removal.

After the filter, syngas is cooled above the tar dew point to avoid condensation and enters the collector which is operated using a scrubbing liquid to absorb the heavy condensable tars while the syngas is cooled down to condense heavy tar compounds. Due to these tars being insoluble, the scrubbing liquid is regenerated, and tars are recovered. In this configuration, tars will be recirculated to the AR. The scrubbing liquid chosen for this operation is biodiesel. The syngas, almost free of heavy tars is led to the absorber where lighter, and in these temperatures gaseous, tars are absorbed in the scrubbing liquid. The temperature of syngas should be kept above water dew point which is typically around 80^{o}C. The scrubbing liquid from the absorber is led to another column, the desorber, where it is regenerated, and the recovered tars are led back to the AR to utilize their energy content [92].

Considering the low tar production of a biomass CLG unit and foreseeing the additional measures for BTX removal, the use of a simpler design consisting only of a collector could be investigated to remove heavy tars. However, due to the simultaneous goal of making this process capable of handling more feedstocks than just woody biomass and the factors that could lead to higher tar production it is not further examined as a scenario as it is too case specific. Different configurations for OLGA allowing for more gas cleaning options are presented in [93].

4.2.5.3 Condenser

After the OLGA unit, heavy tars are successfully removed, and the tar dew point is sufficiently low. The syngas exiting OLGA is cooled down with the aim to condense as much of the syngas moisture as possible because moisture inhibits BTX adsorption to the activated carbon beds while the design of activated carbon beds should have low affinity for moisture [80]. Some of the compounds contained in the syngas are carried with the condensate therefore it should be considered as a wastewater stream.

4.2.5.4 Carbon beds

Activated carbons have been used for hydrocarbon removal, for example in odor control and therefore are a proven technology [86]. They have also been used in syngas cleaning applications but mainly for H_2S removal. Activated carbon beds require lower capital costs compared to the established wet scrubbing with chemical or physical absorption, the use of which is not suited to a small to medium scale application. Because other compounds have an affinity towards activated carbon beds, they can be an alternative for the removal of multiple unwanted compounds. In this configuration activated carbon beds are used first for BTX and residual tar removal and then for the final H_2S removal.

Activated carbon beds' operation for tar removal has been investigated in pilot scale [86] and in industrial scale in the GoBiGas demonstration plant [79]. The GoBiGas plant is a 32 MW_{th} input plant, on an LHV dry-ash free basis. It was demonstrated that sufficient BTX and heavy tar removal was attainable and many issues on the use of

activated carbons were understood. Emphasis was given on the regeneration of activated carbon beds because despite high temperature steam being necessary for their almost full regeneration it could decrease the need for replacement by 10 times. According to GoBiGas operation, the existence of heavier tars than BTX compounds and especially heavier than naphthalene, made the employed steam regeneration temperature of 160^{o}C insufficient and the activated carbon bed's capacity would decrease with each cycle. It is reported that if steam regeneration temperature is at 400-500^{o}C, almost complete bed regeneration would be possible [85]. Steam consumption for bed regeneration is estimated in the range of 3-5 kg of steam per kg of desorbed organic compound [94]. Another study found that to be 6 kg of steam per kg of adsorbent [95]. The regeneration of activated carbon beds depends on the adsorbed compounds and the activated carbon bed structure with heavier tar compounds adsorbed making regeneration more difficult and a wider pore size distribution easier [80]. After steam regeneration of the beds, the desorbed tars are recirculated to the AR.

The optimization of heavy tar removal is very important to prolong activated carbon bed lifetime, as is the appropriate steam regeneration temperature. In this configuration the goal is for activated carbon beds to remove BTX compounds while heavier tars being removed in the OLGA unit. A suggestion is to operate the beds at lower temperatures (<30^{o}C) as this would lead to increased capacity of the activated carbon bed [85].

In [80], a successful carbon bed configuration at 30^{o}C was used for both BTX and H_2S removal. Their design employed two activated carbon beds for bulk BTX and H_2S removal. During the tests, a higher concentration of benzene led to breakthrough of benzene from the first bed but fully removed at the second bed. It was reported based on experimental findings from pilot tests that most of COS and HCN were also removed by the activated carbon beds which would make them a very attractive solution to make much of the dedicated equipment for COS and HCN removal superfluous. COS concentration was reduced to 7 ppm and HCN probably due to bed saturation was only removed in the 2nd bed to below 0.05 ppm, but it should be noted that HCN concentration was low from the start.

Activated carbon bed adsorption is an equilibrium-based process and the equilibrium capacity of commercially available carbons being up to the range of 200-350 mg/g_{Carbon} for benzene, toluene and other hydrocarbons [80].

Apart from BTX and residual tar removal, activated carbon is used for its conventional purpose, as desulfurization. However, this could not be achieved in low steam and oxygen syngas therefore an air injection is used to enhance H_2S removal, leading to the need of a following deoxygenation step using for example a Cu/Zn catalyst [86].

4.2.5.5 Hydrolysis reactor

While many impurities can be sufficiently removed in the employed gas cleaning process steps and the guard bed could remove any impurities to the appropriate levels, the quick saturation of the guard bed is undesired because it is expensive, and issues arise with its disposal. Without hydrolysis of COS and HCN, they will break through the activated carbon beds and the water scrubber and will be adsorbed by the guard bed. To prolong the lifetime of the guard bed they will be converted to H_2S and NH_3 respectively using a hydrolysis reactor and therefore allowing the removal of NH_3 in the scrubber and some of the H_2S in the smaller activated carbon bed prior to the guard bed. Hydrolysis of COS and HCN follow R. 12 and R. 13 respectively.

$$COS + H_2O \rightleftharpoons H_2S + CO_2 \qquad \textit{R. 12}$$

$$HCN + H_2O \rightleftharpoons NH_3 + CO \qquad \textit{R. 13}$$

4.2.5.6 Water Scrubber

NH_3 is highly soluble in water therefore after HCN has been hydrolyzed to NH_3, together with the produced NH_3 during gasification, ammonia is removed from the syngas by a two-stage water scrubber during which water is sprayed from the top of the column and syngas flows counter-currently. An alkali solution of water and NaOH can be used to facilitate HCl removal [96].

4.2.5.7 ZnO guard bed and deoxygenation

Guard beds are used as final polishing steps for the syngas prior to impurity sensitive fuel synthesis. They can be either warm guard beds to facilitate catalytic reactions or cold guard beds. In this configuration, an activated carbon bed is used after the water scrubber prior to a warm guard bed consisting of two beds, one with ZnO and the other with a Cu/Zn deoxygenation catalyst to remove oxygen present in the syngas from the prior air injection. Before the guard bed, an activated carbon bed is used for H_2S removal.

4.2.6 Fischer-Tropsch synthesis

FTs is a catalytic process that converts CO and H_2 into a mixture of short to long-chain hydrocarbons. The produced mixture is referred to as FT-crude or syncrude and the wide range of hydrocarbons contained can be upgraded to meet fuel specifications and used for example as transportation fuel. This is done either on-site on the processing plant or at an oil refinery.

FTs can be classified based on the operating temperature in low temperature Fischer-Tropsch (LTFT) operating at 220-250 ^oC, medium temperature Fischer-Tropsch (MTFT) at 250-300^oC or high temperature Fischer-Tropsch (HTFT) at 300-350^oC [97]. Many catalysts can be used for FTs, but for commercial applications Co- and Fe-based are used. For LTFT the catalysts used, are Co- or Fe-based and it is suitable for production of long chained hydrocarbons while for HTFT, Fe-based catalysts are used. The product

distribution of FT follows the Andrew-Schultz-Flurry (ASF) distribution, and the main products include n-olefins which are mostly α-olefins and n-paraffins, and to a lesser extent, alcohols. The ASF distribution is based on the chain growth probability factor α that expresses the probability of chain propagation rate r_p and termination r_t. The weight distribution based on carbon atoms number is given by Eq. 10 and the chain growth probability factor is given by Eq. 11. A higher α means that the FTs product distribution is shifted to the longer chained hydrocarbons. For LTFT, a usual α value is higher than 0.85 and for HTFT the usual value is around 0.7, highly dependent on catalyst and operating conditions. A proposed reason for the lower α values of HTFT is that an increase in temperature favors the endothermic desorption process, therefore the adsorbed CO or CO_2 are released from the catalyst surface.

$$\frac{W_n}{n} = (1-\alpha)^2 \alpha^{n-1} \quad \text{Eq. 10}$$

$$\alpha = \frac{r_p}{r_p + r_t} \quad \text{Eq. 11}$$

The main reactions taking place during FTs are R. 14 - R. 17. Many aspects of FTs reaction routes and product distribution are presented in [98].

Paraffins:	$nCO + (2n+1)H_2 \rightarrow C_nH_{2n+2} + nH_2O$	R. 14
Olefins:	$nCO + 2nH_2 \rightarrow C_nH_{2n} + nH_2O$	R. 15
Water Gas Shift (WGS):	$CO + H_2O \rightleftharpoons CO_2 + H_2$	R. 16
Oxygenates:	$nCO + 2nH_2 \rightarrow C_nH_{2n+2}O + (n-1)H_2O$	R. 17

While FTs is usually done after removing CO_2 from the syngas, this step is not required if proper catalyst and operating conditions are chosen. An alternative way for FTs is to feed the FT reactor a CO_2 containing syngas and convert both CO and CO_2 to hydrocarbons. Syngas conditioning when CO_2 is removed is usually done with a WGS reactor converting enough of CO to produce CO_2 and H_2 to obtain the necessary H_2/CO ratio which is targeted to be around 2.1 because the ratio of H_2 to CO affects the product distribution. If CO_2 is not removed, then WGS equilibrium probably will not be able to provide the necessary H_2 for the necessary ratio to be obtained. Therefore, hydrogen will be fed to obtain the appropriate $H_2/(CO+CO_2)$ ratio and this will be considered as the conditioning step for this process train.

In the examined configuration, CO_2 is not removed, leading to further equipment cost reduction as the use of an expensive acid gas removal unit is no longer needed. However, operational expenditure increases due to external green hydrogen demand. FTs is performed at elevated temperature and pressure and the use of a Fe-based catalyst at HTFT is necessary to enhance CO_2 conversion as it can catalyze both FTs and rWGS reactions. Additionally, the catalyst, for the specific application, will need to suppress C_1-C_4 hydrocarbons to enhance the selectivity of C_{5+} hydrocarbons which is

the desired hydrocarbon fraction. HTFT compared to LTFT has a lower chain growth probability factor governing the product distribution leading to shorter hydrocarbons. It should be mentioned that despite the ASF distribution being a good approximation of the product distribution, the production of C_1-C_3 hydrocarbons deviates from it and especially for C_1 and C_2.

The mechanism for FT CO_2 hydrogenation is considered to be a two-step reaction where rWGS reaction happens first and then CO is converted via FTs [99]. The two-step reaction is FT kinetically limited meaning that it is observed rWGS reaches equilibrium because Fe-based catalysts catalyze WGS and the elevated temperatures of reaction. CO is consumed via the kinetically slower FTs reaction and produced by the rWGS reaction until the latter reaches equilibrium. Note, the production of H_2O from FTs shifts the rWGS equilibrium towards CO_2 and H_2.

The path of not removing CO_2 leads to a higher carbon utilization in the overall process if recirculation of the FT gaseous products is considered, therefore less CO_2 is emitted. The gaseous FT products coming from FT-crude separation are recirculated and passed through a catalytic steam allothermal reformer to convert light HCs into CO and H_2 while reducing inert hydrocarbon recirculation and hydrocarbon product loss.

A significant remark about FTs is that it is strongly exothermic, and the relatively high reaction temperature allows for the recuperation of heat at elevated temperature. This is done by using water at elevated pressure to increase saturation temperature to the level where sufficient temperature difference is available for heat transfer and most of the heat is transferred as latent heat of evaporation as the pressurized water enters the reactor with a small subcooling and exits with a slight superheating.

4.2 Process modelling

Process modelling is done using Aspen Plus™ software. The aim of developing a model for the proposed process is to integrate available literature data, validate the model's accuracy in using the data and simulate the process under different conditions. This allows to evaluate the process from the thermodynamic and technoeconomic sides, based on the process modelling results. The modelling includes a simple model for the drying, a modified-equilibrium model for the CLG unit, simple gas cleaning process steps modelling, a FTs unit with recirculation of gaseous products and a HRSG system.

Aspen has information about many conventional components; however, biomass and ash are considered non-conventional components. Biomass composition is specified using proximate and ultimate analysis, and ash component is specified as containing 100% ash in its proximate and ultimate analysis. Gases and liquids are in the stream class "MIXED", and solids are in the stream class "CLSOLID". Non-conventional components are in the stream class "NC". If not otherwise specified, the property

method used is the RKS-BM method which is a commonly used method in similar applications.

The process representative feedstock used in the process simulation is OTP with the composition of Table 26.

Table 26: Olive Tree Prunings composition.

	OTP
Proximate analysis (% d.b.)	
Moisture	25.2
Fixed Carbon	17.1
Volatile Matter	78.4
Ash	4.5
Ultimate analysis (% d.b.)	
Ash	4.5
Carbon, C	50.43
Hydrogen, H	6.79
Nitrogen, N	1.27
Sulphur, S	0.12
Chlorine, Cl	0.07
Oxygen, O	41.32
LHV (MJ/kg d.b.)	17.56

The overall Aspen Plus model flowsheet is depicted in Figure 12.

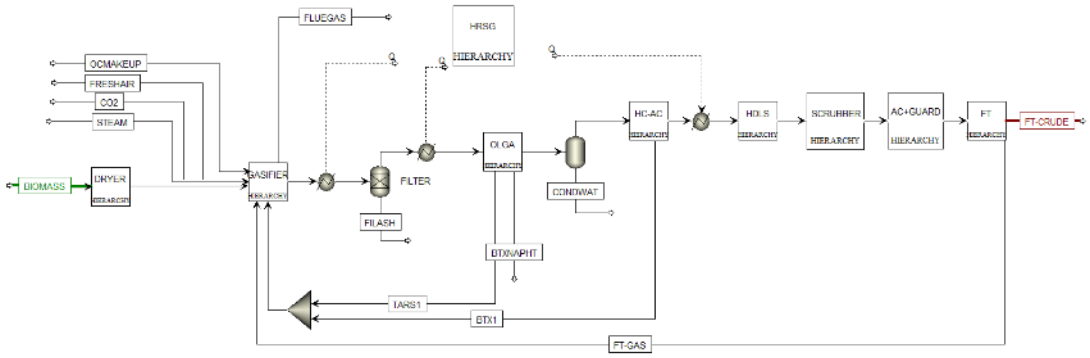

Figure 12: Complete process model in Aspen Plus™.

4.2.1 Dryer

A belt dryer is used for feedstock drying which based on results from chapter 3 enters the dryer with an initial moisture content of 20% while the outlet moisture content is set to be 12%. The outlet moisture content can be as low as 8% according to literature [100]. The available unit operation to simulate a dryer in Aspen Plus™ requires a lot of information. Therefore, a simpler method is followed in which literature data on heat and power consumption are used to calculate energy demands of the dryer and the

dryer is simulated by an Rstoic block in which the reaction of inlet biomass with high moisture content yields a biomass component with lower moisture content. The difference between moisture content yields the released water upholding mass balance. A 15°C temperature increase of biomass is assumed to occur during drying. The reaction set in the Rstoic block is R. 18 while biomass moisture content is redefined to the value after the dryer. The conversion of biomass is set appropriately to ensure mass balance.

$$BIOMASS \rightarrow 0.05550843506\ H_2O \qquad R.\ 18$$

For a belt dryer using air as drying medium and a closed water circuit operating between 60/90°C, the specific heat requirement is 1300 kWh/t_{H2O} and power consumption is 115 kJ/kg of dry biomass [100] while 20% of the heat requirement can be covered by low temperature heat, less than 60°C [101].

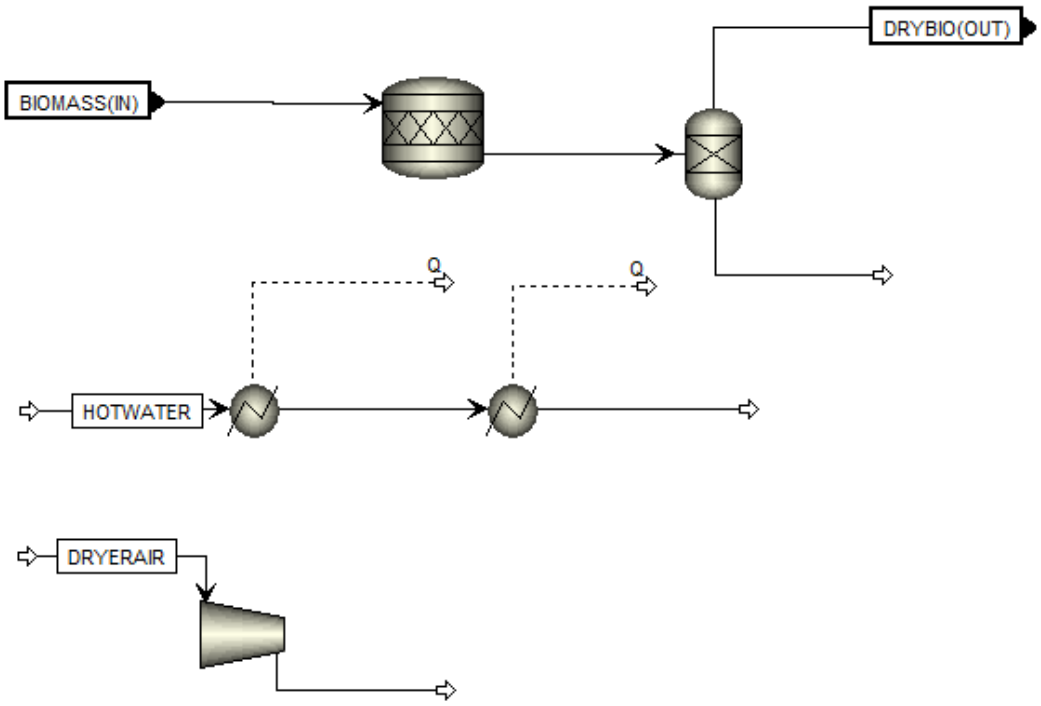

Figure 13: Dryer model-Aspen Plus™ flowsheet.

4.2.2 Chemical Looping Gasification

The developed CLG model is based on modified equilibrium as it predicts the formation of non-equilibrium components and the incomplete char gasification complementing the insufficiencies of purely equilibrium-based models. The whole gasification unit is operated at atmospheric pressure although slight pressurization will lessen the need for downstream blowers to compensate pressure losses.

The stream with dried biomass coming from the dryer enters the gasification model at the specified dryer outlet conditions. It is assumed that biomass is instantly devolatilized into its basic elements based on the provided biomass ultimate analysis and proximate analysis with the new moisture content.

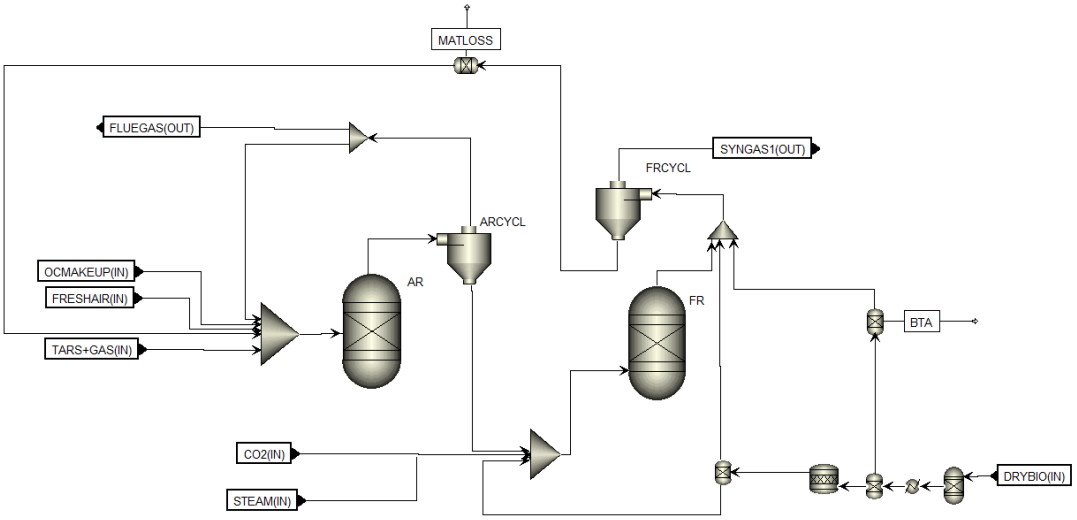

Figure 14: Chemical Looping Gasification unit-Aspen Plus™ flowsheet.

Biomass enters the modelled CLG unit after the dryer and is devolatilized based on the ultimate analysis in an RYield block. Then, a separator simulates the split of unreacted carbon and ash. Unreacted carbon is set based on carbon conversion and ash is fully separated in this separator. A part of these will exit the gasifier as bottom ash so it was assumed that 1% of the unreacted carbon and all of the biomass contained ash end up in the bottom ash. In reality, some of the ash content will make it to the FR cyclone and even to the filter after which particulates will be fully removed. The part of the unreacted carbon that continues to be in the process mixes with the syngas after the gasifier and before the gasifier cyclone. The main part of the biomass proceeds from the first separator and goes to an Rstoic block in which reactions for CH_4, C_2H_4, C_2H_6, C_3H_8, C_6H_6, $C_{10}H_8$, NH_3, HCN, H_2S, COS, HCl are included. This is the part of the model that predicts non-equilibrium products from the gasification process, because their formation is due to non-equilibrium conditions in the gasifier thus an RGibbs reactor would not correctly predict their formation. The conversion of C to each hydrocarbon compound is based on fitting the model predictions to experimental data. The production of C_2-C_3 species is represented by C_2H_4, C_2H_6, C_3H_8 and tars have been separated in BTX compounds represented by benzene (C_6H_6) and heavy tars represented by naphthalene ($C_{10}H_8$). The conversion of N, S, Cl is based on literature data. More on the selection of the appropriate conversions will be presented in the model validation while the used values are presented in Table 27 together with other parameters. After the Rstoic block, the produced compounds are separated from the stream and C, CO, H_2, CO_2, O_2, H_2O are directed to the RGibbs reactor representing the equilibrium part of the FR. Steam used for FR fluidization and CO_2 used for fuel feeding

via a feeding screw and connecting equipment fluidization are added to the fuel reactor in pre-determined ratios based on inlet w.b. biomass to the CLG unit. OC enters the gasifier, and the reactants reach equilibrium in the RGibbs block. The product from the FR is mixed with the abovementioned unreacted char and led to the cyclone after the FR. The cyclone is assumed to have 0.1% loss of circulated OC by employing an SSplit block for gas-solid separation and then a separator to remove 0.1% of each component of circulated OC [102]. The carbon slip stream is separated here and led back to the AR. OC make-up stream is not considered here. Instead, OC stream is assumed to circulate continuously to the AR in the fully reduced state and at the outlet FR conditions. OC is assumed to be composed only of ilmenite for modelling simplicity. The OC circulation flow is subject to a design specification which leads to convergence issues in the model if a recirculation stream is assumed from the FR therefore the outlet OC is not redirected to the AR.

A special attention is paid for the origin of the CO_2 for fluidization. In this analysis, it is assumed that biogenic CO_2 is purchased from external supplier, e.g. from a biogas upgrading plant. The alternative option is to consider a separation unit for CO_2 capture from the flue gas derived from the FT synthesis unit. The latter would be beneficial for the investment in the case that the CO_2 production cost was less than the purchased cost.

AR fluidization control is done with recirculating part of the AR flue gas which is an almost inert gas. Inlet stream to the AR apart from the recirculated OC is the fresh pre-heated air carrying the necessary oxygen to oxidize the recovered fuel entering the AR and the OC that will be transferred to the FR. The AR is also used as the plant's oxidizer to recuperate fuel energy that would be burned to an oxidizer. The pre-heated air is mixed right before the AR with the recirculated flue gas stream to fluidize the reactor. The recirculation factor does not affect modelling and its results. The recovered heavy tars and BTX from the OLGA unit and the activated carbon beds are fed to the AR without scrubbing liquid and air from OLGA and moisture being accounted. The last stream entering the AR is the gaseous products from FTs that are not separated and not recirculated to the steam reformer, and elsewise would be burned in an oxidizer. In the AR, oxygen is assumed to oxidize all the combustible gases and the rest of the oxygen, which is regulated to be sufficient for the gasifier, is used to oxidize the OC. The outlet AR stream is led to the AR cyclone which is represented by an SSplit block that fully separates gas from solids. OC is the only solid present after the AR and the flue gas is directed to the recirculation controller from which the uncirculated flue gas exits the CLG unit.

Control of the CLG unit

The constant parameters throughout the model simulation are the carbon conversion, operating temperature of the AR and FR, biomass devolatilization, steam to biomass ratio, non-equilibrium reaction conversion extent, CO_2 used for fluidization.

The parameters subject to design specifications are:

- The inlet air flow with the target being autothermal operation of the CLG unit by accounting for 1% heat loss of the whole unit.
- The OC circulation rate targeting the transfer of all available heat from the AR.

The reaction taking place in the AR for the OC is R. 19.

$$4\,FeTiO_3 + O_2 \rightarrow 2Fe_2TiO_5 + 2TiO_2 \qquad R.\ 19$$

The included reactions for the non-equilibrium products are R. 20 - R. 30:

$$N_2 + 3\,H_2 \text{ --> } 2\,NH_3 \qquad R.\ 20$$

$$S + H_2 \text{ --> } H_2S \qquad R.\ 21$$

$$CL_2 + H_2 \text{ --> } 2\,HCL \qquad R.\ 22$$

$$C + 2\,H_2 \text{ --> } CH4 \qquad R.\ 23$$

$$2\,C + 2\,H_2 \text{ --> } C2H4 \qquad R.\ 24$$

$$2\,C + 3\,H_2 \text{ --> } C2H6 \qquad R.\ 25$$

$$3\,C + 4\,H_2 \text{ --> } C3H8 \qquad R.\ 26$$

$$6\,C + 3\,H_2 \text{ --> } C6H6 \qquad R.\ 27$$

$$10\,C + 4\,H_2 \text{ --> } C10H8 \qquad R.\ 28$$

$$S + C + 0.5\,O_2 \text{ --> } COS \qquad R.\ 29$$

$$N_2 + 2\,C + H_2 \text{ --> } 2\,HCN \qquad R.\ 30$$

4.2.3 Syngas cleaning

The syngas exiting the FR cyclone is cooled down from the FR temperature of 850°C to the filtration temperature of 550°C by a heater block. The filter is able to remove all remaining solids such as the OC, char and ash that passed through the FR cyclone despite the model not predicting a breakthrough of solids. Alkali and heavy metals despite not being accounted for in the model, they are also captured in the filter. Also, the model has not predicted the formation of solid chlorides or other nitrogen compounds going to ash. The chlorine that manages to pass through the filter is in the HCl compound while nitrogen in the N_2, NH_3 and HCN compounds. Therefore, the filter is represented by a separator block that splits the compounds that are captured. The

split fraction of Cl_2 representing solid chlorides is set to 1. For N_2, an assumed split fraction value of 0.2 is set to represent part of the remaining nitrogen going to ash compounds. Solids and ash split fractions are also set to 1 for complete solid removal.

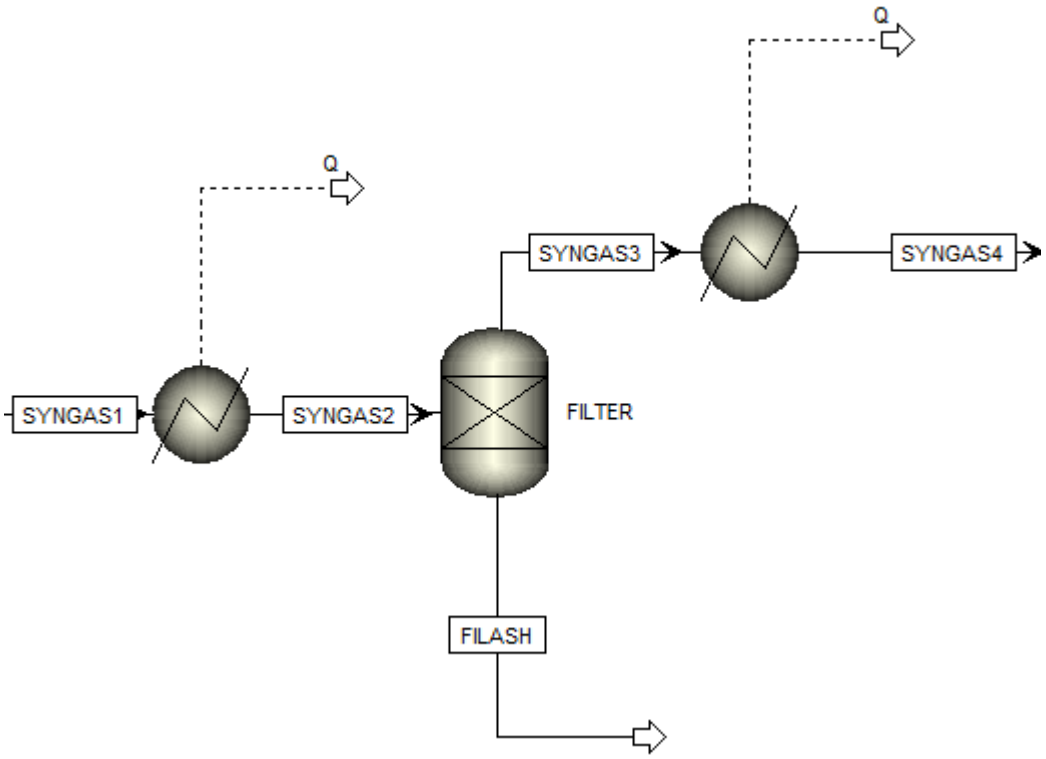

Figure 15: Syngas coolers and filter-Aspen Plus™ flowsheet.

After the filter, the particulate free syngas is led through another heater block to further lower the syngas temperature down to an acceptable OLGA inlet temperature which must be above tar dew point, in this case 400°C being a safe temperature considering the low tar content of CLG syngas. OLGA is modelled as two separator blocks and two coolers. The first separator simulates the collector in which heavy tars condense through cooling while the scrubbing liquid absorbs them. The split fraction is arbitrarily, without impact to the overall modelling, set to 0.8 for $C_{10}H_8$, which is the representative of heavy tar compounds. The scrubbing liquid which for this case can for example be biodiesel and plays no role in the modelling, is regenerated and tars are recovered but this part is not modelled. After the first separator is a heater block to model the syngas cooling down to 120°C happening in the collector. Then, the absorber is modelled as a separator block in which a 0.3 split fraction is set for benzene which represents BTX compounds and the rest of $C_{10}H_8$, is removed simulating complete heavy tar removal and partial BTX removal overall achieved in the OLGA unit. A heater block follows the absorber to cool down the syngas to 80°C. The stripper is responsible for the regeneration of scrubbing liquid, but this part is not modelled. The tar and BTX containing streams are combined and led to the AR to be combusted. As mentioned earlier, tar formation is relatively small, and thus carbon exploitation of the

retrieved tars and BTX is insignificant relative to the possible issues of circulating them to the FR. Experiments carried out in [103] using ilmenite, among other OCs, considered the recirculation of tar compounds to the FR and at the current operating temperature of 850°C, 80% Benzene conversion was achieved. Large scale experiments were not available, and the saturation of activated carbon beds is unwanted. Thus, it was decided to recirculate tars to the AR, so under high temperatures and highly oxidative environment the tars are fully cracked and oxidized.

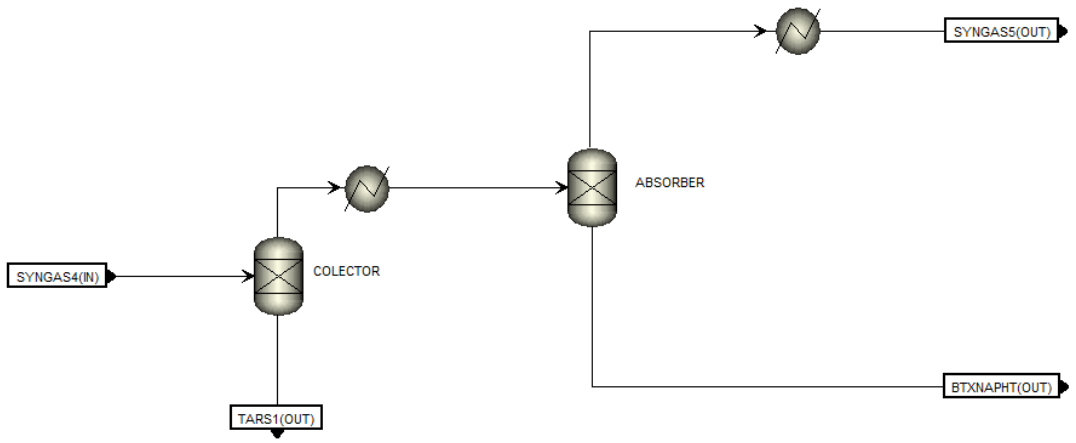

Figure 16: OLGA unit -Aspen Plus™ flowsheet.

The heavy-tar free syngas exiting the OLGA unit is led to a condenser to remove its moisture. The condenser is simulated as a flash separator that cools the syngas down to an appropriate temperature of 30°C which is enough to condense most of the moisture and is a suitable operating temperature for the subsequent activated carbon beds. There are two activated carbon beds operating for the complete removal of remaining BTX compounds from the syngas. To facilitate H_2S adsorption an air injection is included at the second bed at a 7 mol ratio between oxygen and H_2S. The beds are represented by separator blocks. The first one has a 0.8 split fraction for benzene representing BTX adsorption and the second separator removes the remaining BTX and all H_2S in two separate streams. The H_2S containing stream goes to an Rstoic block with the oxidation of H_2S to elemental sulfur taking place. The stream exits the Rstoic block, and the oxygen contained that would in reality be contained in the syngas is discarded via a separator block as it is in small quantity to cause any significant change to the syngas composition. Elemental sulfur is led to a wastewater stream as explained in the following section.

Activated carbon bed regeneration is realized using steam at 1bar and 500°C as this is a sufficiently high temperature for almost full bed regeneration. The necessary amount of steam is approximately 12 kg_{steam}/kg_{BTX} based on 4 kg_{steam}/kg_{carbon} [95] and 0.25 kg_{BTX}/kg_{carbon} [80]. To model the regeneration, steam is mixed with the outlet BTX containing streams and the mixture, after being cooled down to 40°C in a heater block,

is led to a flash block separator in which almost full recovery of the very volatile BTX compounds is achieved. In reality, the activated carbon beds have adsorbed many impurities in different amounts. An in-depth investigation of the adsorption of other compounds is necessary, firstly to understand what wastewater treatment is needed, secondly to optimize the activated carbon beds operation because they can be a versatile low-cost solution. In this model, elemental sulfur which is the only other considered adsorbed compound is mixed with the condensate water from the flash and the outlet water-sulfur stream is considered wastewater.

The configuration of activated carbon beds should be assessed in the detailed plant layout because the use of three or four beds is possible to allow normal plant operation while one or two of the beds are regenerated.

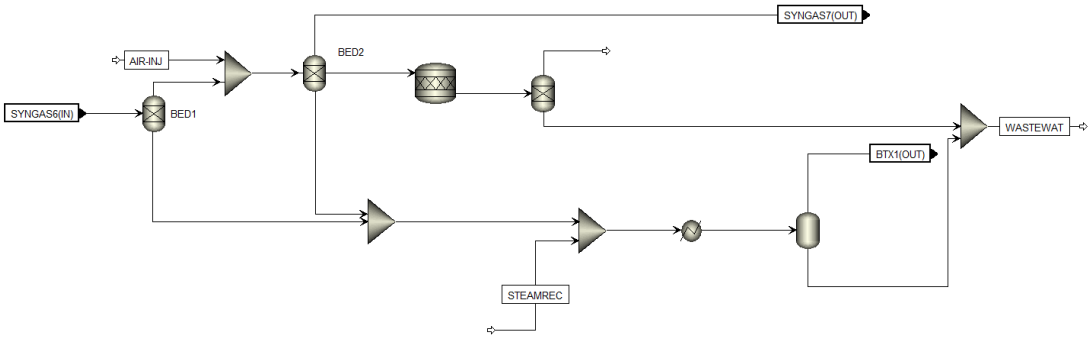

Figure 17: Activated carbon beds--Aspen Plus™ flowsheet.

Following the carbon beds a hydrolysis reactor is used to convert COS and HCN. A heater block heats the syngas up to the reactor temperature of 205°C [86], [96]. The reactor is modelled by a REquil block in which the two reactions are specified with their respective temperature approach to equilibrium [101].

$$COS + H_2O \rightleftharpoons \mathrm{H_2}S + CO_2, \qquad T_{app} = 0^oC$$

$$HCN + H_2O \rightleftharpoons \mathrm{N}H_3 + CO, \qquad T_{app} = 10^oC$$

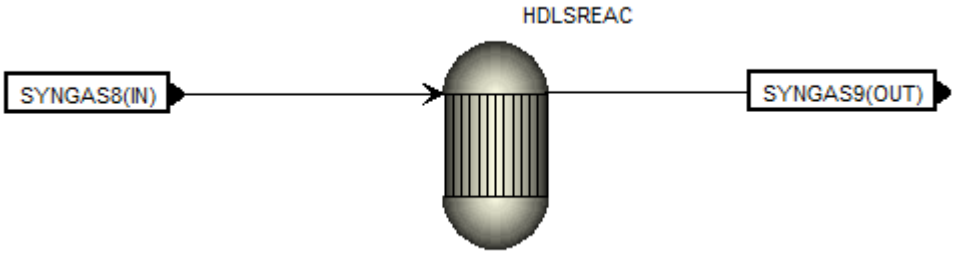

Figure 18: Hydrolysis reactor-Aspen Plus™ flowsheet.

Following the hydrolysis reactor is a two-stage water scrubber. The first stage cools down the gas to 60°C while the second stage cools it further down to 30°C. Enough water flows to each scrubber for the desired cooling. Complete NH_3 and HCl removal

are assumed, and it is modelled via a separator block after the two flash separators simulating the two-stage scrubbing [104]. The removed NH_3 and HCl are mixed with the previous water streams in the model. A bleed stream from the scrubbing water is split to control contaminant concentration. The scrubber wastewater together with other wastewater is treated on-site or disposed bearing the additional cost. The NaOH addition and wastewater treatment are not modelled. The used property method is SRK.

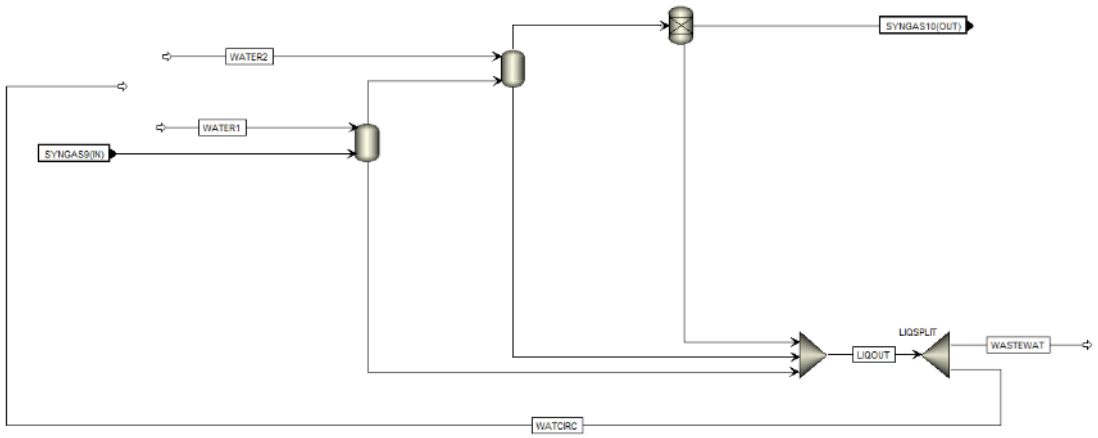

Figure 19: Scrubber-Aspen Plus™ flowsheet.

The final removal step consists of an activated carbon bed with microporous structure ideal for H_2S removal, the warm guard bed responsible for the syngas to meet FTs specifications and the deoxygenation catalyst which removes any remaining oxygen leftover from the prior air injection. The activated carbon bed is operated at 30°C which is the scrubber's outlet temperature. The warm guard beds operate at 200°C, so the syngas is heated to the operating temperature. The beds are modelled as separator blocks with the activated carbon bed removing any remaining tars and a 0.9 split fraction for H_2S despite no tars being predicted to breakthrough the previous activated carbon beds. The two latter beds are modelled by a single separator block that removes all O_2, tars, NH_3, H_2S, COS, HCN. The assumption of complete contaminant removal is done for modelling reasons, but the guard bed will sufficiently lower the contaminant levels of the syngas to meet downstream fuel synthesis specifications.

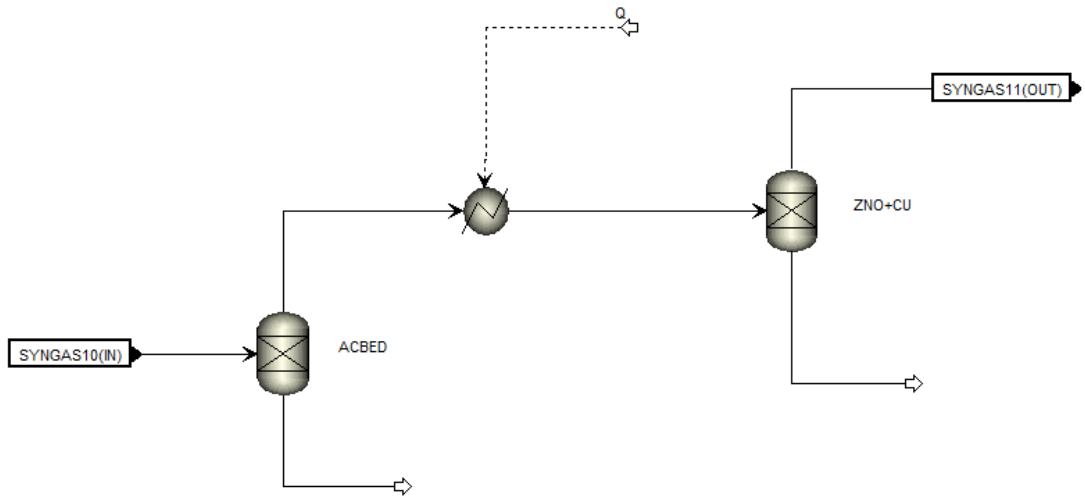

Figure 20: Activated carbon bed and guard bed – Aspen Plus™ flowsheet.

4.2.4 Fischer-Tropsch synthesis

The FTs process modelling is based on incorporating experimental data from [105] and some guided assumptions because experimental data reporting does not include all necessary information. The data available are for various concentration ratios of CO_2/ (CO+ CO_2) under the reactor operating conditions of 300°C and 15 bar with the catalyst 100Fe/6Cu/16Al/6K of 12.5 g_{cat}*h/mol and H_2/(CO+CO_2) equal to 1.87. The available data regard the CO_2, CO and total carbon conversions to hydrocarbon products, in addition to carbon selectivity for the CH_4, C_2-C_4, C_{5+} and the olefin content in C_2-C_4. The chain growth probability factor was not reported but for Fe-based catalysts with potassium as a dopant for CO_2 hydrogenation, 300°C, 15bar was found to be around 0.7 in [106]. This value is accurate enough to calculate the ASF product distribution for C_{5+} hydrocarbons despite not necessarily being the exact experimental one for different CO_2/ (CO+ CO_2) ratios. The average selectivity for C_{5+} occurring in the experiments based on the ASF distribution is close to an α=0.7, but in reality, multiple alpha values could be used for different C_{5+} fractions to better approximate hydrocarbon distribution. The results will not significantly change for slight alpha variation. It is only important if more detailed approximations are needed, e.g., for the on-site refining of FT-crude. The olefin content in C_{5+} hydrocarbons is taken from a similar experimental work for different CO_2/ (CO+ CO_2) ratios [107]. First, second or third grade polynomial curves are fitted to the experimental data curves and are included in a calculator block. The polynomials are a function of the CO_2/ (CO+ CO_2) ratio so the calculator takes as input this ratio at the inlet of the FT reactor and calculates the carbon conversions and product distribution according to the experimental results. This way the kinetic or more detailed modelling is not necessary. The property method used in the FTs block is NRTL.

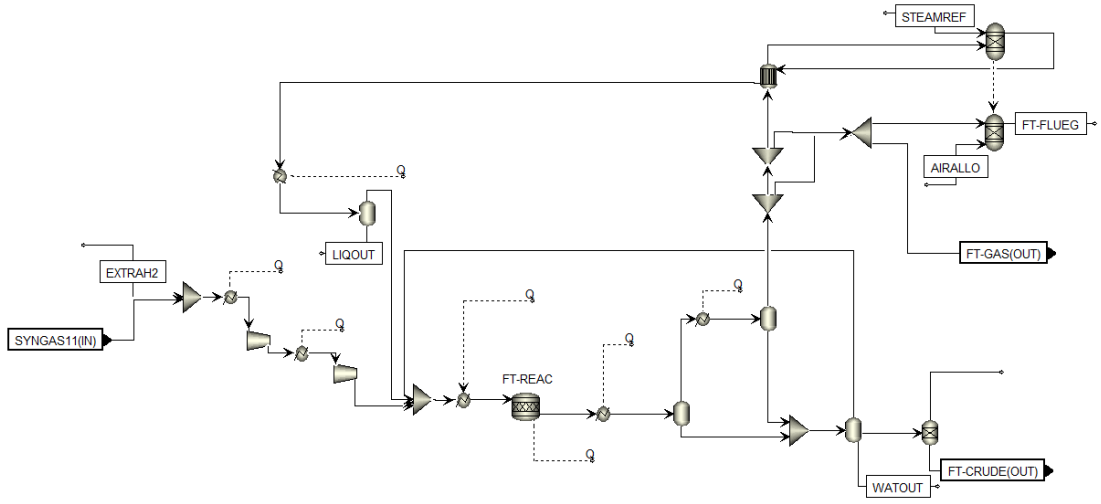

Figure 21: Fischer-Tropsch synthesis - Aspen PlusTM flowsheet.

The modelling of the FT reactor is an Rstoic block with two reactions occurring in series, the rWGS converting CO_2 and H_2 to CO and H_2O and then the FTs reaction with reactants being CO and H_2 and products being the considered hydrocarbons. The model takes into account hydrocarbons from C_1-C_{20} and uses three lumped components to represent the rest of the hydrocarbons. The lumped components are C_{24} for the C_{21}-C_{24} range, C_{28} for the C_{25}-C_{28} range and C_{48} for the rest carbon atoms.

Syngas exiting the gas cleaning process is mixed with sufficient H_2 to meet the necessary ratio of $H_2/(CO+CO_2)$ at the point right before the FT reactor to meet the experimental conditions. This can be considered as the gas conditioning step of the process. The conditioned syngas enters a two-stage compression train with intermediate cooling up to FTs pressure and the compressed syngas is mixed with the recycled streams. If pressure drops were considered, each of the recycled streams would need a compressor to bring them up to mixing pressure. This was not considered in this model, so the mixed syngas is then heated up to the FTs reactor temperature and enters the reactor. The FT products are a mixture of syngas species and short or long-chained hydrocarbons from which the FT-crude needs to be separated. It is realized by two-stage cooling and liquid separation at 120°C and 31°C with two heater blocks cooling the FT-products down to flash temperature modelled by a flash2 block in which the condensed product is separated. In the model, the liquid products are mixed and sent to a three-phase separator operating at 30°C in which water is removed, gaseous product is recirculated and FT-crude with a few light gases exit which are recirculated to the FTs reactor. A separator block is then used to separate C_{5+} product which usually is considered as the FT-crude product in the literature and therefore the results will be easily comparable to literature. The gaseous product exiting the second flash drum contains many light hydrocarbons and would be beneficial to reform them into fresh CO and H_2. This is done by leading the gaseous product to a steam allothermal reformer that operates at a steam to methane ratio of

3 and 900°C, 15bar. Heat for the endothermic reforming reactions is provided by combusting part of the recirculated FT gases with air in a reactor with the flue gas exiting temperature set at 950°C. Steam and air are at the reactor pressure and pre-heated to enhance efficiency in terms of chemical energy. Burning part of the recirculated gaseous product simultaneously prevents the accumulation of inert compounds in the system. The recycle ratio of gaseous products is set to 1, but the effective recycle ratio is around 0.75 because the combusted part of the recirculated products does not allow for higher effective recirculation. A heat exchanger is used to pre-heat FT product entering the reformer and cool down the reformed FT product which is further cooled down to 80°C to remove the moisture coming from the FTs reaction and the reformer. The gaseous products coming from the condenser and the three-phase separator are mixed with the inlet syngas.

4.2.5 Heat integration with Heat Recovery Steam Generation (HRSG)

The integrated process provides many opportunities for heat recovery due to the high temperature syngas exiting the CLG unit being cooled down, the high temperature flue gases exiting reactors and the highly exothermic FTs reaction. An effective heat integration configuration will balance heat recovery and techno-economics. With high temperature heat available in the integrated process, it is possible to include in the heat integration an HRSG system for electricity production therefore lowering external energy, heat or electricity, requirements. It does however increase capital expenditure countered by lower operating costs.

The modelling of HRSG is done using heat exchangers instead of heater blocks allowing the inclusion of heat exchanger's pinch points. The considered pinch points of heat exchangers are 30K for gas-gas, 15K for gas-liquid, 10K for liquid-liquid heat transfer [108].

Known technical limitations are taken into account in the configuration. The practical limitations may limit the amount of available heat from one stream or completely exclude the stream from heat recovery. Another set of limitations regard plant layout because the extensive piping required for complex heat integration will be even more impractical if not foreseen to some extent and should be thought of in this assessment. A final limitation can be the one-step cooling and heating of streams entering two-phase stage avoiding increased costs for equipment. These considerations allow for a practical configuration of heat integration with an HRSG system.

A case specific configuration of heat integration will be explained in this section. Based on this configuration the overall process will be evaluated at the expected operation point.

Heat recovery can be completed in the following streams:

- AR flue gas from reactor temperature to 150°C outlet.

- Allothermal reformer flue gas from allothermal temperature to 150^{o}C outlet.
- Syngas cooling from FR temperature to filter temperature.
- Syngas cooling after OLGA.
- Syngas cooling prior to syngas compression train to FTs.
- Intermediate cooling of syngas compression train prior to FTs.
- Intermediate cooling of air compression to allothermal reactor.
- Reformed FT gaseous product two-stage cooling.
- Syngas cooling by OLGA scrubbing liquid, steam for the activated carbon bed regeneration and syngas cooling in the scrubber are not considered in heat recovery. These streams will provide low temperature heat if needed for drying or other purposes but for now, the scrubbing water and steam used for bed regeneration are cooled with water without utilizing this heat. In the OLGA unit, internal heat exchangers will be used to heat up the medium used in the stripper and any excess heat requirements are expected to be met by the residual heat from the heat integration and HRSG system developed.

Heat is required for the following streams:

- Close water circuit for drying.
- Steam for the FR.
- Air pre-heating for the AR.
- Air pre-heating for the activated carbon bed air injection.
- Syngas heating to hydrolysis reactor temperature.
- Syngas heating to warm guard bed temperature.
- Syngas heating to FT-reactor temperature.
- Steam pre-heating for the FT- allothermal reformer.
- Air pre-heating for the FT-allothermal reformer.
- FT product pre-heating prior to FT- allothermal reformer**.**
- OLGA unit.
- Plant heating demand.

Electrical power is required for the following:

- Initial pre-treatment
- Dryer power consumption.
- Air-fan to the AR.
- Two-stage compression of syngas prior to FTs.
- Two-stage compression of air prior to FT- allothermal reformer**.**
- Pump for HRSG system.
- Circulators and additional pumps, compressors not accounted for in the model.
- Heat utilities covered by electrical heating.
- Plant electricity needs.

Heat integration main guidelines considered:

- FT-product cooling is done in one step when prior to flash drum.
- The heat recovery of FTs products should be done in close proximity to minimize piping and in a simple manner to minimize complexity.
- FT-reactor cooling is done by pressurized water, undergoing phase change and close to the reactor temperature but at sufficient temperature difference.
- Syngas exiting the FR with heavy tar compounds should be cooled by high temperature medium to avoid a cold heat-exchanger surface on which tars will be condensed.
- Combustible components heat-exchanging with air should be avoided for safety reasons.
- When two-step cooling or heating is required, technoeconomic criteria should be considered to assess less energy-efficient, but more cost-effective solutions.

The modelling of heat integration begins by introducing a water stream and increasing its pressure to 48 bar which exhibits a sufficient temperature difference between the FT-reactor operating temperature of 300^{o}C and the water saturation temperature of 260^{o}C. It is assumed that the water would enter the FT-reactor at 5K of subcooling and exit at 5K superheating. Enough water will be passed from the reactor cooling system to extract the necessary heat at these design specifications. In the modelling done, there is more pressurized water flow than necessary for FT-reactor cooling. Therefore, a splitter is used to split the excess water flow while allowing for more water flow to be passed to the FT-reactor if more cooling is required. The heating of the medium-pressure water stream is done by 5 streams, of which 1 to 3 of them can be controlled to provide more or less heat therefore giving flexibility to the FT-reactor cooling system. The total flow of pressurized water is calculated to cool down the FT-product prior to the first flash drum in a heat-exchanger with 15 K pinch point. The pressurized water flows in, firstly cooling down the FT-product prior to the second flash drum, then the FT-product prior to the first flash drum. Then the remaining goal is to recover heat from the FT-allothermal reformer stream while no condensation occurring in the stream, the syngas' intermediate cooling of the FTs compression train and the steam exiting the second turbine at 1bar. The three latter streams' outlet temperature can be controlled to provide more or less heat for the pressurized water to reach 5K of subcooling.

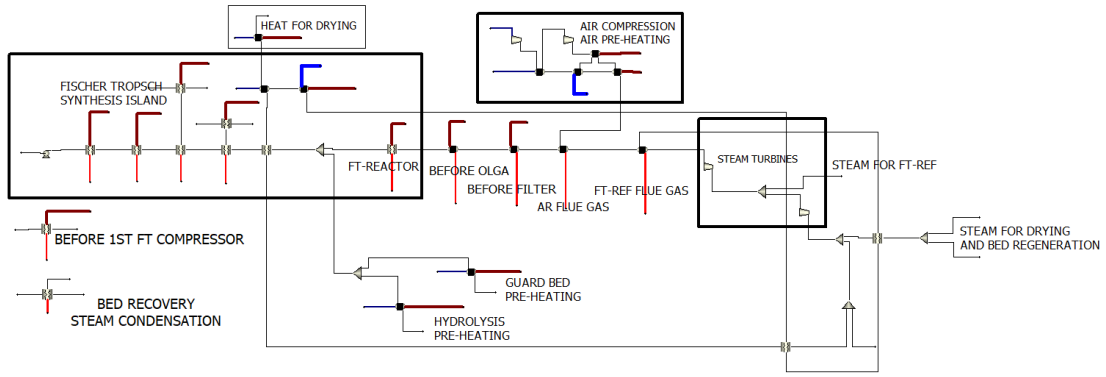

Figure 22: HRSG - Aspen Plus™ Flowsheet.

The water is vaporized in the FT-reactor and is led to be superheated by firstly the syngas cooling after the filter, then the syngas cooling after the FR and then by oxygen depleted air and FT-allothermal reformer flue gas. The superheated medium pressure steam is expanded in two stages with the first stage exit being at 15bar to extract the steam necessary for the FT-allothermal reformer. The temperature of this stream will be a little higher than the one used in modelling, but due to convergence issues it was not set as the new steam inlet temperature to the reactor. Then, the second expansion stage at 1 bar outlet pressure. Part of the exit steam will be separated and heated to produce the steam going to the gasifier and the activated carbon bed regeneration. The necessary heat will be provided by the FT-allothermal reformer flue gas which then goes on to provide heat to the rest of the split 1 bar steam coming out from the second expansion stage. The 1bar steam then provides heat to the pressurized water and the rest of its heat is transferred to the syngas prior to the FT-reactor which needs to be heated up to the FT-reactor temperature. The rest of the required heat for this stream is given by the FT-allothermal reformer flue gas.

An air-air-AR flue gas configuration has been devised to heat up the air necessary for gasification and in parallel heat up and pressurize the air necessary for the FT-allothermal reformer which is pressurized by a compression train with intermediate cooling. After the first stage pressurization, air for the gasification is used to cool down the pressurized air. The pressurized air proceeds to the second compression stage and is almost at the inlet temperature set for air entering the FT-allothermal reformer. AR flue gas still has high temperature heat to give as it did not manage to give all of its heat to the medium pressure steam. Therefore, a three-heat exchanger configuration is used to utilize its heat by firstly giving its high temperature heat to the air going to the AR, then to the compressed air and again to the air going to the AR as in Figure 23.

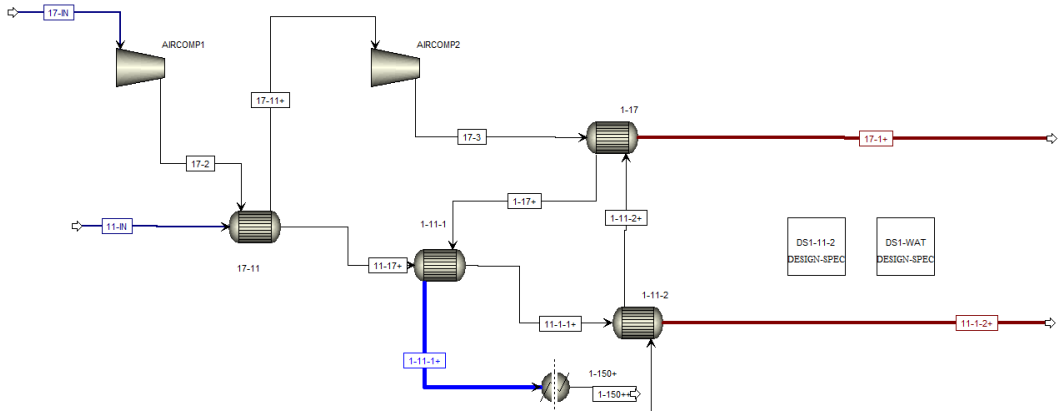

Figure 23: Air pre-heating configuration- Aspen Plus™ flowsheet

The remaining 1bar steam is used to produce hot water for drying and the rest of its heat is not further utilized in the process.

The stream of pressurized water split from going to the FT-reactor is used to heat syngas for the hydrolysis reactor and the warm guard bed.

Cooling water is used to complete the cooling of the following streams:

- FT-allothermal reformer.
- Intermediate cooling of syngas compression train prior to FTs.
- Steam regeneration of activated carbon beds.
- Syngas cooling prior to syngas compression train to FTs.

Operating parameters and information about the developed model are summarized in Table 27.

Table 27: Operating parameters of the model.

	Parameter	Unit	Value
Dryer	T_{bio-in}	°C	25
	$T_{bio-out}$	°C	40
	Moisture-in	%	20
	Moisture-out	%	12
	Heat consumption	kWh/t_{H2O}	1300
	Power consumption	kJ/kg	115
	Water circuit inlet/outlet	°C	90/60
Gasifier	T_{AR}	°C	950
	T_{FR}	°C	850
	S/B		0.6
	CO_2/B		0.2
	T_{steam}	°C	500
	T_{air}	°C	450
	CC	%	98

	Heat loss	% Heat input (LHV)	1
	OC loss	% Circulation	0.1
	Non-equilibrium compounds		
	Hydrocarbon yields:		
	CH_4	mol/kg dry bio	4.434
	C_2H_4	mol/kg dry bio	1.227
	C_2H_6	mol/kg dry bio	0.316
	C_3H_8	mol/kg dry bio	0.01452
	C_6H_6	mol/kg dry bio	0.03846
	$C_{10}H_8$	mol/kg dry bio	0.00391
	Nitrogen conversion to:		
	NH_3	%	70
	HCN	%	0.5
	N_2	%	29.5
	Sulfur conversion to:		
	H_2S	%	95
	COS	%	5
	Chlorine conversion to:		
	HCl	%	20
Filter	T_{filter}	°C	550
	Particulate removal	%	100
	Solids removal	%	100
OLGA	T_{in}	°C	400
	T_{out}	°C	80
	Heavy Tar removal	%	100
	BTX removal	%	30
Condenser	T_{out}	°C	30
Activated carbon beds	T_{bed1}	°C	30
	T_{bed2}	°C	30
	BTX removal	%	100
	H_2S removal	%	100
	O_2/H_2S	mol/mol	7
	T_{steam} regeneration	°C	500
	m_{steam}/m_{carbon}	kg_{steam}/kg_{carbon}	4
	m_{BTX}/ m_{carbon}	g_{BTX}/g_{Carbon}	0.25
Hydrolysis	$T_{reactor}$	°C	205

Scrubber	$T_{stage1\text{-}out}$	°C	60
	$T_{stage2\text{-}out}$	°C	30
	NH_3 removal	%	100
	HCl removal	%	100
Activated carbon bed	T_{bed}	°C	30
	H_2S removal	%	90
Guard beds	T_{bed1}	°C	200
	Impurity removal	%	100
	T_{bed2}	°C	200
	Deoxygenation	%	100
FT unit inlet	T_{cool}	°C	35
	1st Comp. P_{out}	bar	5
	T_{int_cool}	°C	35
	2nd Comp. P_{out}	bar	15
FTs	$T_{reactor}$	°C	300
	$P_{reactor}$	bar	15
	$H_2/(CO+CO_2)$	mol/mol	1.87
	α	-	0.7
	CO conversion		$-0.6957x^2+ 0.2225x + 0.95$
	CO_2 conversion		$-0.776x^2 + 1.558x - 0.492$
	CH_4 selectivity		0.0206x + 0.1588
	C_2-C_4 selectivity		0.0344x + 0.345
	C_2-C_4 O/P selectivity		-0.0205x + 0.7739
	C_{5+} O/P selectivity		$0.035429x^2 + 0.040971x + 0.76163$
	C_{5+} selectivity		$1\text{-}SCH_4\text{-}SC_2\text{-}C_4$
FT product separation	T_{flash1}	°C	120
	T_{flash2}	°C	31
	T_{flash3}	°C	30
FT product recirculation	RR	-	1
FT allothermal reformer	$T_{fluegas}$	°C	950
	$T_{reformer}$	°C	900
	Steam/Methane	mol/mol	3
FT condenser	T_{cond}	°C	80

4.3 Process modelling results

4.3.1 CLG model validation

The performed modelling has been mostly based on integrating experimental data rather than creating a predictive model able to extrapolate the used data therefore, it is valid only within the range of validation. The CLG model is a modified-equilibrium model predicting the formation of non-equilibrium components. The models' accuracy has been validated for different operational parameters and fuels and it can be used in the range of validation as the results show no significant deviation from the experimental results. Available experimental data from pilot plants using ilmenite as an OC were used for the model in addition to an autothermal CLG operational point calculated by a validated model. Information about the data used are summarized in Table 28.

Table 28: Pilot plant experimental data summary.

	Regime*	Feedstock	Ref
1 MW_{th}	Turbulent	Pine Forest Residue	[71]
50 kW_{th}	Turbulent	Wheat Straw Pellets	[109]
	Turbulent	Pine Forest Residue	[69]
1.5 kW_{th}	Bubbling	Pine Wood	[110]
CLARA model		Forest Residues	[102]

*Information about operating regime taken from [69].

Figure 24 shows the summary of all comparisons between the experimental results from pilot plants and the model's results under the same operational points. In Annex II more analytical information and comparisons are included. The factors included in the model are fuel composition, FR temperature, steam to biomass ratio, air equivalence ratio (ER) of the FR and carbon conversion in the FR. The results evaluated in the model validation are CO_2, CO, H_2, CH_4, H_2O and when given, the C_2-C_3 and tar content. Tar content, C_2-C_3 and CH_4 concentrations were determined mostly by the reaction extent set in the non-equilibrium reactor, so their formation in the model is not related to gasifier operating conditions. Rather, based on the experimental results a certain formation extent was set, through fitting to experimental data, to predict non-equilibrium compound formation with sufficient accuracy. Carbon conversion is not predicted by the model as it is highly variable for different reactors and operating conditions, so the one calculated in the experimental results is used for the model validation. In industrial applications a carbon conversion of 98% or near 100% is expected [71]. The model has with sufficient accuracy predicted the syngas composition for T_{FR}, S/B, ER_{FR} within the ranges specified in Table 29.

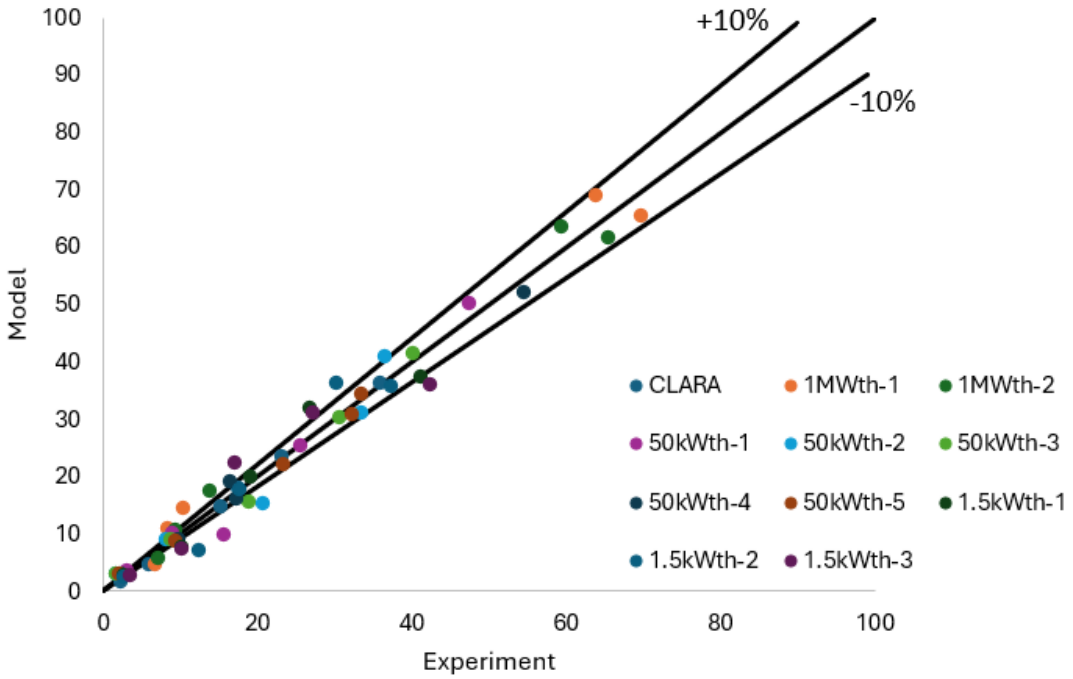

Figure 24: Model predictions and results from operational points at pilot tests. (see Annex II)

Table 29: Model parameter range of validation.

	Min	Max
T_{FR}	804	940
S/B	0.6	0.93
ER_{FR}	0.24	0.44

4.3.2 Key Performance Indicators (KPIs)

The following KPIs were chosen to evaluate the process.

- Cold Gas Efficiency (CGE)

$$CGE = \frac{\dot{m}_{syngas} * LHV_{syngas}}{\dot{m}_{bio} * LHV_{bio} + \dot{m}_{tars} * LHV_{tars} + \dot{m}_{RR} * LHV_{RR}}$$

CGE is calculated for the CLG unit battery limits with inlet streams being the biomass and recirculated streams i.e., tars including BTX, FT gaseous products.

- Cold Gas efficiency including gas cleaning (CGESC)

$$CGESC = \frac{\dot{m}_{syngas} * LHV_{syngas}}{\dot{m}_{bio} * LHV_{bio}}$$

The battery limit is extended from the CLG to right before fuel synthesis.

- Mass conversion efficiency (MCE)

$$MCE = \frac{FTcrude}{\dot{m}_{bio}(d.b.) + \dot{m}_{CO_2} + \dot{m}_{H_2}}$$

Where m_{CO_2} is the mass flow of CO_2 used for fluidization in the CLG unit and m_{H_2} is the mass flow of added H_2 prior to FTs.

- Energy conversion efficiency (ECE)

$$ECE = \frac{\dot{m}_{FTcrude} * LHV_{FTcrude}}{\dot{m}_{bio}(a.r.) * LHV_{bio} + m_{H_2} * LHV_{H_2}}$$

- Carbon Utilization (CU)

$$CU = \frac{Total\ C\ atoms\ in\ FTcrude}{Total\ C\ atoms\ in}$$

CU is calculated for the whole process battery limits with inlet streams being the biomass and CO_2 used in the CLG unit.

- Overall plant efficiency (OPE)

$$OPE = \frac{Q_{FTcrude} + P_{el,prod} + Q_{excess}}{Q_{bio} + Q_{H_2} + P_{el,cons}}$$

The Q_{excess} is the excess heat of the process however it is not utilized further in this case, and it is set equal to zero.

- Jet Fuel Carbon Utilization (JFCU)

$$JFCU = \frac{Total\ C\ atoms\ in\ C_{10} - C_{16}\ FTcrude\ fraction}{Total\ C\ atoms\ in}$$

This KPI quantifies the ratio of the total carbon atoms going to the Jet Fuel fraction of FT-crude, considered here to be C_{10}-C_{16}.

- Naphtha Carbon Utilization (NACU)

Similar to JFCU but for C_5-C_9 and quantifies the ratio of the total carbon atoms going to the naphtha fraction of FT-crude.

- Heavy and wax fraction Carbon Utilization (HWCU)

Similar to JFCU for C_{17+} and quantifies the ratio of the total carbon atoms going to long-chain hydrocarbons and wax.

- Yearly FT-crude production expressed as energy. (FTE)

$$FTE = FTcrude * LHV_{FTcrude}$$

4.3.3 Results

The biomass inlet flow for the model runs is set based on the resulting cost-supply curves considering 8000 h of operation yearly. The chosen plant capacity is 70kt_{DM} of biomass per year thus, 3.03 kg/s of wet biomass at the assumed 20% moisture content when it enters the dryer. Because more than 50% of supplied biomass in all cases is OTP, and the other feedstocks have only slightly different composition, OTP was chosen as the representative feedstock for the model simulations.

The results on KPIs from section 4.3.2 are summarized in Table 30. In addition, FT-crude production in mass flow terms, the available excess heat for utilization above 60°C, electricity production and consumption. This table provides a good overview of the process, showing its great efficiency. The high CGE and CU mean that a large part of biomass is converted to FT-crude which shows promise in GHGs emission reduction while utilizing much of the inlet energy. Furthermore, the electricity balance is slightly deficient, requiring grid electricity, however, an optimization would likely yield enough electricity to counterbalance any further electricity demand. Lastly, the high excess heat available for applications like district heating or providing low grade heat for other industries in the region reveals the potential for much higher overall plant efficiencies if it is considered. Unmentioned results will be discussed in the following sections.

Table 30: Key results of the overall process.

	Value	Unit
Cold Gas Efficiency (CGE)	79.54	%
Cold Gas Efficiency incl. Syngas Cleaning (CGESC)	77.38	%
Mass Conversion Efficiency (MCE)	28.14	%
Energy Conversion Efficiency (ECE)	50.37	%
Carbon Utilization (CU)	57.99	%
Jet Fuel Carbon Utilization (JFCU)	12.94	%
Naphtha Carbon Utilization (NACU)	34.76	%
Heavy-wax Carbon Utilization (HWCU)	1.98	%
FT-crude production	0.937	kg/s
Yearly Fischer-Tropsch product energy (FTE)	$1.2 \cdot 10^6$	GJ
Overall Plant Efficiency (OPE)	35.83	%
Electricity consumption	9.03	MW_e
Electricity production	8.78	MW_e
Heat above 60°C	26.79	MW_{th}

Results of the model simulations on OTP CLG are summarized in Table 31. The CLG unit operates at ~42MW_{th} producing a syngas with high concentration of CO_2, partly because of the large amount of CO_2 used for fluidization. Due to the unreacted char and tar recirculation, the FR ER is slightly lower than the AR ER and this is calculated here to quantify the amount of oxygen that oxidizes combustibles in the AR. OC

circulation is 3.88 kg/s/MW_{th}, in the range achieved in a 1 MW_{th} pilot plant [71], transferring 15.7 MW_{th} of heat to the FR along with oxygen and produce 0.68 $Nm^3/kg_{dry\text{-}bio}$ of syngas ($CO+H_2$). Syngas yield is in line with experimental results and predictions considering the high char conversion assumed and the high ER needed for autothermal operation [69]. It needs to be highlighted that this model represents an industrial scale CLG unit with optimal operation regarding char conversion and heat loss.

Table 31: Results from the CLG unit model.

	Unit	Value
Feedstock		OTP
Biomass flow (MC 12%)	kg/s	2.762
Thermal input (LHV)	MW_{th}	41.87
FR fluidization steam	kg/s	1.66
Fresh air to AR	kg/s	6.00
Inert & fluidization CO_2	kg/s	0.55
Tar recirculation	kg/s	0.0086
AR equivalence ratio	-	0.38
FR equivalence ratio	-	0.35
CGE	%	79.54
OC circulation	kg/s	162.6
OC heat transfer to FR	MW_{th}	15.7
Syngas yield	Nm^3/kg	0.68
Syngas composition		
X_{H2O}	vol%	0.424
X_{CO2}	vol%-dry	0.421
X_{CO}	vol%-dry	0.180
X_{H2}	vol%-dry	0.291
X_{CH4}	vol%-dry	0.069
$X_{C2\text{-}C3}$	vol%-dry	0.024
Heavy tars	g/Nm^3 dry	0.349
BTX	g/Nm^3 dry	2.097
AR outlet		
O_2	vol%	0
H_2O	vol%	0.0019
CO_2	vol%	0.0160
CO	vol%	0
H2	vol%	0
N2	vol%	0.9821

A summary of the main streams is given in Table 32 with each stream corresponding to the streams in Figure 25. The progression of impurity removal can be seen and the expected syngas composition entering the FTs island. The syngas meets FT catalyst specifications with the guard bed sufficiently removing impurities and for the purposes of this simulation it is assumed they are 100% removed.

Table 32: Main process streams.

	Unit	WET-BIO	DRY-BIO	SYNGAS-1	SYNGAS-3	SYNGAS-4	SYNGAS-6	SYNGAS-8
Mass flow	kg/s	3.038	2.762	6.144	6.138	4.173	4.228	4.202
Temperature	°C	25	40	850	80	30	205	200
Pressure	bar	1	1	1	1	1	1	1
O_2	Mole fraction			0	0	0	0	0
H_2O				0.4237	0.424	0.032	0.031	0.033
CO_2				0.2426	0.243	0.408	0.402	0.406
CO				0.1038	0.104	0.175	0.173	0.175
H_2				0.1678	0.168	0.282	0.278	0.281
CH_4				0.0400	0.040	0.067	0.066	0.067
C_2H_4				0.0111	0.011	0.019	0.018	0.019
C_2H_6				0.0028	0.003	0.005	0.005	0.005
C_3H_8				0.0001	0.000	0.000	0.000	0.000
C_6H_6				0.0003	0.000	0.000	0	0
$C_{10}H_8$				3.52E-05	0	0	0	0
N_2				0.0010	0.001	0.001	0.015	0.015
NH_3				0.0057	0.006	0.010	0.010	0
CL_2				7.12E-05	0	0	0	0
HCL				3.56E-05	3.56E-05	5.98E-05	5.90E-05	0
H_2S				3.20E-04	3.21E-04	5.38E-04	2.78E-05	0
COS				1.69E-05	1.69E-05	2.83E-05	1.98E-07	0
HCN				4.09E-04	4.09E-04	6.87E-04	3.44E-07	0
BIOMASS	Mass fraction	1	1					

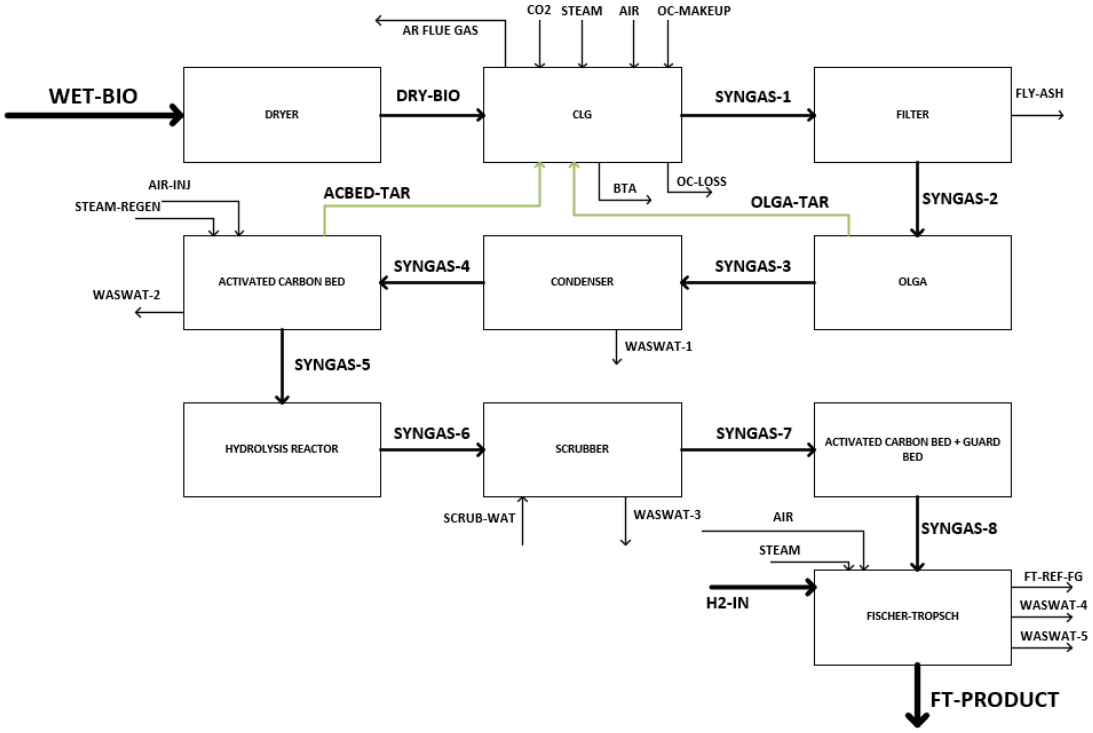

Figure 25: Simple block flow diagram of the overall process.

The heat balance of the process is depicted in Figure 26. The low heat demand of the dryer is due to the low moisture content of the feedstock entering the dryer. The CLG unit has low heat losses, and the rest of the chemical energy decrease is going to inlet stream heating part of which can be useful high temperature heat. Minimal losses are observed during the gas cleaning process. Most of the efficiency loss comes from the FTs island due to the highly exothermic FTs and the part of the syngas combusted to sustain steam reforming.

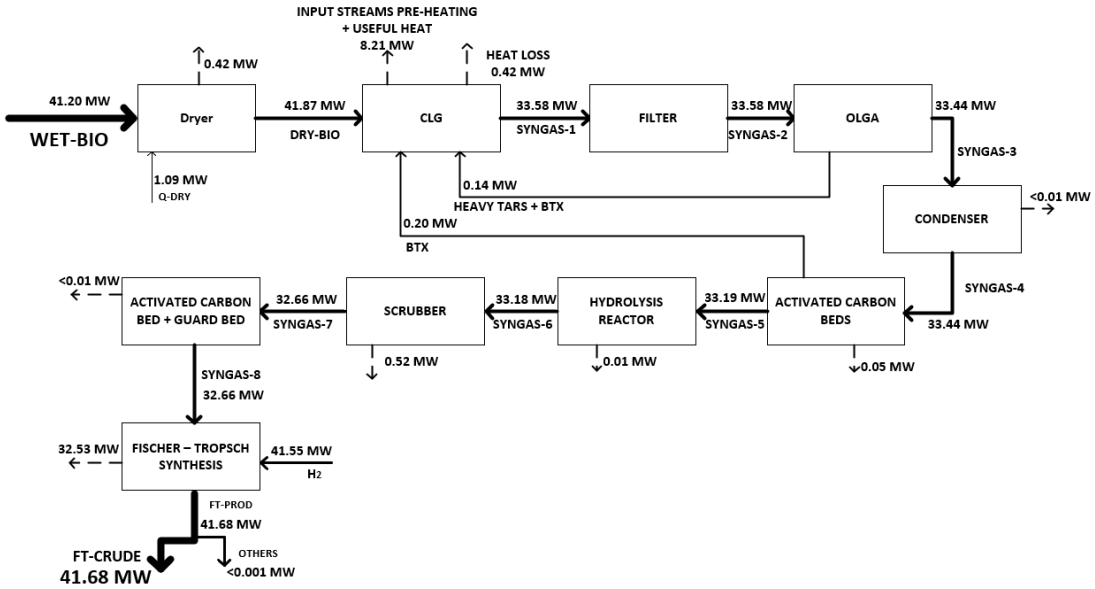

Figure 26: Heat balance of the process.

The carbon balance of the process is depicted in Figure 27. Unreacted char going to the AR of the CLG along with recirculated tars end up in the AR flue gas as CO_2. Low carbon losses occur in the condenser as they are carried with condensed water and similarly in the scrubber some carbon species leave the system with condensed water. The FT-PRODUCT stream refers to the whole product as it is not separated fully from lighter carbon species and a separation is shown for FT-crude matching carbon utilization. Most of the carbon losses occur in the flue gas of the allothermal steam reformer which shows there is potential to increase carbon utilization with another strategy such as using an autothermal reformer. Also, this carbon balance has been based on the assumption that CO_2 used for fluidization is external. It should be underlined that in case of partial recirculation of CO_2 captured from FTs off gases, carbon utilization is calculated to 67.2%.

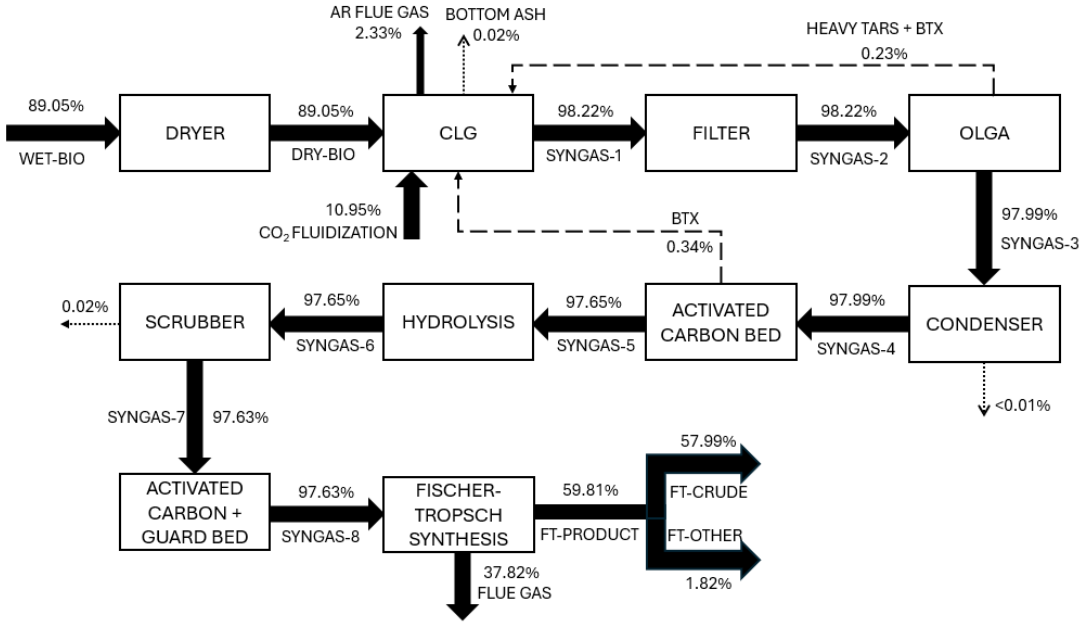

Figure 27: Carbon balance of the process scheme.

The FT-crude composition in mass fractions is depicted in Figure 28.

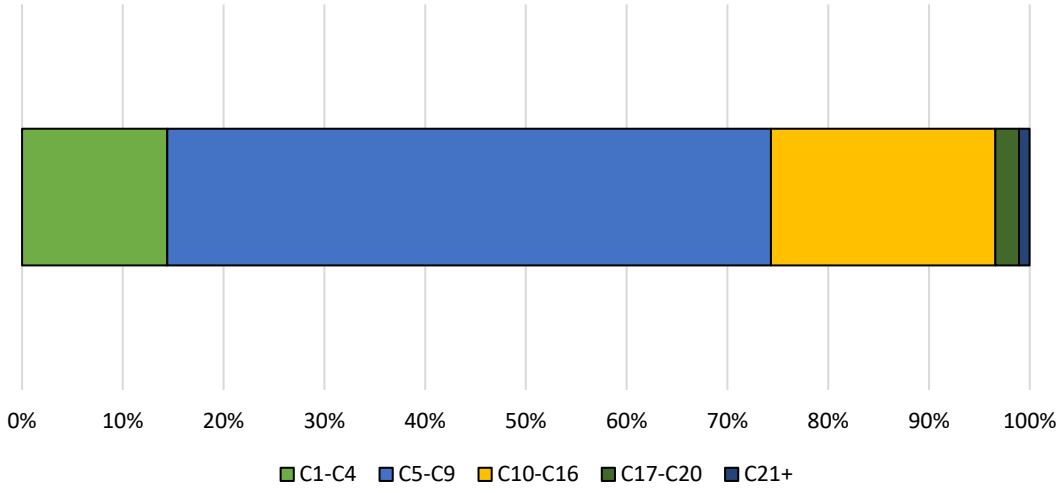

Figure 28: Mass fraction composition of FT-crude.

An important note on the previous and following figures is that the mass fraction is depicted and not the calculated yields of naphtha, jet fuel and heavier HCs which were on total carbon basis. Also, the produced FT-crude refers to the separated fractions of the HC mixture exiting the FT reactor. The low temperature of 30°C allowed for some of the produced C_1-C_4 fraction to be separated as well as the C_{5+} fraction which in many cases would be sold as LPG. However, the produced FT-crude from HTFT with a Fe-based catalyst has a high olefin content. The mass fraction of olefins and paraffins at each fraction of the FT-crude is depicted in Figure 29. The high olefin content and high C_5-C_9 yield with simultaneously considerable C_{10}-C_{16} yield allow for targeted production of aviation biofuels which will be a product of high demand in the market. The light HCs and the C_5-C_9 can be oligomerized and turned into longer-chain HCs.

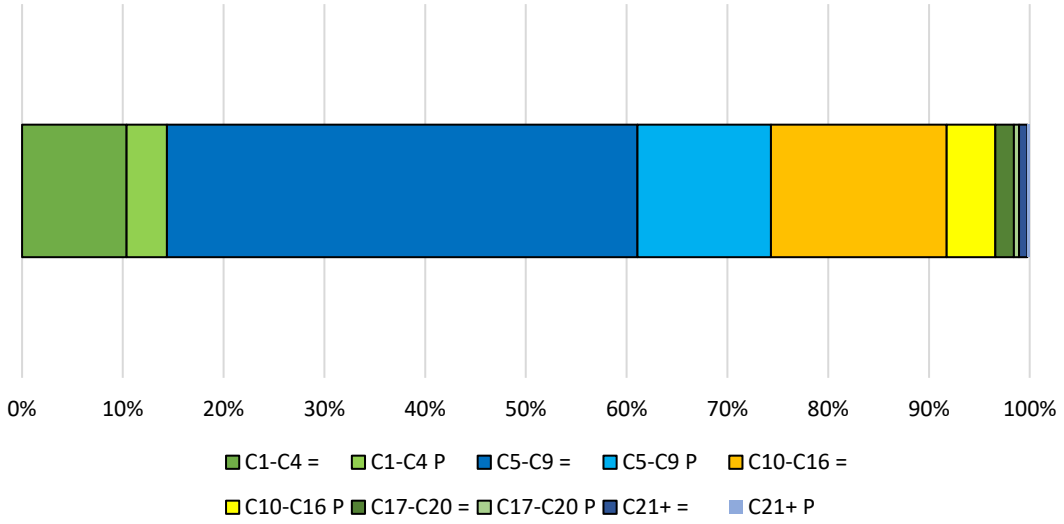

Figure 29: Olefin and paraffin distribution in the FT-crude fractions.

4.3.3.1 Sensitivity analysis

Based on the previously explained results it would be interesting to see how the specific steps and the overall process are affected by changing gasification operating parameters. Thus, a sensitivity analysis was performed on the gasification operating parameters within the model's validated range under autothermal operation. Because of autothermal operation, ER is a dependent variable in the sensitivity analysis.

At first, the CGE behavior was investigated relative to the FR temperature for different S/B and moisture content and the results are illustrated in Figure 30, Figure 31. There are two main trends observed. In particular, the CGE drop when S/B or moisture increases and when FR temperature increases. The fuel is oxidized to sustain endothermic gasification reactions and heating streams to the reactor temperature. Increasing the inlet streams' flow without increasing temperature or lowering the FR temperature will cause a CGE decrease as more chemical energy of the fuel is converted to heat. A different trend would be possible if higher steam addition would mean more char is converted in the FR, but this effect is not as important in DFBG or CLG as the heat from char combustion would be eventually transported from the AR to the FR.

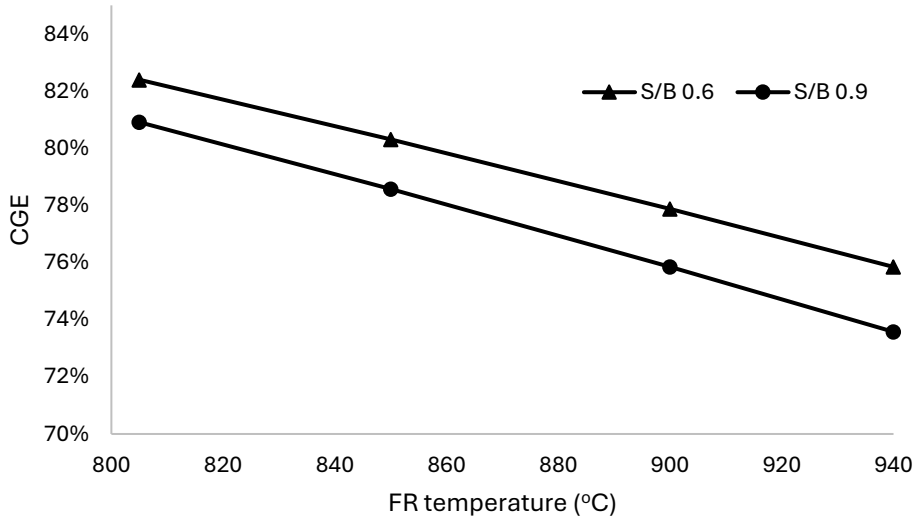

Figure 30: CGE versus fuel reactor temperature for moisture content 9% and S/B of 0.6 and 0.9.

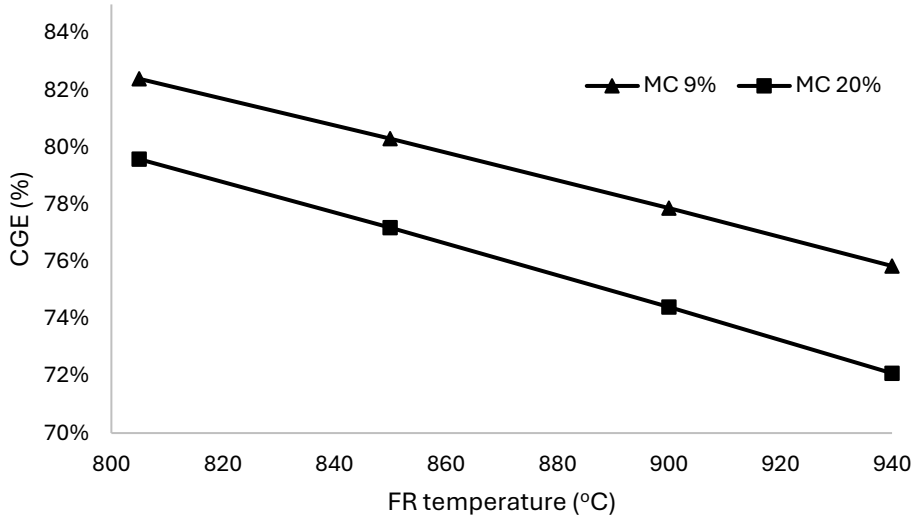

Figure 31: CGE versus fuel reactor temperature for S/B =0.6 and Moisture Content of 9% and 20%.

The next step was to study syngas composition changes with varying FR temperature, moisture and S/B and the results are depicted in Figure 32, Figure 33 and Figure 34. The equivalence ratio is also shown in the following figures. From the results, it can be seen that an increase in S/B or moisture will lead to a more oxidized fuel with only small variations in syngas composition for the investigated range.

The FR temperature was shown to have the greatest impact in syngas composition and the significant changes can be attributed to two factors. One factor is similar to the CGE explanation, that with increased FR temperature, more fuel is oxidized to provide heat for inlet streams. The other factor is that under higher temperatures, the endothermic reactions are favored like the rWGS reaction that seems to play a role in the observed changes. Despite the continuously increasing ER with higher FR temperature, CO_2 concentration only slightly increases together with CO at the expense of H_2. Therefore, it can be deduced that rWGS consumes H_2 producing CO and H_2O while the oxidation of CO takes place further pushing the rWGS which is also favored by the higher operating temperature shifting equilibrium towards CO and H_2O. An optimal point of FR temperature should be determined also by other factors such as char conversion and tar production both of which are better with higher operating temperatures.

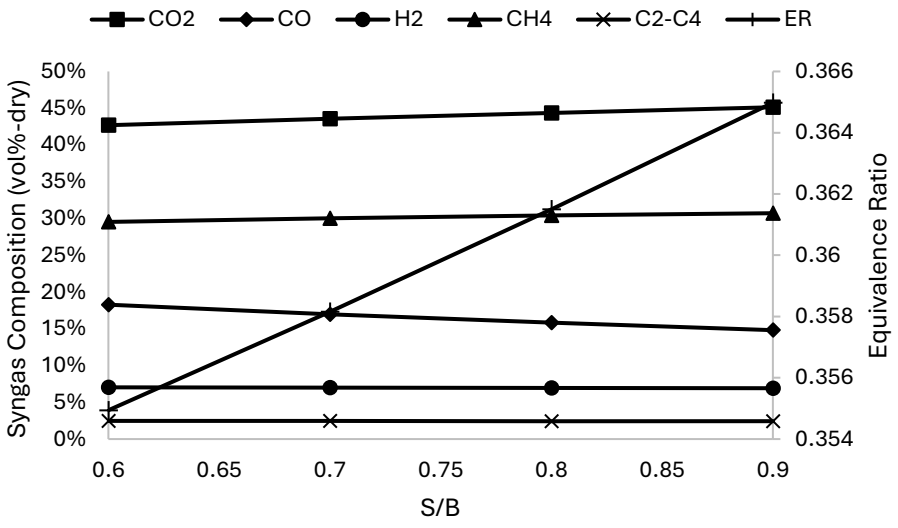

Figure 32: Syngas composition versus S/B at 850oC FR temperature and 12% moisture.

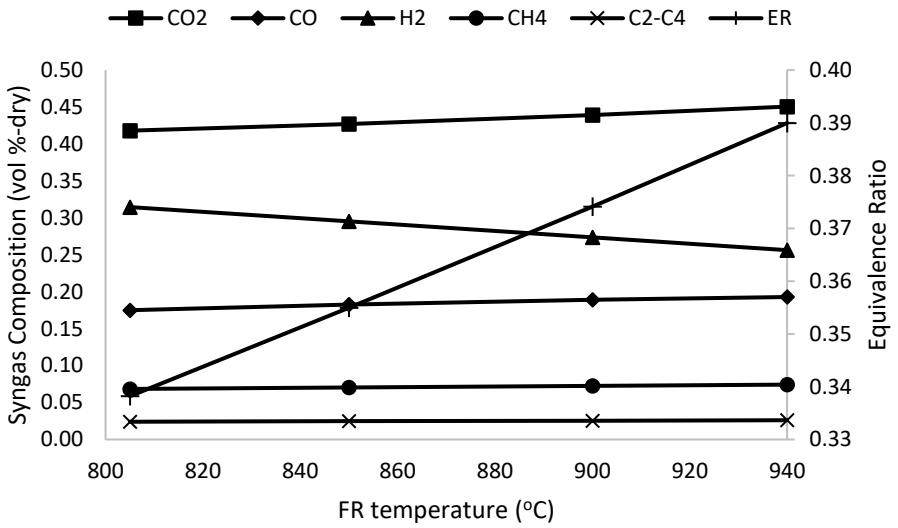

Figure 33: Syngas composition versus FR temperature at 12% moisture and 0.6 S/B.

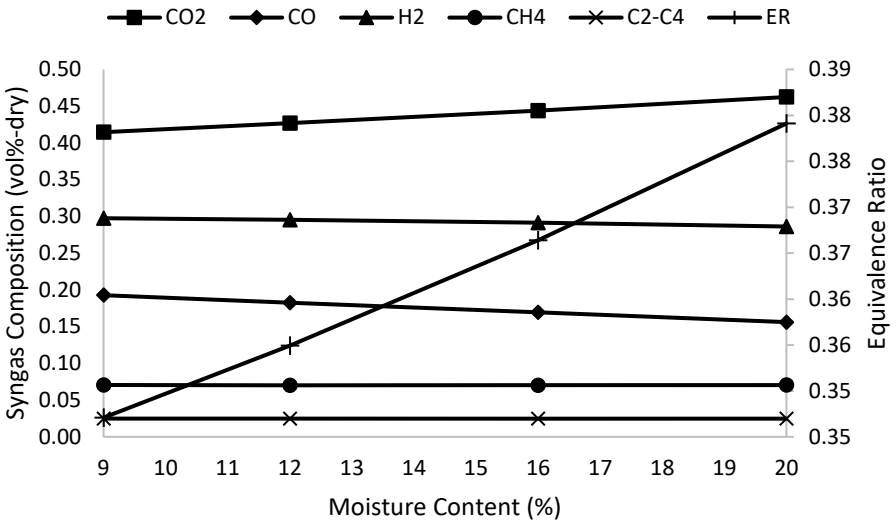

Figure 34: Syngas composition versus moisture at 850oC FR temperature and 0.6 S/B.

A main efficiency of the process is considered its ability to utilize carbon therefore it was investigated in the sensitivity analysis for FR temperature, S/B and moisture. The resulting curves are shown in Figure 35, Figure 36. The FR temperature increase, slightly increased total carbon utilization with the relative difference within a constant S/B being around 0.1%. This difference could be attributed to a very slight decrease of the CO_2/ ($CO+CO_2$) ratio with increasing FR temperature, resulting to a higher total carbon conversion slightly. This difference is quite small, so an additional factor might play a role. In particular, the difference in composition of the product after the FT reactor will affect the product separation step. Therefore, if more product is separated, it results in higher carbon utilization. Moving on, a considerable increase is observed when increasing S/B or moisture. This is due to a higher CO_2/ ($CO+CO_2$) ratio leading to a lower carbon utilization. The differences in carbon utilization are small, so operational advantages from different parameters might justify a carbon utilization decrease.

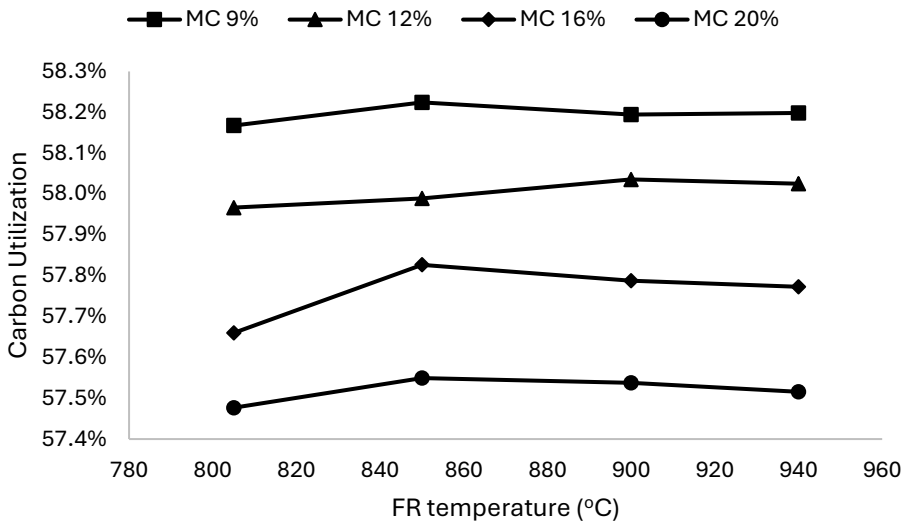

Figure 35: Carbon utilization versus the FR temperature for different moisture at 0.6 S/B.

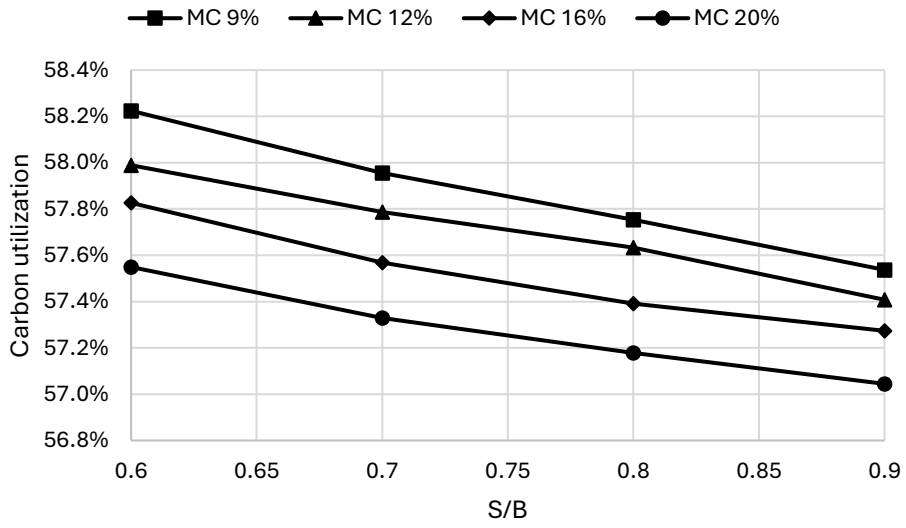

Figure 36: Carbon utilization versus S/B for different moisture at 850oC.

The jet fuel yield, on total carbon basis, was also investigated with the results shown in Figure 37, Figure 38. Similar trends to carbon utilization are observed with small relative differences which can be explained by the same factors with an additional one. The total carbon conversion due to a CO_2/ ($CO+CO_2$) ratio increase is accompanied by a higher C_{5+} selectivity therefore based on the ASF distribution, more jet fuel fraction HCs will be produced and separated, ending up in the FT-crude.

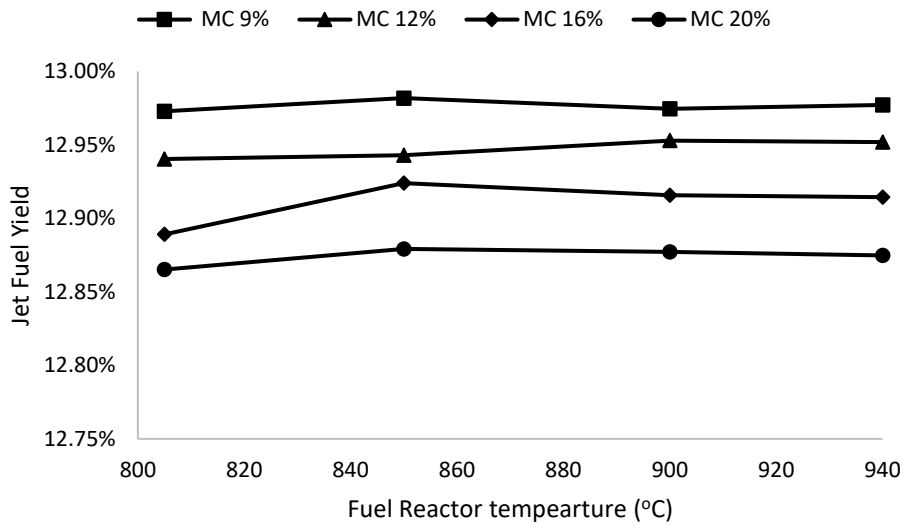

Figure 37: Jet Fuel Yield versus the FR temperature for different moisture contents at 0.6 S/B.

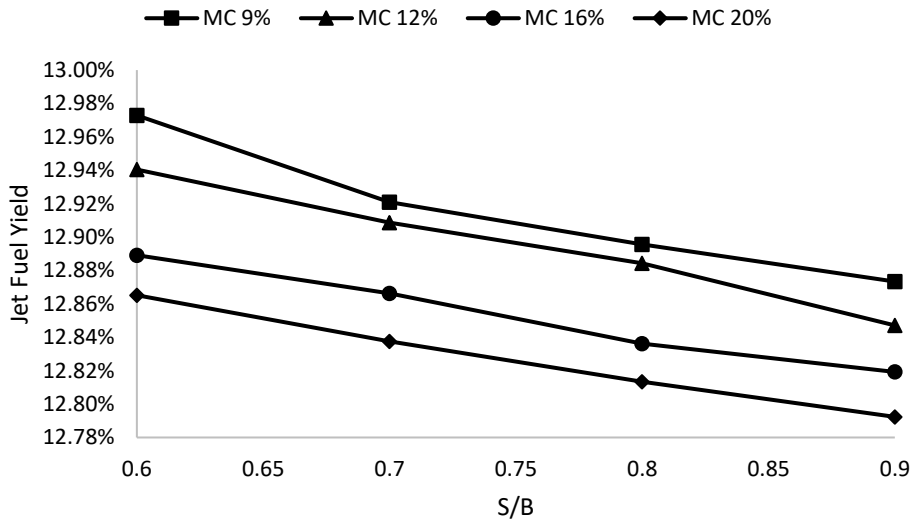

Figure 38: Jet Fuel Yield versus S/B for different moisture at 850oC.

As a general bottom line, the operating parameters of the CLG unit have small impact to the overall plant's performance in terms of biofuels production. This can be explained by the FTs converting both CO_2 and CO, while the reformer due to lack of CO, H_2O and the high operating temperature, converts much of the CO_2 to CO leading to a high total carbon conversion. Thus, CLG operational parameters will be chosen based other criteria, such as minimizing tar production or achieving high H_2 content.

4.4 Discussion

The CLG unit operated under autothermal conditions with ilmenite as an OC and OTP as feedstock. Inlet stream pre-heating is set at 400°C and 450°C for air and steam respectively, the CGE of the unit was 79.54%. This result is in line with [111] that achieved ~80% with ilmenite as OC and higher than a work with LD-slag as an OC in

which a maximum of 76% CGE was obtained, but with slightly different operating conditions [112]. The sensitivity analysis of CGE for different FR temperature, moisture and S/B showed a CGE higher than 71% in all cases. Therefore, a sufficient pre-heating of inlet streams will ensure the gasification unit has a high CGE under many different operating conditions. The pre-heating of streams should be optimized with other criteria besides the maximum technically obtainable pre-heating. One such criterion could be a technoeconomic one, of configuring the HRSG system to produce more electrical power, in which case lower pre-heating is achieved.

Moving on to the gas cleaning process train, the employed processes do not significantly decrease the chemical energy content of the produced syngas with the CGE dropping slightly to 77.38% which means a good gas cleaning configuration is employed.

Because CO_2 was not removed from the syngas, a greater part of the available carbon, entered the FT reactor. Coupled with the recirculation of part of the FT gases and the support from the external green H_2, part of CO_2 was eventually converted to HCs yielding a high CU of ~58%. This can be compared to results from [111] that achieved a CU of 32.48% revealing the immense gains from keeping CO_2 in the process as much as possible. Further increase in carbon utilization will be possible if instead of the allothermal reformer, an autothermal reformer is employed, but this alternative requires oxygen to be purchased or produced on-site. Another option is to use O_2-rich air which will lower the compression work and enhance carbon efficiency of the process. The current designs' maximum effective recirculation of FT gases is approximately 75%.

The energy conversion efficiency of this configuration is 50% which considers as input the biomass and hydrogen energy content. This efficiency is lower than the achieved in [111] of 53% and the difference is mostly due to the higher efficiency of the FTs unit in the latter case. The exact cause of this efficiency loss is unknown, but it could be due to a more exothermic FTs or due to the allothermal reformer operation.

The last important beneficial aspect from utilizing the CO_2 content is the increase in mass-percentage yield of FT-crude which in this case is 28.1% while in [111] is 20.6%. However, the FT-crude of the latter case is composed of C_{5+} HCs while in this case the C_1-C_4 fraction separated with the conventional FT-crude of C_{5+} HCs is also considered. A great part of the C_1-C_4 fraction is olefins that can be turned into long-chain HCs by oligomerization and are thus considered as a sold product within the FT-crude. The part of C_1-C_4 is not high enough to fully explain the mass conversion difference of the two configurations.

The use of available excess heat, allows for feedstock with higher moisture content to be used which means that cheaper feedstock and with less pre-treatment can be bought from biomass suppliers, lowering the biomass price. For the considered dryer a low energy demand is calculated of 1 MW_{th} or approximately 2.4% of the biomass energy content on a LHV (d.b.). The CLG unit shows good behaviour with a high CGE

under the expected operating parameters of industrial scale CLG units and the results agree with literature data. Ilmenite seems to be a good OC option for CLG with low tar production and considering the low contaminant level of the feedstock there will be economic and technical benefits in gas cleaning. The syngas cleaning process train was configured using cost-effective solutions suitable for medium scale applications. In large-scale applications the benefits of using other established methods start to show due to economies of scale. This gas cleaning train makes use of dedicated process steps for specific impurity removal in parallel to the activated carbon beds which can serve a multifunctional purpose removing multiple contaminants, according to the chosen design. This will improve the operational flexibility of the processing plant as it creates a more robust gas cleaning train able to handle not only the initially chosen feedstocks, but also other more difficult feedstocks. The energy input to the plant comes from biomass and hydrogen that leads to the gasification and gas cleaning parts being at 42 MW_{th} scale while the FTs island is at 74 MW_{th} scale. Hydrogen addition prior to FTs is necessary to achieve the desired ratio of $H_2/(CO+CO_2)$ because at low ratios the FTs reactor will face catalytic issues, and most importantly, lower product yield. The present configuration requires a high amount of hydrogen addition with part of its energy being used to the allothermal reformer. Using hydrogen energy content to produce heat for the reformer does not seem appealing. Alternative configurations should be considered employing pressure swing adsorption (PSA) units and possibly some carbon discharge. Lowering carbon utilization could improve technoeconomics, but an investigation of efficiency penalties should be done.

Around 50% of biomass and hydrogen energy input is converted to useful product. The generated heat is recuperated via the HRSG system so part of it is internally exchanged, wasted via cooling water, lost to the environment or becomes electricity. The final excess heat available for utilization or in need for further cooling is 26.79 MW at temperature above 60^{o}C or 32% of biomass and hydrogen heat input. Heat available above 60^{o}C could be directed to district heating or other applications.

The plant, under this configuration, is almost self-sufficient with a slightly negative balance on electricity needs. With an optimized HRSG it is possible to cover many of the demands, even from the equipment compensating the pressure drops. This could be facilitated, if needed, by a small boiler increasing steam temperature, since the power generation equipment already exists in the configuration.

An overall plant efficiency of 35.83% is obtained without the utilization of excess heat and almost 27000 tonnes of FT-crude are produced corresponding to $1.2 \cdot 10^6$ GJ or 333 GWh of energy content. The mass conversion of input dry biomass, CO_2 and hydrogen is 28% with a jet fuel yield of 13% on carbon basis. According to data from ELSTAT on aviation fuel consumption in Greece [113], assuming that 50% of FT-crude will be converted to C_{10}-C_{16}, this plant can cover 2.4% of the aviation fuel demand or 7% of SAF demand in 2040 without projecting consumption increase.

5. Technoeconomic assessment

The technoeconomic assessment of the proposed processing plant was performed according to the method described by Peters, Timmerhaus and West [114]. It will result in the Total Capital Investment (TCI) and the break-even selling price (BESP) of FT-crude, which is calculated on the basis of 10% IRR through a discounted cash flow analysis.

Literature data were used to find equipment and utility prices. The developed model was used to size equipment units and calculate utility needs. It is estimated that, done right, the method used will provide an accuracy of +/- 30% with only major equipment costs needing to be considered. The actual accuracy of this method though is not expected to be in this range, as there are many hurdles in correctly estimating the necessary variables.

Product specification

FT-crude is the C_{1+} HC fraction of the separated product, thus excluding inert compounds without market value. Literature usually refers to FT-crude as the C_{5+} fraction because it is the dominant fraction in LTFT characterized by the high chain growth probability. Sometimes, FT-crude is defined as the C_{1+} fraction and this approach is chosen here due to the olefin content in FT-crude from the employed Fe-based HTFT being more than 70%. Olefins can through oligomerization be upgraded to longer-chain HCs, and by using proper catalysts increasing the yield of the desired fractions. The opposite approach is followed in LTFT where the wax fraction of FT-crude is cracked to form shorter-chain HCs. Hence, the divergence from the usual literature definition of FT-crude is prudent in this case.

5.1 Methodology

The methodology used to determine TCI is schematically illustrated in Figure 39 as a simple diagram. Almost all of the necessary factors are considered as a percentage of the total purchased equipment cost (TPEC), making its calculation essential to the methodology. TPEC is the total cost of equipment without the additional costs related to installation as they are defined in [114]. This proves to be difficult to find in literature because the reporting methods differ, so which factors are included in the reported costs is not always clear, but even when it is clear, the included factors are only sometimes reported. Moreover, many of the available literature data on equipment cost are old, in some cases, more than 15-20 years. Therefore, they lack accuracy when transposed to more recent years despite accounting for inflation and other changes by the use of specially designed indexes. The use of old equipment costs should be avoided whenever possible as with time and technological advancement, the equipment cost will change. The cost index used in this analysis is the Chemical Engineering Plant Cost Index (CEPCI). It requires the conversion of estimates made in

different currencies, to USD incurring further uncertainty in the calculations due to currency value change. It is therefore prudent to assume that this analysis will most likely provide an estimate of the TCI even beyond the initially stated +/- 30%.

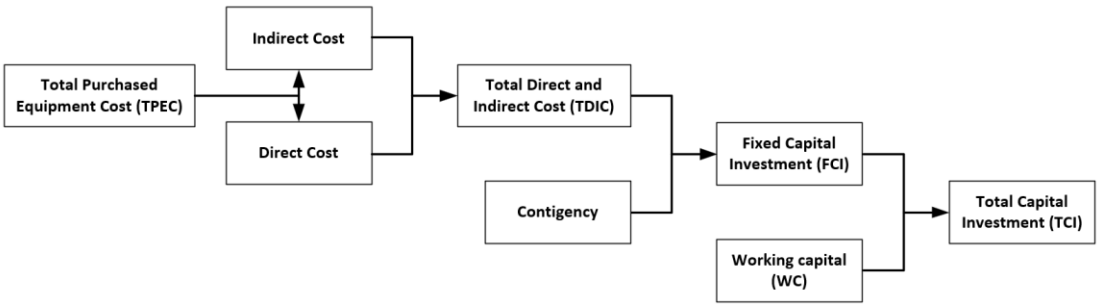

Figure 39: TCI calculation methodology.

The method for calculating equipment cost at a different scale and year based on the reference year's equipment cost and size relies on the use of scaling factors and the aforementioned CEPCI values. The reference size of the equipment is a variable suitable to approximate its cost at a different scale by the use of a scaling factor on the ratio of the actual and the reference value of the variable. When including the ratio of CEPCI values between the year that the cost is reported and the year basis for the assessment then, Eq. 12 can be used to transpose the cost at the desired size and year. The year basis for this assessment was chosen to be 2023 and a comparison is also done, for 2020 that had a lower CEPCI value and therefore costs would be more comparable to other literature costs. The exchange rates for every currency for the reference and the base year are taken from the European Central Bank.

$$EC_i = EC_{ref} \cdot \left(\frac{D_i}{D_{ref}}\right)^{sf} \cdot \frac{CEPCI_{year}}{CEPCI_{ref}} \qquad \textit{Eq. 12}$$

The individual purchase equipment cost can be summed to yield the TPEC. Based on it, the factors to estimate total direct and indirect costs are incorporated. Alternatively, if known, individual factors can be used for each equipment to determine the fixed capital investment (FCI) upon which the working capital (WC) will be added to yield the TCI. Between the two approaches, the former is chosen for this analysis, according to which an installation factor is used to determine the direct cost. The installation factor includes the installation cost, instrumentation and controls, piping, electrical, buildings including services and yard improvements. Additionally, the indirect costs include engineering and supervision, construction, legal expenses and contractor's fees and are referenced to the TPEC. Based on the direct and indirect costs, the contingency is calculated which yields the FCI. The FCI is used to calculate the WC which is added to the FCI yielding the TCI. In reality, these factors will vary with plant scale and region. The cost assessment is done for the n^{th} plant, meaning that the proposed plant has either already been built, so knowledge is acquired, or there is

extensive knowledge of the components, and their connection is not an issue. The abovementioned factors and their values are summarized in Table 33.

Table 33: Factors used to calculate the TCI, Start-up expenses and land purchase.

Description	**Value**	
Direct Costs		
TPEC	100	
Purchased equipment installation	39	% TPEC
Instrumentation and controls	26	% TPEC
Piping	31	% TPEC
Electrical systems	10	% TPEC
Building (including services)	29	% TPEC
Yard improvements	12	% TPEC
Total Direct Cost (DC)	247%*TPEC	
Indirect Costs		
Engineering and Supervision	32	% TPEC
Construction	34	% TPEC
Legal and contractor's fees	23	% TPEC
Total Indirect costs (IC)	89%*TPEC	
Total direct and indirect costs (TDIC)	TDC+IC	
Contingency	20	% TDIC
Fixed Capital Investment (FCI)	120%*TDIC	
Working Capital	10	% FCI
Total cost of investment (TCI)	110%*FCI	
Startup expense	5	% FCI
Land purchase	6	% TPEC

Apart from TCI, the operating costs need to be considered. These include the fixed operating costs and the variable operating costs. The estimation of fixed operating costs is approached by relating them to the FCI and the yearly salaries. They include general expenses, maintenance and repairs, taxes and insurance. The values used in this assessment are summarized in Table 34.

Table 34: Factors used to calculate the Fixed Operating Costs.

Fixed Operating Costs	**Value**	
Maintenance and Repairs	5	%FCI
Taxes and Insurance	2	%FCI
General expenses	60	% Salaries

The variable operating costs include the raw material used in the process, the utilities, catalysts etc. and the operating labor. The electrical balance of the plant yields only a slight deficiency in produced electricity. While the pressure compensating equipment would increase power consumption, the optimization of HRSG is expected to cover the increased demand, thus, the plant is considered self-sufficient. Prices of raw materials, utilities and catalysts used in this assessment are summarized in Table 35. The necessary quantities are extracted from literature or the simulation results.

Table 35: Prices of raw material, utilities and catalysts.

Raw material	**Value**	**Unit**	**Ref**
Biomass	70.31	€/t_{DM}	Chapter 3
CO_2	40	€/t	[115]
Green H_2	3.5	€/kg	Assumed
Utility prices			
Ilmenite	300	€/t	[104]
Ash disposal	25	€/t	[104]
OLGA scrubbing liquid	1.12	€/lt	[116]
Fresh water	2	€/t	[104]
Wastewater discharge	4	€/t	[104]
Catalysts			
Hydrolysis [a]	16000	€/t	[104]
Fischer-Tropsch	2000	€/t	Note b
Reformer catalyst	7700	€/t	[117]

a) Assumed to be the same as a WGS catalyst, but this is an overestimation.
b) Based on catalyst composition and current market prices of the components with sufficient price increase due to catalyst preparation associated costs. As a reference point the Cobalt catalyst price in [104] versus the price of Cobalt were compared.

Operating labor is calculated based on a methodology proposed in [114] that considers process steps and plant production capacity to determine the amount of labor hours needed. The relevant process steps in this process are 5 and the product capacity is 0.936 kg/s. Considering that each labor works 40 hours per week and 230 working days per year, the labors needed are 65 and with the average labor cost per employee in Greece estimated to be 32000 €, the yearly labor cost is calculated at 2.09M€.

To calculate the break-even selling price of FT product, a discounted cash flow model is used. The financial parameters used in this analysis are summarized in Table 36.

Table 36: Financial parameters for the technoeconomic assessment.

Financial parameter	**Value**	**Unit**
Yearly operation	8000	h
Discount rate	8	%
Interest rate	6	%
Tax rate	22	%

Depreciation period	10	years
Construction period	3	years
Construction expenses breakdown		
1st year	8	% FCI
2nd year	60	% FCI
3rd year	32	% FCI
Capital breakdown		
Own capital	100%	
Subsidy	0%	
Loan	0%	

As seen on the described methodology the calculation of TPEC is essential with all other costs being based on it. When TPEC is overestimated, the TCI can be many times higher yielding unrealistic results. Overestimating TPEC based on literature data is easy when the associated costs included in the reported equipment cost are not clearly specified. Often, the available costs are for a version of uninstalled equipment cost, meaning that some factors are already included in the reported cost and an installation factor is given. In other cases, an installed equipment cost was stated. Therefore, a strategy was used to overcome this issue, according to which when the reported equipment cost was clearly specified as uninstalled purchase equipment cost and without including any related costs, it was taken as an uninstalled equipment cost according to its definition in this thesis. When equipment cost was given as uninstalled purchase equipment cost already including some costs, but the authors had specified an installation factor for the specific equipment, the installed cost was calculated, and the purchase equipment cost was back calculated from the installed cost. When the equipment cost was clearly specified as installed equipment cost then the purchase equipment cost was again back calculated. The factor used to derive the purchase equipment cost was 2.47 according to Table 33.

The justification for the employed methodology is based on the reporting methods of literature being more consistent with the installed equipment cost definition. TPEC is defined as the sum of purchase equipment cost, but in this methodology this cost is only needed to estimate the constituents of TCI. Therefore, for the purposes of this assessment, TPEC is only an approximated value based on which, components of the TCI and TCI are calculated. Calculating the installed equipment cost of the processing plant and back calculating TPEC using the factor considered to yield the installed equipment cost in the employed methodology will be a more consistent method. Basing the TCI calculation on the reported uninstalled equipment costs containing some of the factors would be more wrong as it would in all likelihood lead to a significant overestimation of the TCI.

5.2 Results

The resulting BESP of FT-crude is 3.54 €/kg for 2023 as the basis year and 3.00 €/kg for 2020. The difference between the selling price, highlights the importance of the chosen basis year. This cost is considered high and is mostly due to the assumption of the hydrogen price being 3.5 €/kg. The TCI of the plant is 248 M€ with 2023 as the basis year and 175.6 M€ for 2020, a 29% cost decrease relative to 2023.

The results were obtained based on the equipment costs found in literature for the major units of the proposed processing plant and have been summarized in Table 37. Along with the equipment cost are their scaling factor, reference year and currency, reference size, installation factor and the installed cost in €2023. The reference year costs are either in Euro (€) or USD ($) and the installation factor of 1 indicates an installed reference equipment cost.

Table 37: Installed equipment costs of the plant.

Unit	Scaling unit	Ref. size	Actual size	Scaling factor	Ref. Year	Ref. Cost	Installation factor	Installed Cost	Reference
Pre-treatment									
Feedstock handling	Wet biomass MWth (LHV)	157	41.20	0.31	€ 2010	5.30	1	6.22	[68]
Dryer	Evaporated water (kg/s)	0.342	0.276	0.28	€ 2010	1.90	1	3.18	[68]
Gasification [a]	Dry biomass (kg/s)	17.8	2.431	0.75	€ 2010	12.60	1.5	7.54	[118]
Syngas cleaning									
Hot gas filter	Syngas flow (kmol/s)	1.466	0.270	0.67	€ 2010	5.90	1.15	3.88	[118]
OLGA unit [b]	Normal vol. flow (Nm^3/s)	1000	21751	1	€ 2004	0.20	1	8.99	[92]
Activated carbon beds [c, d]	MW_{th} of gasifier	32	41.87	0.7	€ 2014	1.17	1	2.40	[119]
Hydrolysis reactor	Normal. vol. flow (Nm^3/s)	81.2	3.644	0.67	$ 2005	0.37	2.47	0.18	[120]
Scrubber	Syngas input, kmol/s	1.446	0.163	0.67	€ 2010	5.20	1	2.14	[68]
Activated carbon bed [e]	MW_{th} of gasifier	32	41.87	0.7	€ 2014	0.23	1	0.48	[119]
Guard beds	Syngas MWth	260	32.66	0.85	€ 2010	5.20	1.15	1.82	[121]
FT synthesis									
Syngas compressor 1	Work (MWe)	10	2.229	0.67	€ 2010	5.00	1	3.25	[68]
Syngas compressor 2	Work (MWe)	10	1.390	0.67	€ 2010	5.00	1	2.37	[68]
FT reactor	Feed (kg/s)	23.79	10.35	0.72	$ 2014	12.06	1	8.48	[122]
Steam reformer [f]	Syngas feed (kmol/s)	2.037	0.258	0.67	€ 2010	14.50	1.5	9.67	[108]
Boiler [f]	Boiler input (MWth)	355	24.10	1	$ 2007	52.00	1.49	7.39	[123]
Air compressor 1	Work (MWe)	10	2.372	0.67	€ 2010	5.00	1	3.39	[68]
Air compressor 2	Work (MWe)	10	2.459	0.67	€ 2010	5.00	1	3.47	[68]
Heat integration & Power									
HRSG	Heat transferred (MW_{th})	43.6	61.4	0.8	€ 2010	5.20	1.15	13.97	[68]
Steam turbine 1	Power out (MWe)	15.2	3.905	0.85	€ 2010	6.80	1.15	4.38	[68]
Steam turbine 2	Power out (MWe)	15.2	5.341	0.85	€ 2010	6.80	1.15	5.71	[68]

a) The gasification unit is approximated by two Circulating Fluidized beds and the mentioned installed cost is for one CFB.
b) The cost was based on old data and as a specific investment cost for the OLGA unit without considering scaling effects. Also, the unit is designed for dirtier operation, so the flexibility of this process configuration will allow for cost reduction.
c) The activated carbon bed reported cost also contains the cost for their regeneration system.
d) Unclear which installation costs are included in the mentioned cost, so it should be used with caution.

e) This bed is approximated to be at 1/5 of the activated carbon beds with the regeneration system, but it is likely lower.
f) The allothermal reformer was approximated by a steam reformer and a boiler leading to an overestimation of the cost.

Figure 40 shows the break-down of TCI into its basic constituents, direct and indirect costs, contingency and working capital. Indirect costs are higher than direct costs when contingency is added, emphasizing their importance.

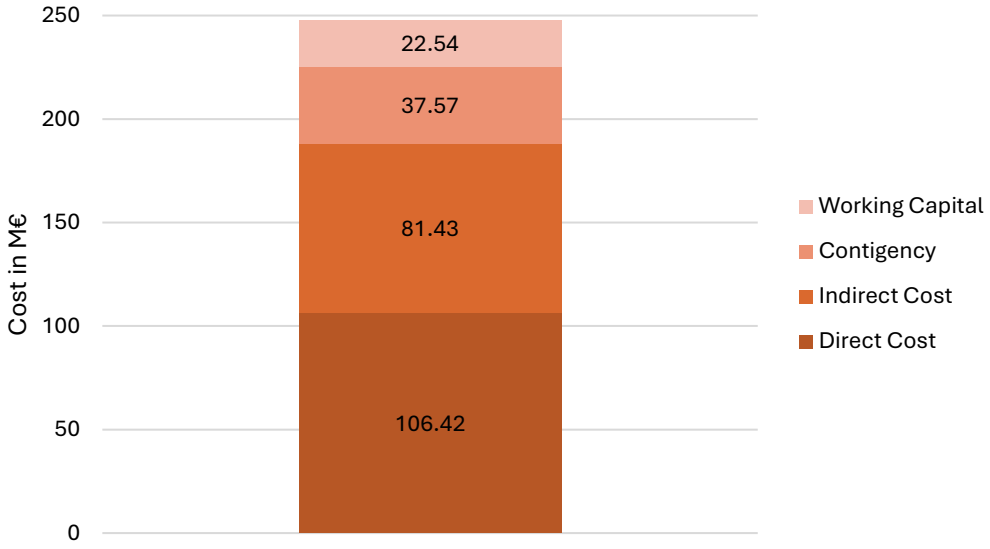

Figure 40: TCI break-down.

The direct costs in this case are considered as the installation costs their break-down is illustrated in Figure 41.

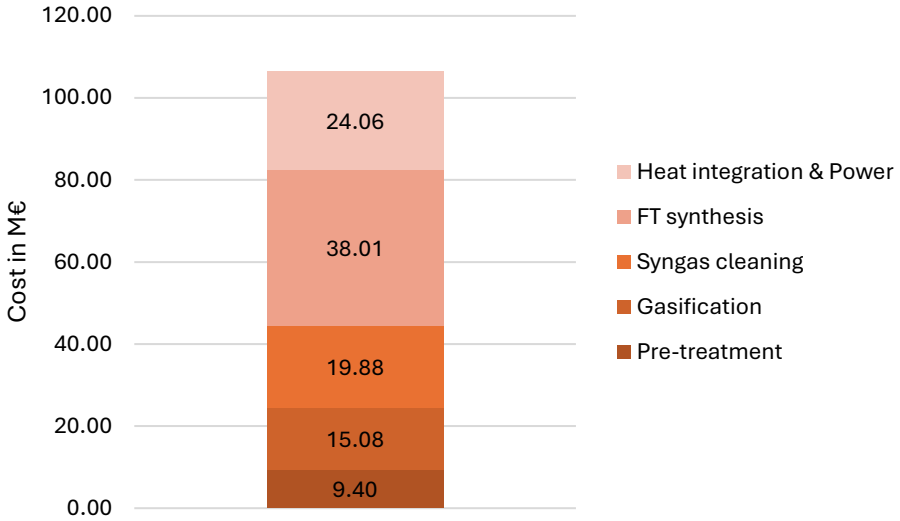

Figure 41: Installed equipment cost breakdown.

As can be seen, the greatest share of installed equipment cost is for the FTs island and the heat integration. This is due to the plant's scale effectively being doubled at the FTs island.

The higher scale of the FTs island explains the high cost for the HRSG system as the fuel synthesis step has most of the cooling and heating demand. The highly exothermic

reactions and the recirculation of gases leading to increased equipment size, lead to a higher overall cost for FTs and HRSG. However, a large share of HRSG is for the power generation.

The gas cleaning section installed equipment costs are broken down in Figure 42.

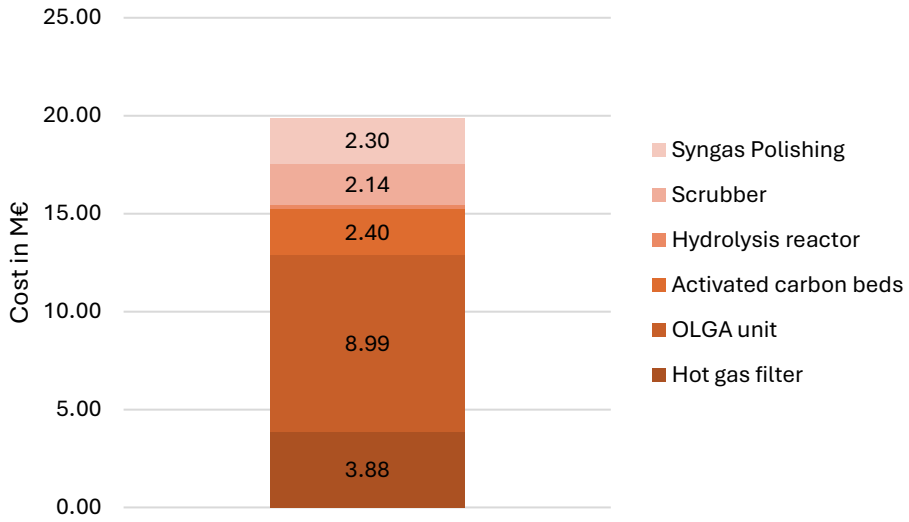

Figure 42: Installed Equipment Cost break-down for the syngas cleaning section.

The gas cleaning section was a major part of the process configuration development. The goal was to employ cost-effective technologies that would allow to remove both the ASU and the AGR unit. From the cost break-down in Figure 41 it is visible that the cost of the gasification unit is close to that of the syngas cleaning process. If this is compared to a similar configuration [104], with an AGR unit, it can be seen that there is a major relative difference between syngas cleaning and chemical looping gasification. In this configuration, the OLGA unit is a large share of the total gas cleaning section's installed cost. Additionally, it is expected that an overestimated cost of the OLGA unit is included. After the OLGA unit, the hot gas filter is the second most expensive equipment while other parts of gas cleaning are in the same cost range. The hydrolysis reactor is not visible as it represents only a very slight cost of 180k€. From this cost breakdown, a goal of this work to propose a cost-effective, robust gas cleaning configuration has been achieved.

The FTs island installed costs are broken down in Figure 43 in its three main parts, the FT reactor, the reforming section and the compression of streams. The FT reactor seems to have the lowest price followed by the compressors. The reforming section is the most expensive and might be due to overestimating the cost of an allothermal steam reforming system by assuming it is a reformer and a boiler. An interesting result would also be to separate the HRSG into each section, which would reveal the cost of the HRSG system in the FTs island.

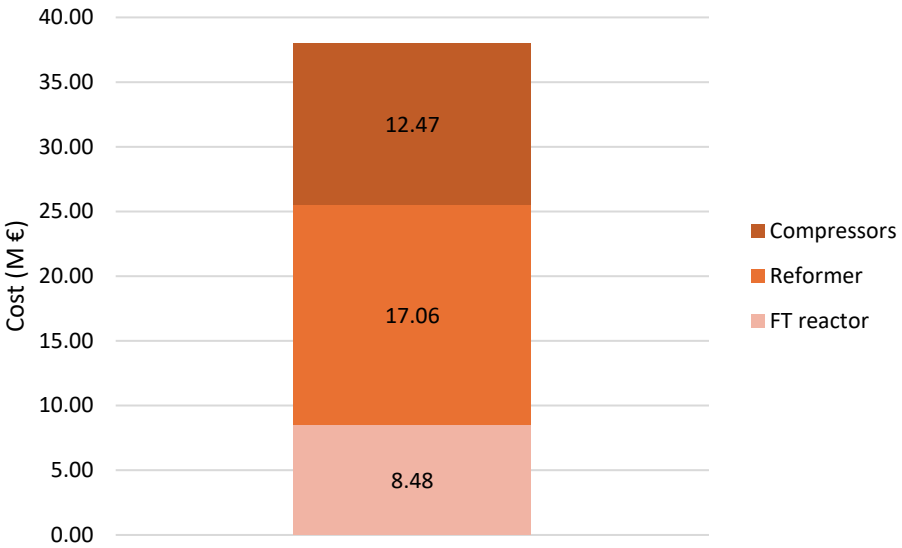

Figure 43: Installed Equipment Cost break-down for the FT island.

The operating costs breakdown is shown in Figure 44. The raw materials which include biomass, H_2 and CO_2 have the largest share of the operating costs and from Figure 45 it is obvious that H_2 is the main contributor to the raw material costs. Regarding utilities, the OC make up followed by OLGA scrubbing liquid are the main material utilities and there can be significant benefits in minimizing these utilities.

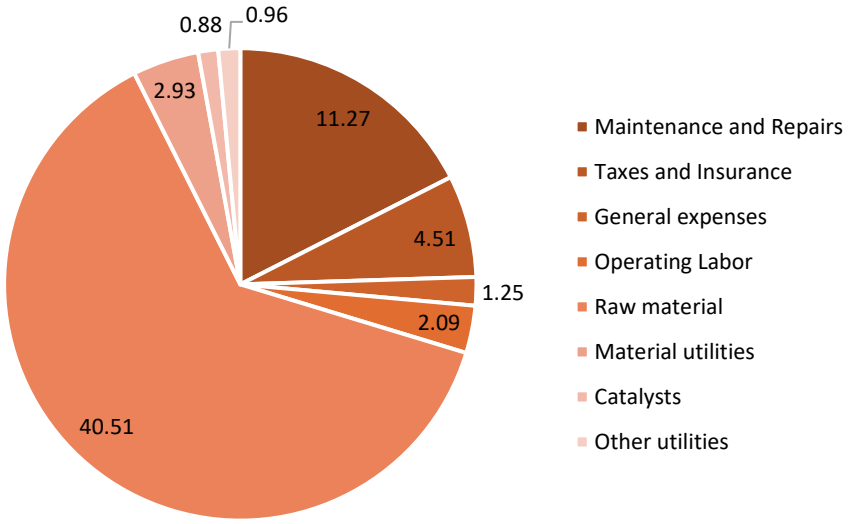

Figure 44: Operating costs break-down in M€.

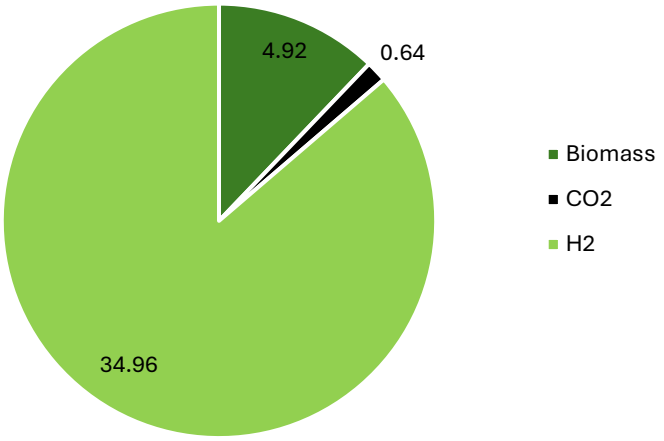

Figure 45: Raw material costs break-down in M€.

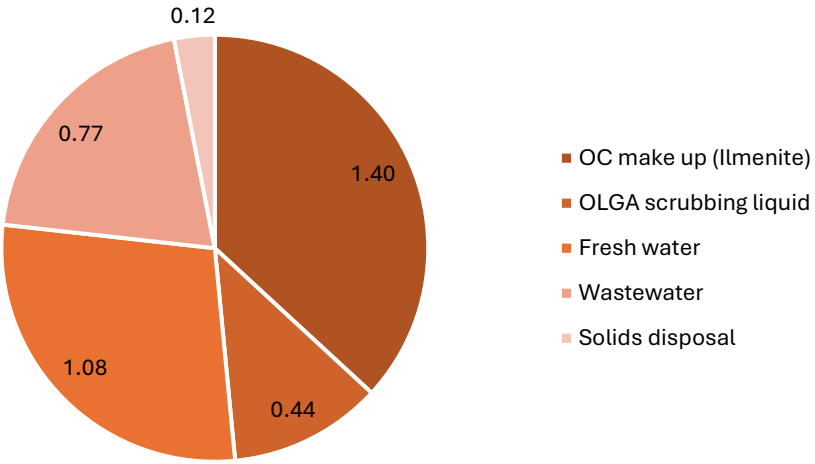

Figure 46: Material utilities cost break-down in M€.

Lastly, Figure 47 and Figure 48 show the contribution of the FCI, OPEX and others i.e., land purchase, start-up expense and working capital for the year basis 2023 and 2020 respectively. For more insight, H_2 and Biomass costs are depicted separately from the OPEX to assess visually the part of BESP related to them. As can be seen, the contribution of H_2 costs surpasses those of the FCI and the biomass even when added. This is, as explained before, due to the large amount of H_2 needed and its high price. Biomass cost has a small contribution because the plant doubles in thermal input at the FTs unit, thus all costs increase while biomass quantity remains low. Comparatively, between the two basis years, the equipment cost for 2020 is lower and operates under the same utility prices. Therefore, hydrogen share of contribution to BESP increases in the 2020 year basis.

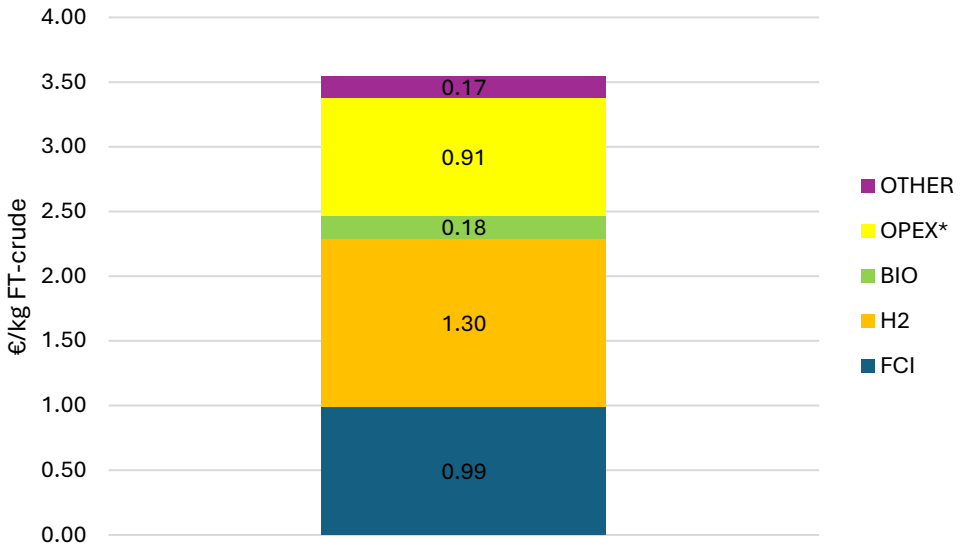

Figure 47: Contribution to BESP for basis year 2023.

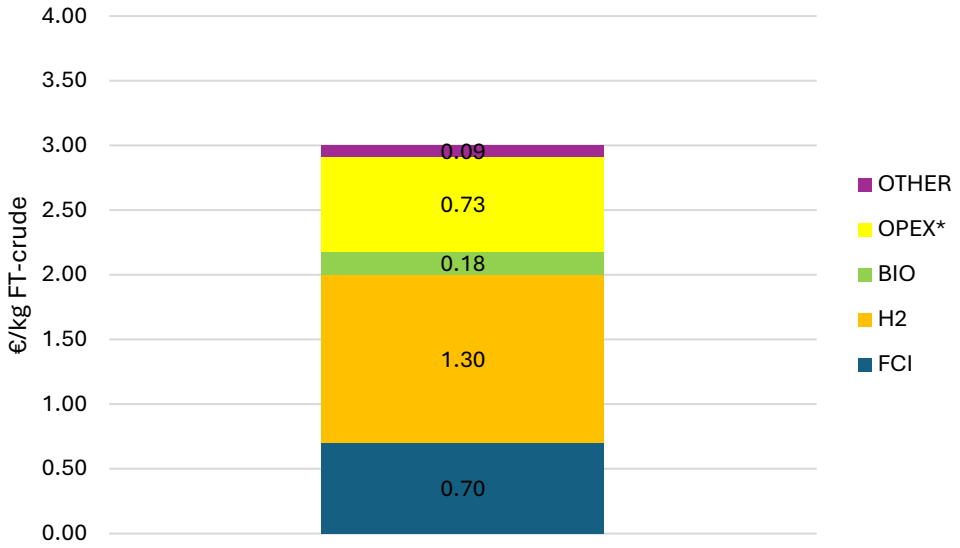

Figure 48: Contribution to BESP for basis year 2020.

5.2.1 Sensitivity Analysis

The results from the analysis of a base case scenario revealed the major contributors to the BESP. A sensitivity analysis regarding the price of H_2 and biomass will provide insight into the effect a potential increase or decrease in their price will have on BESP. Additionally, the plant's capacity is based on the supply security analysis and a 70kt annual biomass supply is chosen. However, if a lower or higher capacity is chosen, supported by the appropriate plan on how to attain the necessary feedstock, it will result in a different TCI and operating costs, thus plants' capacity is also investigated. The last parameter chosen to change is the IRR value based on which the BESP is calculated to show the effect a divergence from the standard 10% IRR will have on BESP. The parameters and their low, base and high case are in Table 38. The results are illustrated in Figure 49 for 2023 basis year and in Figure 50 for 2020.

Table 38: Economic parameter sensitivity analysis cases.

Parameter	Low	Base	High
Hydrogen (€/kg)	2	3.5	5
Biomass (€/t_{DM})	50	70.31	90.4
Capacity (kt_{DM})	50	70	120
IRR	8%	10%	12%

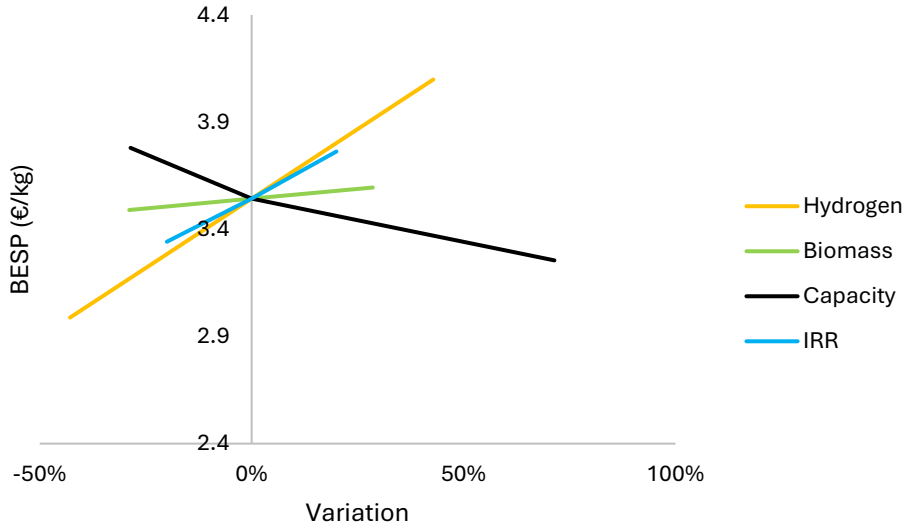

Figure 49: Sensitivity analysis results for year basis 2023.

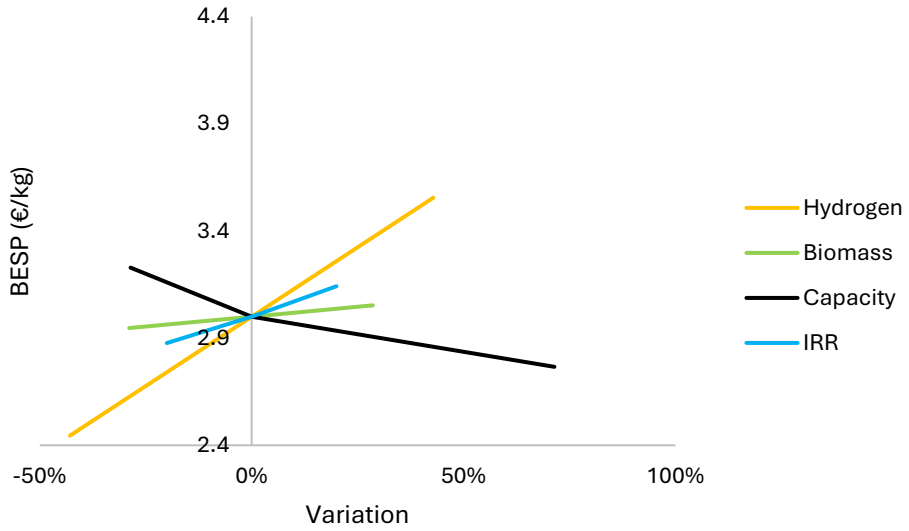

Figure 50: Sensitivity analysis results for year basis 2020.

The results highlight that hydrogen price variation offers the steepest cost reduction while the biomass price variation plays a small part in price reduction. The high case for biomass price was chosen to be the current market's share corresponding SMP. A realistic time frame this production plant can begin operation is close to 7-10 years, at which time, domestic green hydrogen production will have increased, and imports will

be possible to compensate domestic green hydrogen supply deficit or high domestic prices. Additionally, state subsidization of the hydrogen price is a real possibility making the assumed 3.5 €/kg hydrogen price in the base case all the more reasonable.

To isolate plant capacity increase as a factor affecting BESP and due to the low BESP increase with biomass price increase, the accompanied biomass price increase with plant capacity was not considered. It is evident that the economy of scale significantly affects BESP with lower scales, quickly increasing BESP while higher scales steadily decrease it. Increasing plant capacity past a certain point will not be the optimized solution as technologies with lower operating costs will offer bigger BESP reductions.

The last factor in sensitivity analysis was the IRR basis for BESP calculation to show the significance of choosing a suitable IRR value to evaluate the investment. A 10% IRR is commonly used thus it was chosen as the base case.

Comparing the results between the years 2023 and 2020, the same trends are observed, and the results are included for the complete comparison between the two basis years.

5.3 Discussion & Remarks

The analysis in this chapter is deliberately conducted for two basis years instead of one, since it was foreseen, that higher costs would be calculated using recent data. Indeed, the resulting BESP of FT-crude in 2023 basis is 3.54 €/kg while for 2020 basis is 3.00 €/kg, a relative increase of 18%. This means that comparing results based on 2023 to past years is very difficult. The cost increase is attributed to the steep increase in CEPCI values. A factor that might also play a role is the difference in currency exchange rate, in this case between the Euro and USD, for the two basis years.

The technoeconomic evaluation for the proposed advanced biofuels production plant was insightful on the main factors determining BESP and the investment cost. A well based comparison with other works is difficult to perform due to the different financial and other parameter used in the assessment. Also, due to different distribution of HCs in the FT-crude, a pathway with higher BESP can actually be closer to the market, so there is uncertainty in the comparative. Therefore, no extensive comparison is done with literature reported values as the comparison can only provide a rough estimate of the relative BESP values. The FT crude density is assumed to be 750 kg/m^3 for comparison reasons. Since the difference in FT crude composition will yield different density, a more general density is better to transpose the calculated BESP. The BESP to compare is for the 2020 basis year calculations and therefore a base case BESP of 2.25 €/lt is used. Also, expressed in energy content the BESP is 243 €/MWh or 67.5 €/GJ. Comparing with literature, in [124] a BESP of 31 €/GJ of FT-crude was obtained using CLG and CO2 removal indicating the proposed configuration, due to the FTs, resulted in a much higher BESP. The same is observed compared to [125] where the worst cases yield around 120-140 €/MWh and considering carbon tax credit, they go down to 60-70 €/MWh. Other costs in similar ranges were also reported. The calculated BESP is however comparable with synthetic fuels cost of 250 €/MWh in 2020 [126].

Considering the medium plant scale of approximately 40MW biomass and 74MW Fischer-Tropsch the results are encouraging as the sensitivity analysis revealed major economic benefits of scale. Considering, the high impact cost of H_2 has to the BESP, there can be major benefits from improving the configuration for less H_2 consumption.

Results from chapter 3 showed that at a high local market share, the annual supply of 120kt_{DM} biomass is possible, thus exploiting the economy of scale. This biomass supply corresponds to 80MW plant scale, so a less than doubling of the plant scale leads to an improved BESP of 2.76 €/kg. Much larger scales than 70MW will need to be comparatively assessed with different gas cleaning configurations as the lower operating costs of certain capital-intensive solutions might be economically better.

Also, the production plant's feasibility can be significantly improved by operating parameter changes to the two main contributors to the total installed equipment cost, the FTs island and the HRSG system. Reducing the compression needs by operating at a lower pressure or lowering recirculation ratio can reduce the need for electricity production, and HRSG costs, in the latter case, also decreasing the equipment size. However, if operating pressure or the recirculation ratio decrease, the production capacity and efficiencies will be negatively affected. This matter requires a cost-benefit analysis on different operating conditions.

6. Conclusions

A comprehensive framework was used to evaluate different aspects relevant to a commercial advanced biofuels production plant for a case study in the Peloponnese region of Greece. First, major policies of EU and Greece were investigated to set a basis for understanding the current policy landscape and future trends. This part offered a better view of how policy hopes to affect the market, more specifically regarding the goals set by policymakers and the regulatory measures to support or discourage the use of biomass. Following an overview of Greece's regions and available biomass, the Peloponnese region was chosen for the case study and its most promising biomass sources were evaluated. The cost-supply curves were calculated for a hypothetical plant location and used to determine plant capacity, share of biomass types in annual feedstock supply and average cost of feedstock supply. Then, a preliminary level analysis of the proposed plant was conducted. This part included the use of mass and energy balances to evaluate the processing scheme from a performance point of view, and the technoeconomic assessment based on results from previous work in chapters 3 and 4. Thus, a methodological approach was followed to assess the prospects of the proposed plant and the individual or combined results of the employed processes, but also of the region.

The current policy landscape of Greece and the EU favors advanced biofuel production. Policy measures are in place or under development to encourage biomass mobilization and utilization towards biofuel production. From the analysis, it is concluded that both Greece and the EU have recognized the central role biofuels will play in decarbonizing certain sectors in the near-term. Biofuel production apart from SAF, biodiesel and bioethanol will include others, like biogas and biomethane. Regarding transportation biofuels production, the EU and the Greek State have set mandates for the inclusion of biofuels in the fuel mix and will support advanced biofuel production plants.

The analysis conducted in chapter 3, has retrieved data from various literature sources and incorporated them to a methodology for biomass potential estimation. The use of various data sources and filtering between under and over-estimations ensures that this analysis is within the realistic potential of the Peloponnese region regarding the investigated biomass sources which show the most promise to fuel an expansion of the bioeconomy in the future. The assumptions regarding the theoretical potential should be further supported by on-field measurements about pruning and forest residue productivity to better estimate the theoretical potential of each regional unit or municipality. The availability and harvesting efficiency of biomass should be better calculated to include local practices and conditions. The conservative assumption of cumulatively 36% of prunings being left on the field is a good starting point to ensure reliability of the feedstock security assessment and the general biomass availability of the Peloponnese region. The inclusion of the mobilization rate and market share

capture allows for a more realistic estimate of the feedstock's cost at the processing plant gate, as it constrains the use of the cheap biomass sources which would lead to unrealistic estimates of the feedstock cost. The mobilization rate has been assumed to be 50% for prunings and 20% for forest residue on a 10-year projection. However, it could be much higher, close to 100% for prunings, if the state imposes policy measures regarding pruning handling and disposal. Forest residue mobilization will depend on the extent that the state supports forest management, and forest agencies make the necessary forest management plans. The two factors greatly affecting market available biomass potential are availability constraints, restricting the total biomass that can be mobilized, and the mobilization rate depending mostly on market dynamics, and in particular, stakeholder engagement and incentives. From the technical side, it is important to improve harvesting equipment, increasing harvesting efficiency and capability which would increase the technical potential and reduce harvesting costs.

The Peloponnese region is rich in sustainably available woody biomass, suitable for the proposed process plant's configuration. The technical potential of the region regarding the assessed types is 752.3 kt_{DM} for rather unfavorable availability and sustainability conditions. A biomass processing plant in the region with a capacity of 70kt_{DM} seems to be possible with an average price of biomass being 70.31€/t_{DM}. The low price is due to this biomass being residual from normal pruning and logging activities, thus a byproduct with no current market value. If a market value is assigned to it, then the developed approach calculating the SMP can be used to evaluate the scenario in which cheaper biomass types can benefit from market dynamics. In that case an average biomass price of 90.4€/t_{DM} is foreseen. The SMP approach in future biomass pricing was not found in literature, thus to the knowledge of the author it is applied for the first time in this work. The local market share significantly affects the average biomass price, thus, it should be a central target in the business plan. It is encouraging that the proposed processing scheme can handle different feedstocks, hence, broadening the available biomass types and allowing for flexibility, increasing feedstock security and for cheaper feedstocks to be used.

Extending from the work in chapter 3, in chapter 4 an advanced biofuels production plant is proposed utilizing novel technologies. Considering that most likely only a medium to low scale biomass processing plant is possible in the region, the employed processing scheme was adjusted to be suitable for these plant scales. The goal was to use promising solutions that would alleviate the process from the use of an ASU or other oxygen production units, and the use of an AGR unit for CO_2 removal.

A model for CLG under various conditions and feedstocks was developed and validated against experimental data to obtain results from simulations in Aspen Plus^{TM}. The model considered an industrial scale CLG unit with relevant operating parameter assumptions reflecting industrial scale operation. A CGE of 79.54% was obtained showing the promise of this technology as an alternative gasification unit. Control

methods are very important from the technical side due to the complexity of managing operational parameters' interrelations, as was explained in the respective section.

An effective gas cleaning process was inspired by the GoBiGas demonstration plant with the modification of using the more suitable OLGA process. This change is expected to bring significant improvements to the use of activated carbon beds for BTX removal especially on the requirements regarding the steam regeneration process. The combination of these technologies will likely be cheaper in the small to medium scales than the alternative tar removal processes. For the downstream gas cleaning steps, dedicated gas cleaning steps were employed to ensure the robustness of the gas cleaning. The fuel synthesis process is chosen to be FTs using a Fe based catalyst making CO_2 removal unnecessary. This gas cleaning process configuration has a good efficiency with only a slight drop in the overall CGE to 77.38%.

A model was developed for the FTs process step to evaluate the overall process. The model was based on using experimental findings and with input the resulting syngas from the upstream process, calculate product yield and HC distribution. The FTs island model included basic product separation and a FT gases loop that included a reforming section allowing for higher carbon utilization. The current FTs configuration proves effective in converting a great part of input carbon into FT-crude yielding an overall CU of 58% for the integrated process.

Lastly, the developed HRSG configuration considered and highlighted many constraints but should be further optimized based on criteria such as electricity production or inlet stream pre-heating and include heat transfer losses and pressure drops. Heat recovery plays a central role in cases with highly exothermic reactions and when multiple heating and cooling steps exist in the process.

Overall, this chapter has provided a detailed description of the developed model for drying, CLG, gas cleaning, FTs island and HRSG system with the necessary detail to perform the plants' technoeconomic assessment.

The technoeconomic assessment yields a TCI of 175.6 M€ and BESP of 3€/kg of FT-crude for 2020 basis year. A high olefin content of the produced FT-crude differentiates it from the typical LTFT produced FT-crude by allowing the targeted production of many HC fractions via oligomerization under a proper catalyst. This makes BESP comparison to literature more difficult, however the calculated BESP is higher than conventional paths and comparable to that of synthetic fuels. The cost breakdown and sensitivity analysis provide insight on the main areas of focus for cost reduction potential. The cost of H_2 determines most of the operating costs and the FTs island followed by the HRSG system determine most of the capital costs. Optimizing operating parameters for these areas using technoeconomic criteria will have major economic benefits. The current configuration demands a high hydrogen input, approximately equal to the biomass produced syngas. Due to this intricacy, that can be mitigated by an alternative configuration, the advanced biofuels production plant

resembles a synthetic fuel production plant. Therefore, this production plant is in the middle ground between synthetic fuels and biofuels despite being considered a biofuel production plant. Altering the current configuration should also be considered to minimize H_2 demand.

The developed case study showed that a medium scale advanced biofuel production plant in Peloponnese can cover ~7% of national SAF demand in 2040. This is an important finding which shows a significant biomass mobilization will strengthen energy security in Greece.

7. Future work

Based on the conducted work some possible future works are suggested.

- On-field measurements of pruning productivity from various locations and years across the Peloponnese or other regions to conduct a more accurate potential assessment to facilitate the development of a bio-based industry.
- Further experimental study on CLG focusing on the assessment of OC losses and OC composition after multiple redox cycles.
- Experimental or modelling study on CLG with dirtier feedstocks to assess its capability to produce low tar containing syngas under various feedstocks.
- Investigation of a configuration with only the collector part of OLGA, relying on the activated carbon beds for remaining BTX removal. Detailed modelling of activated carbon beds operation under these conditions and the regeneration process.
- Experimental or modelling investigation on the multifunctional capabilities of activated carbon beds, especially regarding COS and HCN removal.
- A hybrid approach with in-situ production of hydrogen and oxygen allowing for alternative configurations with higher efficiency and operational advantages. One such configuration change would be the use of an autothermal reformer instead of the allothermal steam reformer, increasing FT-crude production, lowering the energy penalty and electrical consumptions by decreasing the necessary compression work.
- Comparative assessment of different fuel synthesis steps coupled to the upstream configuration. One such could be a methane synthesis step, since a goal of Greece is to produce biomethane.
- Optimization of the overall process and mainly the FTs island and the HRSG system. A cost-benefit analysis for different recirculation ratios of FT gases and operating parameters to assess possible economic benefits.
- Life cycle assessment of the biomass supply chain and processing. Comparative assessment of alternative FTs and biofuel production configurations to the one proposed in this thesis.

References

[1] UNFCCC, “ADOPTION OF THE PARIS AGREEMENT - Paris Agreement text English.”

[2] “EUROCONTROL Aviation Outlook 2050 Main Report,” 2022. Accessed: Sep. 19, 2024. [Online]. Available: https://www.eurocontrol.int/sites/default/files/2022-04/eurocontrol-aviation-outlook-2050-main-report.pdf

[3] “International Air Transport Association (IATA), ‘Our Commitment to Fly Net Zero by 2050.’” Accessed: Sep. 19, 2024. [Online]. Available: https://www.iata.org/en/programs/sustainability/flynetzero/

[4] Avitabile V, Baldoni E, Baruth B, and Bausano G, “Biomass production, supply, uses and flows in the European Union Integrated assessment,” doi: 10.2760/811744.

[5] “Assessment of the potential for new feedstocks for the production of advanced biofuels (ENER C1 2019-412) Final Report,” 2021. Accessed: Sep. 19, 2024. [Online]. Available: https://op.europa.eu/en/publication-detail/-/publication/ec9c1003-76a7-11ed-9887-01aa75ed71a1/language-en

[6] S. López, “Trends in the EU bioeconomy JRC SCIENCE FOR POLICY REPORT,” doi: 10.2760/835046.

[7] ICAO, “‘CORSIA: Carbon Offsetting and Reduction Scheme for International Aviation.’” Accessed: Sep. 19, 2024. [Online]. Available: https://www.icao.int/environmental-protection/CORSIA/Pages/default.aspx

[8] IATA, “‘Unveiling the biggest airline costs.’” Accessed: Sep. 19, 2024. [Online]. Available: https://www.iata.org/en/publications/newsletters/iata-knowledge-hub/unveiling-the-biggest-airline-costs/

[9] *DIRECTIVE (EU) 2023/2413 OF THE EUROPEAN PARLIAMENT AND OF THE COUNCIL of 18 October 2023 amending Directive (EU) 2018/2001, Regulation (EU) 2018/1999 and Directive 98/70/EC as regards the promotion of energy from renewable sources, and repealing Council Directive (EU) 2015/652*.

[10] *European Union. (2021). Regulation (EU) 2021/2115 of the European Parliament and of the Council of 2 December 2021 establishing rules for support for strategic plans to be drawn up by Member States under the Common Agricultural Policy (CAP Strategic Plans) for the period 2023-2027. Official Journal of the European Union, L 435/1.*

[11] “Hellenic REPUBLIC (2023), Ministry of Environment and Energy, NATIONAL ENERGY AND CLIMATE PLAN —PRELIMINARY DRAFT REVISED VERSION OCTOBER 2023.”

[12] EAGF and EAFRD, "'CAP STRATEGIC PLAN OF GREECE 2023-2027,'" 2022. Accessed: Sep. 19, 2024. [Online]. Available: https://www.minagric.gr/images/stories/docs/agrotis/KAP2023_2027/egkekrimeno_ss_kap_2023_2027.pdf

[13] A. and rural development European Commission, "Approved 28 CAP Strategic Plans (2023-2027)," Jun. 2023.

[14] F. Scala, "Particle agglomeration during fluidized bed combustion: Mechanisms, early detection and possible countermeasures," Mar. 01, 2018, *Elsevier B.V.* doi: 10.1016/j.fuproc.2017.11.001.

[15] "AGROinLOG, H2020 project, GA 727961, Available from: http://agroinlog-h2020.eu/en/."

[16] "AGROinLOG (2019), D6.3: Comprehensive identification of opportunities for the production of biomass & biocommodities and for a logistics integration".

[17] "S2BIOM, 7th Framework Programme for Research , GA 608622, Available from: http://www.s2biom.eu/."

[18] "ΜΕΛΕΤΗ ΑΞΙΟΠΟΙΗΣΗΣ ΠΑΡΑΓΟΜΕΝΗΣ ΒΙΟΜΑΖΑΣ ΣΤΟ Ν. ΛΑΡΙΣΑΣ ΜΕ ΚΑΥΣΗ ΓΙΑ ΣΥΜΠΑΡΑΓΩΓΗ ΗΛΕΚΤΡΙΣΜΟΥ ΚΑΙ ΘΕΡΜΟΤΗΤΑΣ." Accessed: Sep. 20, 2024. [Online]. Available: http://agreng.agr.uth.gr/node/81

[19] "PROFORBIOMED, Task 4.1.7, Deliverable 5, 'Πλήρης φάκελος με τα στοιχεία για την παραγωγή βιομάζας από τον αγροτικό και δασικό τομέα και οικονομικά στοιχεία εξαγωγής και διάθεσης της βιομάζας Δυτικής Μακεδονίας.,'" 2013. Accessed: Sep. 20, 2024. [Online]. Available: http://bit.ly/47z8vcM

[20] ΑΔΑΜΑΝΤΙΑ Γ. ΚΑΠΑΡΕΛΟΥ, "'ΔΙΑΧΕΙΡΙΣΗ ΚΑΙ ΑΞΙΟΠΟΙΗΣΗ ΓΕΩΡΓΙΚΩΝ ΑΠΟΒΛΗΤΩΝ: ΜΕΛΕΤΗ ΠΕΡΙΠΤΩΣΗΣ ΓΙΑ ΤΗΝ ΠΕΡΙΦΕΡΕΙΑ ΠΕΛΟΠΟΝΝΗΣΟΥ.'" Accessed: Sep. 20, 2024. [Online]. Available: https://apothesis.eap.gr/archive/item/81992

[21] "AgroBioHeat, H2020 project, GA 818369, Available from: https://agrobioheat.eu/."

[22] "Up_Running, H2020 project, GA 691748, Available from: http://www.up-running.eu/ (not available as of 22/7/2024)."

[23] "CHRISGAS, 6th EU Research Framework Programme, GA 502587, https://cordis.europa.eu/project/id/502587?isPreviewer=1."

[24] "Biomasud Plus, H2020 project, GA 691763, Available from: http://biomasudplus.eu/en_GB/."

[25] "Google. (n.d.). Peloponnese. Google Maps. Retrieved [2024], from https://www.google.com/maps."

[26] M. A. Kougioumtzis, E. Karampinis, P. Grammelis, and E. Kakaras, “Integrated harvesting and biomass haulage of olive tree prunings. Evaluation of a two year harvesting campaign in central Greece and fuel characterization of the prunings collected,” *Biomass Bioenergy*, vol. 165, Oct. 2022, doi: 10.1016/j.biombioe.2022.106572.

[27] ΠΑΝΑΓΙΩΤΗΣ Α. ΝΤΟΓΚΟΥΛΗΣ, “‘Αξιοποίηση των υπολειμμάτων καλλιεργειών για παραγωγή ενέργειας,’” 2020. Accessed: Sep. 20, 2024. [Online]. Available: https://ir.lib.uth.gr/xmlui/handle/11615/57914

[28] “Δύο νέες θυγατρικές από τη Motor Oil στην κυκλική οικονομία - Ποιες είναι οι VERD και Πράσινο Λάδι.” Accessed: Sep. 20, 2024. [Online]. Available: https://www.capital.gr/epixeiriseis/3746951/duo-nees-thugatrikes-apo-ti-motor-oil-stin-kukliki-oikonomia-poies-einai-oi-verd-kai-prasino-ladi/

[29] “Cnn.gr, Jul. 15, 2024 ‘Ανακύκλωση τηγανέλαιων: Πώς επιχειρήσεις και νοικοκυριά μπορούν να προστατέψουν το περιβάλλον;’ Available at: https://www.cnn.gr/oikonomia/nea-tis-agoras/story/425190/anakyklosi-tiganelaion-pos-epixeiriseis-kai-noikokyria-boroyn-na-prostatepsoun-to-perivallon.”

[30] “ΠΕΡΙΦΕΡΕΙΑ ΠΕΛΟΠΟΝΝΗΣΟΥ ‘ΠΕΡΙΦΕΡΕΙΑΚΟ ΣΧΕΔΙΟ ΔΙΑΧΕΙΡΙΣΗΣ ΑΠΟΒΛΗΤΩΝ (ΠΕ.Σ.Δ.Α.)’ Available at: https://www.eydpelop.gr/2014-2020/wp-content/uploads/2022/06/PESDA-Peloponnisou.pdf.”

[31] “Deliverable Task 3.2. Biomasud Project Selected biofuels characterization results and quality assessment report.”

[32] “Phyllis2, Available at: https://phyllis.nl/Browse/Standard/CEN-TS-14961#fruit%20biomass.”

[33] C. L. Williams, R. M. Emerson, and J. S. Tumuluru, “Biomass Compositional Analysis for Conversion to Renewable Fuels and Chemicals,” in *Biomass Volume Estimation and Valorization for Energy*, InTech, 2017. doi: 10.5772/65777.

[34] Γκιώνης Σπύρος, Λουκάς Αθανάσιος, Καρούντζος Δημήτρης, and Καρυτσιώτη Ευφορία, “‘ΗΠΙΕΣ ΜΟΡΦΕΣ ΕΝΕΡΓΕΙΑΣ - ΒΙΟΜΑΖΑ,’” 2004, Accessed: Sep. 20, 2024. [Online]. Available: http://library.tee.gr/digital/tri/tri_m30.pdf

[35] S. V. Vassilev, D. Baxter, L. K. Andersen, and C. G. Vassileva, “An overview of the chemical composition of biomass,” May 2010. doi: 10.1016/j.fuel.2009.10.022.

[36] Valter Francescato *et al.*, “‘ΕΓΧΕΙΡΙΔΙΟ ΚΑΥΣΙΜΩΝ ΞΥΛΟΥ,’” 2008. Accessed: Sep. 20, 2024. [Online]. Available: http://www.cres.gr/cres/files/xrisima/ekdoseis/ekdoseis_GR7.pdf

[37] “C. Papadakis, Neakriti.gr (2021), ‘Λιόκλαδα: Ναι ή όχι στην καύση τους; - Τι συμβουλεύει ειδικός’, Available at:

https://www.neakriti.gr/kriti/1603611_lioklada-nai-i-ohi-stin-kaysi-toys-ti-symboyleyei-eidikos , Last accessed: 11/09/2024."

[38] "dasarxeio.com (2024), 'Πρόγραμμα AntiNero III: Η συνδρομή του ΤΑΙΠΕΔ για τη θωράκιση των ελληνικών δασών από την κλιματική κρίση' Available at: https://dasarxeio.com/2024/03/06/133993/ , Last accessed: 11/09/2024."

[39] "Harmonization of biomass resource assessments, Volume I, Best Practices and Methods Handbook," 2010, doi: 10.13140/2.1.4643.8084.

[40] "Hellenic Statistical Authority, Annual Agricultural Statistical Survey, Areas and Production 2021, Available at: https://www.statistics.gr/en/statistics/-/publication/SPG06/-."

[41] L. S. Esteban, P. Ciria, and J. E. Carrasco, "An assessment of relevant methodological elements and criteria for surveying sustainable agricultural and forestry biomass byproducts for energy purposes," *Bioresources*, vol. 3, no. 3, pp. 910–928, Jul. 2008, doi: 10.15376/biores.3.3.910-928.

[42] R. Spinelli and G. Picchi, "Industrial harvesting of olive tree pruning residue for energy biomass," *Bioresour Technol*, vol. 101, no. 2, pp. 730–735, Jan. 2010, doi: 10.1016/j.biortech.2009.08.039.

[43] "uP_running, Biomass Day 2017, Metropolitan Expo, Apr. 7, 2017, 'Ενεργειακή αξιοποίηση αγροτικών κλαδεμάτων στην Ελλάδα: Πώς μπορεί να προχωρήσει; Το έργο uP_running', Available at: http://www.cres.gr/kape/publications/pdf/5_20170407_Biomass%20Day_%CE%9A%CE%91%CE%A1%CE%91%CE%9C%CE%A0%CE%99%CE%9D%CE%97%CE%A3.pdf."

[44] L. Pari, V. Alfano, D. Garcia-Galindo, A. Suardi, and E. Santangelo, "Pruning biomass potential in Italy related to crop characteristics, agricultural practices and agro-climatic conditions," *Energies (Basel)*, vol. 11, no. 6, Jun. 2018, doi: 10.3390/en11061365.

[45] D. García-Galindo, A. Dyjakon, and F. C. Villa-Ceballos, "Building variable productivity ratios for improving large scale spatially explicit pruning biomass assessments," *Energies (Basel)*, vol. 12, no. 5, 2019, doi: 10.3390/en12050957.

[46] "S2Biom, 19.4.2017, D1.1 'Roadmap for regional end-users on how to collect, process, store and maintain biomass supply data.'"

[47] "BIORAISE, Available at: http://bioraise.ciemat.es/Bioraise/".

[48] M.-A. Kougioumtzis, E. Karampinis, P. Grammelis, and E. Kakaras, "Assessment of Biomass Resources for an Integrated Biomass Logistics Center (IBLC) Operating in the Olive Oil Sector." doi: 10.5071/26thEUBCE2018-1DV.1.14.

[49] K. Moustakas, P. Parmaxidou, and S. Vakalis, "Anaerobic digestion for energy production from agricultural biomass waste in Greece: Capacity assessment

for the region of Thessaly," *Energy*, vol. 191, Jan. 2020, doi: 10.1016/j.energy.2019.116556.

[50] "BIOmasud, D2.4 'BIORAISE GIS platform with actualized information of sustainable biomass resources available and costs and stakeholders relevant data for residential heating solid biofuels production, logistics and use in each participating country.'"

[51] L. Pari, A. Suardi, E. Santangelo, D. García-Galindo, A. Scarfone, and V. Alfano, "Current and innovative technologies for pruning harvesting: A review," Dec. 01, 2017, *Elsevier Ltd*. doi: 10.1016/j.biombioe.2017.09.014.

[52] A. Suardi *et al.*, "Pruning harvesting with modular towed chipper: Little effect of the machine setting and configuration on performance despite strong impact on wood chip quality," *PLoS One*, vol. 16, no. 12 December, Dec. 2021, doi: 10.1371/journal.pone.0261810.

[53] A. Suardi *et al.*, "Machine performance and HOG fuel quality evaluation in olive tree pruning harvesting conducted using a towed shredder on flat and hilly fields," *Energies (Basel)*, vol. 13, no. 7, 2020, doi: 10.3390/en13071713.

[54] "uP_running, 14.07.2017, D2.1 'Sector Analysis and Action Plan for the Demo Regions.'"

[55] "BioSFerA, 2021, D2.4: 'Determination of the main input parameters for the case studies.'"

[56] R. Spinelli, N. Magagnotti, and C. Nati, "Harvesting vineyard pruning residues for energy use," *Biosyst Eng*, vol. 105, no. 3, pp. 316–322, 2010, doi: 10.1016/j.biosystemseng.2009.11.011.

[57] T. Bosona, G. Gebresenbet, and A. Dyjakon, "Implementing life cycle cost analysis methodology for evaluating agricultural pruning-to-energy initiatives," *Bioresour Technol Rep*, vol. 6, pp. 54–62, Jun. 2019, doi: 10.1016/j.biteb.2019.02.006.

[58] "Hellenic Republic, Government Gazette, B 6472/17.12/2022."

[59] "Hellenic Republic, Government Gazette, B 6013/17.10.2023."

[60] Ι. Ελευθεριάδης, "ΓΕΝΙΚΗ ΓΡΑΜΜΑΤΕΙΑ ΕΜΠΟΡΙΟΥ ΟΔΗΓΟΣ ΓΙΑ ΤΗ ΔΙΑΚΙΝΗΣΗ ΚΑΥΣΟΞΥΛΩΝ ΜΟΝΑΔΕΣ ΜΕΤΡΗΣΗΣ-ΥΓΡΑΣΙΑ-ΦΥΣΙΚΗ ΞΗΡΑΝΣΗ ΣΥΝΤΑΞΗ." [Online]. Available: www.gge.gov.grΔΙΕΥΘΥΝΣΗΜΕΤΡΟΛΟΓΙΑΣwww.cres.gr

[61] "Chemical Looping gAsification foR sustainAble production of biofuels (CLARA), GA: 817841, 2022, D7.1: Cost estimation for biomass feedstock supply."

[62] "Aspen Technology, Inc. Aspen Plus V11 https://www.aspentech.com/".

[63] F. Marx, P. Dieringer, J. Ströhle, and B. Epple, “Design of a 1 MWth pilot plant for chemical looping gasification of biogenic residues,” *Energies (Basel)*, vol. 14, no. 9, May 2021, doi: 10.3390/en14092581.

[64] J. Mak *et al.*, “An Assessment of Ambient and Heated Forced Air Drying Pre-treatments for Enhancing the Quality of Various Forest Biomass Feedstocks,” *Front Energy Res*, vol. 8, Jan. 2020, doi: 10.3389/fenrg.2020.00007.

[65] C. L. Williams, T. L. Westover, R. M. Emerson, J. S. Tumuluru, and C. Li, “Sources of Biomass Feedstock Variability and the Potential Impact on Biofuels Production,” Mar. 01, 2016, *Springer New York LLC*. doi: 10.1007/s12155-015-9694-y.

[66] A. Alamia, A. Larsson, C. Breitholtz, and H. Thunman, “Performance of large-scale biomass gasifiers in a biorefinery, a state-of-the-art reference,” *Int J Energy Res*, vol. 41, no. 14, pp. 2001–2019, Nov. 2017, doi: 10.1002/er.3758.

[67] A. K. Kumar and S. Sharma, “Recent updates on different methods of pretreatment of lignocellulosic feedstocks: a review,” Dec. 01, 2017, *Springer Science and Business Media Deutschland GmbH*. doi: 10.1186/s40643-017-0137-9.

[68] I. Hannula, “Co-production of synthetic fuels and district heat from biomass residues, carbon dioxide and electricity: Performance and cost analysis,” *Biomass Bioenergy*, vol. 74, pp. 26–46, Mar. 2015, doi: 10.1016/j.biombioe.2015.01.006.

[69] O. Condori, A. Abad, F. García-Labiano, L. F. de Diego, M. T. Izquierdo, and J. Adánez, “Parametric evaluation of clean syngas production from pine forest residue by chemical looping gasification at the 20 kWth scale,” *J Clean Prod*, vol. 436, Jan. 2024, doi: 10.1016/j.jclepro.2023.140434.

[70] K. Göransson, U. Söderlind, J. He, and W. Zhang, “Review of syngas production via biomass DFBGs,” Jan. 2011. doi: 10.1016/j.rser.2010.09.032.

[71] F. Marx, P. Dieringer, J. Ströhle, and B. Epple, “Process efficiency and syngas quality from autothermal operation of a 1 MWth chemical looping gasifier with biogenic residues,” *Applications in Energy and Combustion Science*, vol. 16, Dec. 2023, doi: 10.1016/j.jaecs.2023.100217.

[72] A. Goel, E. M. Moghaddam, W. Liu, C. He, and J. Konttinen, “Biomass chemical looping gasification for high-quality syngas: A critical review and technological outlooks,” Sep. 15, 2022, *Elsevier Ltd*. doi: 10.1016/j.enconman.2022.116020.

[73] N. M. Nguyen, F. Alobaid, P. Dieringer, and B. Epple, “Biomass-based chemical looping gasification: Overview and recent developments,” Aug. 01, 2021, *MDPI AG*. doi: 10.3390/app11157069.

[74] A. Abad, J. Adánez, A. Cuadrat, F. García-Labiano, P. Gayán, and L. F. De Diego, “KINETICS OF REDOX REACTIONS OF ILMENITE FOR CHEMICAL-LOOPING COMBUSTION.”

[75] P. Bartocci, A. Abad, A. C. Flores, and M. de las Obras Loscertales, “Ilmenite: A promising oxygen carrier for the scale-up of chemical looping,” *Fuel*, vol. 337, Apr. 2023, doi: 10.1016/j.fuel.2022.126644.

[76] J. B. Yang, N. S. Cai, and Z. S. Li, “Reduction of iron oxide as an oxygen carrier by coal pyrolysis and steam char gasification intermediate products,” *Energy and Fuels*, vol. 21, no. 6, pp. 3360–3368, Nov. 2007, doi: 10.1021/ef7002377.

[77] P. Dieringer *et al.*, “Fate of ilmenite as oxygen carrier during 1 MWth chemical looping gasification of biogenic residues,” *Applications in Energy and Combustion Science*, vol. 16, Dec. 2023, doi: 10.1016/j.jaecs.2023.100227.

[78] Z. Yu *et al.*, “Iron-based oxygen carriers in chemical looping conversions: A review,” Apr. 01, 2019, *KeAi Publishing Communications Ltd.* doi: 10.1016/j.crcon.2018.11.004.

[79] A. Larsson, I. Gunnasrsson, and F. Tengberg, “The GoBiGas Project Demonstration of the Production of Biomethane from Biomass via Gasification.”

[80] C. Frilund, E. Kurkela, and I. Hiltunen, “Development of a simplified gas ultracleaning process: experiments in biomass residue-based fixed-bed gasification syngas,” *Biomass Convers Biorefin*, vol. 13, no. 17, pp. 15673–15684, Nov. 2023, doi: 10.1007/s13399-021-01680-x.

[81] H. Boerrigter, H. P. Calis, D. J. Slort, H. Bodenstaff, and H. J. Veringa, “Gas Cleaning for Integrated Biomass Gasification (BG) and Fischer-Tropsch (FT) Systems Experimental demonstration of two BG-FT systems (‘Proof-of-Principle’),” 2004.

[82] S. Anis and Z. A. Zainal, “Tar reduction in biomass producer gas via mechanical, catalytic and thermal methods: A review,” Jun. 2011. doi: 10.1016/j.rser.2011.02.018.

[83] N. Abdoulmoumine, S. Adhikari, A. Kulkarni, and S. Chattanathan, “A review on biomass gasification syngas cleanup,” Oct. 01, 2015, *Elsevier Ltd*. doi: 10.1016/j.apenergy.2015.05.095.

[84] J. Li, X. Yao, K. Xu, J. Ge, D. Yang, and B. Fan, “Numerical investigation of a process model integrating gasification and tar removal,” *Biomass Convers Biorefin*, vol. 13, no. 14, pp. 12689–12703, Sep. 2023, doi: 10.1007/s13399-021-02049-w.

[85] H. Thunman *et al.*, “Advanced biofuel production via gasification – lessons learned from 200 man-years of research activity with Chalmers’ research

gasifier and the GoBiGas demonstration plant," *Energy Sci Eng*, vol. 6, no. 1, pp. 6–34, Feb. 2018, doi: 10.1002/ese3.188.

[86] C. Frilund, S. Tuomi, E. Kurkela, and P. Simell, "Small- to medium-scale deep syngas purification: Biomass-to-liquids multi-contaminant removal demonstration," *Biomass Bioenergy*, vol. 148, May 2021, doi: 10.1016/j.biombioe.2021.106031.

[87] P. Simell *et al.*, "Clean syngas from biomass—process development and concept assessment," *Biomass Convers Biorefin*, vol. 4, no. 4, pp. 357–370, Dec. 2014, doi: 10.1007/s13399-014-0121-y.

[88] S. Tuomi, E. Kurkela, P. Simell, and M. Reinikainen, "Behaviour of tars on the filter in high temperature filtration of biomass-based gasification gas," *Fuel*, vol. 139, pp. 220–231, Jan. 2015, doi: 10.1016/j.fuel.2014.08.051.

[89] E. Kurkela, M. Kurkela, and I. Hiltunen, "Pilot-scale development of pressurized fixed-bed gasification for synthesis gas production from biomass residues", doi: 10.1007/s13399-021-01554-2/Published.

[90] P. J. Woolcock and R. C. Brown, "A review of cleaning technologies for biomass-derived syngas," May 2013. doi: 10.1016/j.biombioe.2013.02.036.

[91] E. Kurkela, M. Kurkela, M. Nieminen, and J. Laatikainen-Luntama, "Circulating fluidized bed gasification of solid recovered fuels - Results from gasification and gas filtration tests," *Chem Eng Trans*, vol. 86, pp. 19–24, 2021, doi: 10.3303/CET2186004.

[92] H. Boerrigter *et al.*, "'OLGA' TAR REMOVAL TECHNOLOGY Proof-of-Concept (PoC) for application in integrated biomass gasification combined heat and power (CHP) systems," 2005. Accessed: Sep. 20, 2024. [Online]. Available: https://publicaties.ecn.nl/PdfFetch.aspx?nr=ECN-C--05-009

[93] H. Boerrigter *et al.*, "OLGA Optimum Improving the economics of integrated biomass gasification plants by extension of the functionalities of the OLGA tar washer," 2006. Accessed: Sep. 20, 2024. [Online]. Available: https://repository.tno.nl/SingleDoc?find=UID%201c1e0189-dc0b-40fe-8160-ce91729a576f

[94] I. Khursheed Shah, P. Pre, B. J. Alappat, and B. J. Alappat Steam, "Regeneration of Adsorbents: An Ex-perimental and Technical Review," *Chem Sci Trans*, no. 2, 2013, doi: 10.7598/cst2013.545ï.

[95] B. Djamila, A. Allali, B. Youcef, and M. H. Sellami, "Steam Regeneration of Exhausted Activated Carbon Used in Natural Gas Dehydration by a Triethylene Glycol Unit," *Physical Chemistry Research*, vol. 12, no. 1, pp. 109–119, Mar. 2024, doi: 10.22036/pcr.2023.385578.2287.

[96] Tommy Schmitt *et al.*, “Cost and Performance Baseline for Fossil Energy Plants Volume 1: Bituminous Coal and Natural Gas to Electricity,” 2022, doi: 10.2172/1893822.

[97] Sennai Asmelash Mesfun, “Biomass to liquids (BtL) via Fischer-Tropsch – a brief review,” 2021. Accessed: Sep. 20, 2024. [Online]. Available: https://www.etipbioenergy.eu/images/ETIP_B_Factsheet_BtL_2021.pdf

[98] M. Claeys and E. Van Steen, *Chapter 8 - Basic studies*. doi: 10.1016/S0167-2991(04)80465-8.

[99] Y. Yao, X. Liu, D. Hildebrandt, and D. Glasser, “Fischer-Tropsch synthesis using H 2/CO/CO 2 syngas mixtures over an iron catalyst,” *Ind Eng Chem Res*, vol. 50, no. 19, pp. 11002–11012, Oct. 2011, doi: 10.1021/ie200690y.

[100] S. Tuomi, E. Kurkela, I. Hannula, and C. G. Berg, “The impact of biomass drying on the efficiency of a gasification plant co-producing Fischer-Tropsch fuels and heat – A conceptual investigation,” *Biomass Bioenergy*, vol. 127, Aug. 2019, doi: 10.1016/j.biombioe.2019.105272.

[101] Ilkka. Hannula and Esa. Kurkela, *Liquid transportation fuels via large-scale fluidised-bed gasification of lignocellulosic biomass*. VTT, 2013. Accessed: Sep. 20, 2024. [Online]. Available: https://publications.vtt.fi/pdf/technology/2013/T91.pdf

[102] N. Detsios *et al.*, “A COMPARATIVE ANALYSIS AND ASSESSMENT OF DUAL FLUIDIZED BED AND CHEMICAL LOOPING GASIFICATION: DESIGN CONSIDERATIONS FOR COMMERCIAL USE AND APPLICABILITY IN BTL SCHEMES.”

[103] A. H. Soleimani, T. Mattisson, and C. J. Linderholm, “CLARA, Deliverable D3.2: ‘Investigation of fate of tar surrogates with oxygen carrier materials.’” Accessed: Sep. 20, 2024. [Online]. Available: https://clara-h2020.eu/wp-content/uploads/2020/03/CLARA_Deliverable_3.2.pdf

[104] V. Gogulancea *et al.*, “Technoeconomic and Environmental Assessment of Biomass Chemical Looping Gasification for Advanced Biofuel Production,” *Int J Energy Res*, vol. 2023, 2023, doi: 10.1155/2023/6101270.

[105] Z. X. Wang *et al.*, “Characteristics of bio-oil-syngas and its utilization in Fischer-Tropsch synthesis,” *Energy and Fuels*, vol. 21, no. 4, pp. 2421–2432, Jul. 2007, doi: 10.1021/ef0700275.

[106] A. Fedorov and D. Linke, “Data analysis of CO2hydrogenation catalysts for hydrocarbon production,” *Journal of CO2 Utilization*, vol. 61, Jul. 2022, doi: 10.1016/j.jcou.2022.102034.

[107] M. Rafati, L. Wang, and A. Shahbazi, “Effect of silica and alumina promoters on co-precipitated Fe-Cu-K based catalysts for the enhancement of CO2 utilization

during Fischer-Tropsch synthesis," *Journal of CO2 Utilization*, vol. 12, pp. 34–42, Dec. 2015, doi: 10.1016/j.jcou.2015.10.002.

[108] I. Hannula, "Synthetic fuels and light olefins from biomass residues, carbon dioxide and electricity: Performance and cost analysis", doi: 10.13140/RG.2.1.3059.0802.

[109] O. Condori, A. Abad, M. T. Izquierdo, L. F. de Diego, F. García-Labiano, and J. Adánez, "Assessment of the chemical looping gasification of wheat straw pellets at the 20 kWth scale," *Fuel*, vol. 344, Jul. 2023, doi: 10.1016/j.fuel.2023.128059.

[110] O. Condori, F. García-Labiano, L. F. de Diego, M. T. Izquierdo, A. Abad, and J. Adánez, "Biomass chemical looping gasification for syngas production using ilmenite as oxygen carrier in a 1.5 kWth unit," *Chemical Engineering Journal*, vol. 405, Feb. 2021, doi: 10.1016/j.cej.2020.126679.

[111] P. Dieringer *et al.*, "Chemical Looping Gasification for Sustainable Production of Biofuels Public Report 3 Content." [Online]. Available: https://clara-h2020.eu/public-reports/

[112] Roshan Kumar T, Mattisson T, Rydén M, and Stenberg V, "Process Analysis of Chemical Looping Gasification of Biomass for Fischer-Tropsch Crude Production with Net-Negative CO2 Emissions: Part 1." doi: 10.1021/acs.energyfuels.2c00819.

[113] "Hellenic Statistical Authority, Physical Energy Flow Accounts, 2019, Available at: https://www.statistics.gr/en/statistics/-/publication/SOP11/2019."

[114] "Peters, M. S., Timmerhaus, K. D., & West, R. E. (2002). Plant design and economics for chemical engineers (5th ed.). McGraw-Hill Chemical Engineering Series."

[115] F. Li *et al.*, "Energy, Cost, and Environmental Assessments of Methanol Production via Electrochemical Reduction of CO2 from Biosyngas," *ACS Sustain Chem Eng*, vol. 11, no. 7, pp. 2810–2818, Feb. 2023, doi: 10.1021/acssuschemeng.2c05968.

[116] "US, Department of Energy, April 2024, 'Alternative Fuel Price Report', Available at: https://afdc.energy.gov/fuels/prices.html."

[117] R. M. Swanson, J. A. Satrio, R. C. Brown, A. Platon, and D. D. Hsu, "Techno-Economic Analysis of Biofuels Production Based on Gasification," 2010. [Online]. Available: http://www.osti.gov/bridge

[118] I. Hannula, "Hydrogen enhancement potential of synthetic biofuels manufacture in the European context: A techno-economic assessment," *Energy*, vol. 104, pp. 199–212, Jun. 2016, doi: 10.1016/j.energy.2016.03.119.

[119] H. Thunman, C. Gustavsson, A. Larsson, I. Gunnarsson, and F. Tengberg, “Economic assessment of advanced biofuel production via gasification using cost data from the GoBiGas plant,” *Energy Sci Eng*, vol. 7, no. 1, pp. 217–229, Feb. 2019, doi: 10.1002/ese3.271.

[120] N. Inc and S. Francisco, “Equipment Design and Cost Estimation for Small Modular Biomass Systems, Synthesis Gas Cleanup, and Oxygen Separation Equipment; Task 2: Gas Cleanup Design and Cost Estimates -- Black Liquor Gasification,” 2006. Accessed: Sep. 20, 2024. [Online]. Available: https://www.nrel.gov/docs/fy06osti/39944.pdf

[121] S. Maier, S. Tuomi, J. Kihlman, E. Kurkela, and R. U. Dietrich, “Techno-economically-driven identification of ideal plant configurations for a new biomass-to-liquid process – A case study for Central-Europe,” *Energy Convers Manag*, vol. 247, Nov. 2021, doi: 10.1016/j.enconman.2021.114651.

[122] O. Onel, A. M. Niziolek, J. A. Elia, R. C. Baliban, and C. A. Floudas, “Biomass and natural gas to liquid transportation fuels and olefins (BGTL+C2-C4): Process synthesis and global optimization,” *Ind Eng Chem Res*, vol. 54, no. 1, pp. 359–385, Jan. 2015, doi: 10.1021/ie503979b.

[123] J. Andersson, J. Lundgren, and M. Marklund, “Methanol production via pressurized entrained flow biomass gasification - Techno-economic comparison of integrated vs. stand-alone production,” *Biomass Bioenergy*, vol. 64, pp. 256–268, 2014, doi: 10.1016/j.biombioe.2014.03.063.

[124] M. N. Saeed, M. Shahrivar, G. D. Surywanshi, T. R. Kumar, T. Mattisson, and A. H. Soleimanisalim, “Production of aviation fuel with negative emissions via chemical looping gasification of biogenic residues: Full chain process modelling and techno-economic analysis,” *Fuel Processing Technology*, vol. 241, Mar. 2023, doi: 10.1016/j.fuproc.2022.107585.

[125] T. Roshan Kumar, T. Mattisson, and M. Rydén, “Techno-Economic Assessment of Chemical Looping Gasification of Biomass for Fischer-Tropsch Crude Production with Net-Negative CO2Emissions: Part 2,” *Energy and Fuels*, vol. 36, no. 17, pp. 9706–9718, Sep. 2022, doi: 10.1021/acs.energyfuels.2c01184.

[126] P. Buchenberg *et al.*, “Global Potentials and Costs of Synfuels via Fischer–Tropsch Process,” *Energies (Basel)*, vol. 16, no. 4, Feb. 2023, doi: 10.3390/en16041976.

Annex I: Feedstock distribution coordinates

Table AI 1: Feedstock distribution coordinates in WGS84.

Municipality	Orchards		Vineyards		Olives	
	Longitude	Latitude	Longitude	Latitude	Longitude	Latitude
ARGOS - MYKINES	22.7499	37.6270	22.6459	37.7599	22.6582	37.6976
EPIDAVROS	23.1451	37.6285			23.0484	37.6258
ERMIONIDA	23.2226	37.3834			23.1917	37.3932
NAFPLIO	22.8273	37.6050			22.8513	37.6164
VOREIA KYNOURIA	22.7419	37.3825			22.6781	37.4256
GORTYNIA					21.8526	37.6309
MEGALOPOLI					22.1593	37.4026
NOTIA KYNOURIA					22.8560	37.1647
TRIPOLI			22.4037	37.5615	22.3737	37.4909
AIGIALEIA	22.1038	38.2238	21.9857	38.2351	22.031	38.2453
DYTIKI ACHAIA	21.5654	38.1463	21.5887	38.1064	21.5413	38.0974
ERYMANTHOS	21.7108	38.0903	21.9288	38.1092	21.7363	38.0999
KALAVRYTA			22.0706	37.9061	22.0403	37.8025
PATRA	21.7732	38.2249	21.7148	38.2049	21.6787	38.1682
VELO - VOCHA	22.7700	37.9658	22.7401	37.9132	22.7713	37.8997
KORINTHOS	22.926	37.9103	22.8368	37.9189	22.8567	37.8143
LOUTRAKI - AGIOI THEODOROI	22.9767	37.9516			22.9782	37.9856
NEMEA	22.7708	37.8086	22.6496	37.8349	22.6797	37.8109
XYLOKASTRO - EVROSTINI	22.6767	38.0397	22.5366	38.0256	22.5044	38.0939
SIKYON	22.7343	37.9922	22.6183	37.9727	22.6569	37.9467
ANATOLIKI MANI	22.4286	36.6773			22.3891	36.6615
EVROTAS	22.6854	36.8478			22.5847	36.8802
MONEMVASIA	22.8372	36.6998			22.8784	36.7340
SPARTI	22.4358	37.0674	22.4915	37.1099	22.4328	37.0935
DYTIKI MANI	22.3252	36.7896			22.2252	36.9104
KALAMATA	22.1163	37.0289			22.0408	37.1007
MESSINI					21.9229	37.0390
OICHALIA					21.9648	37.2409
PYLOS - NESTOROS			21.7716	37.0971	21.7436	36.9389
TRIFYLIA			21.6571	37.108	21.6434	37.2076
ANDRAVIDA - KYLLINI	21.3602	37.9316			21.212	37.9176
ANDRITSAINA - KRESTENA	21.6505	37.6305	21.5989	37.6212	21.7041	37.5668
ARCHAIA OLYMPIA	21.699	37.6467			21.6299	37.6865
ZACHARO					21.6789	37.4663
ILIDA			21.3651	37.8333	21.3486	37.8075
PINEIOS	21.3365	37.8936	21.193	37.8397	21.2232	37.8779
PYRGOS	21.3859	37.727	21.4099	37.7262	21.4779	37.6975

Table AI 2: Feedstock distribution coordinates in WGS84. (continued)

Municipality	Conifers		Broadleaved		Mixed	
	Longitude	Latitude	Longitude	Latitude	Longitude	Latitude
ARGOS - MYKINES	22.4545	37.7806			22.6012	37.4630
EPIDAVROS	23.1451	37.6285	23.1550	37.6110		
ERMIONIDA	23.1024	37.3769	23.3046	37.4781	23.3028	37.4867
NAFPLIO	23.1143	37.5114				
VOREIA KYNOURIA	22.6272	37.2700	22.5271	37.3606	22.5585	37.3158
GORTYNIA	22.1103	37.5939	21.8508	37.6684	21.9073	37.6834
MEGALOPOLI	22.2128	37.2005	22.0755	37.3644	22.0185	37.3598
NOTIA KYNOURIA	22.7294	37.0848	22.7541	37.1877	22.8029	37.2795
TRIPOLI	22.2487	37.5879	22.2972	37.3900	22.3412	37.3168
AIGIALEIA	22.031	38.2453	22.0099	38.1909	21.953	38.2832
DYTIKI ACHAIA	21.369	38.1091	21.505	38.0366	21.5663	37.9744
ERYMANTHOS	21.7734	37.9593	21.9313	38.1161	21.7787	38.0524
KALAVRYTA	22.1241	38.0284	22.0177	37.957	22.0264	37.9272
PATRA	21.8178	38.2664	21.7944	38.2616	21.835	38.3079
VELO - VOCHA	22.6783	37.9054			22.7229	37.9309
KORINTHOS	23.0778	37.7845				
LOUTRAKI - AGIOI THEODOROI	23.0451	38.0178				
NEMEA	22.6707	37.8181	22.6063	37.8644		
XYLOKASTRO - EVROSTINI	22.4257	37.9970	22.4627	38.0401	22.5512	37.9971
SIKYON	22.3343	37.9143	22.5746	37.9267	22.4057	37.905
ANATOLIKI MANI	22.4255	36.7848	22.4193	36.7435	22.4667	36.8145
EVROTAS	22.9082	36.9702			22.4920	36.8840
MONEMVASIA	22.9457	36.9735			22.9457	36.9735
SPARTI	22.5292	37.1410	22.3887	37.0427	22.5028	37.2478
DYTIKI MANI	22.3233	36.9216	22.3082	36.8773	22.2977	36.9769
KALAMATA	22.2217	37.1100	22.1131	37.1027	22.1500	37.1401
MESSINI			21.8	37.0083	21.8911	36.9895
OICHALIA			21.9493	37.3601	21.9616	37.4157
PYLOS - NESTOROS			21.7882	37.0124	21.7903	36.9696
TRIFYLIA	21.7464	37.3451	21.7590	37.2398	21.7630	37.2786
ANDRAVIDA - KYLLINI	21.3365	38.0718	21.4254	37.9646		
ANDRITSAINA - KRESTENA	21.6016	37.5599	21.8895	37.4884	21.9025	37.4769
ARCHAIA OLYMPIA	21.7878	37.8773	21.7024	37.7902	21.7141	37.7988
ZACHARO					21.7548	37.4644
ILIDA	21.4722	37.8421	21.6428	37.825	21.2792	37.7841
PINEIOS	21.2562	37.8012	21.3108	37.8798		
PYRGOS	21.5686	37.6317	21.6853	37.7806	21.4621	37.7201

Table AI 3: Theoretical plant location and intermediate pre-treatment facilities.

	Longitude	Latitude
Plant	23.02472	37.92559
Pre-treat Lak	22.14739	37.38535
Pre-treat Ach	22.07776	38.23688

Annex II: Model Validation data

Experimental data comparison to model predictions

- **1 MW_{th} pilot plant** [71]

The compared operational points from the 1 MW_{th} pilot plant are shown in Table AII 1.

Table AII 1: Operational Points of 1 MWth plant.

OP	Units	1	2
T_{AR}	°C	933	898
T_{FR}	°C	840	804
S/B	kg/kg	1.15	0.93
ER_{FR}	-	0.35	0.35
ER_{AR}	-	0.5	0.52
C_c	-	0.75	0.77

The Pine Forest Residue composition used in the 1 MW_{th} pilot plant is shown in Table AII 2.

Table AII 2: Feedstock composition used in the 1 MWth pilot tests

		IWP	
M	8.3	**ASH**	0.3
FC	15.1	**CARBON**	50.7
VM	84.6	**HYDROGEN**	6.1
ASH	0.3	**NITROGEN**	0.33
		CHLORINE	0.008
		SULFUR	0.008
		OXYGEN	42.554

The model predictions are shown in Figure AII 1.

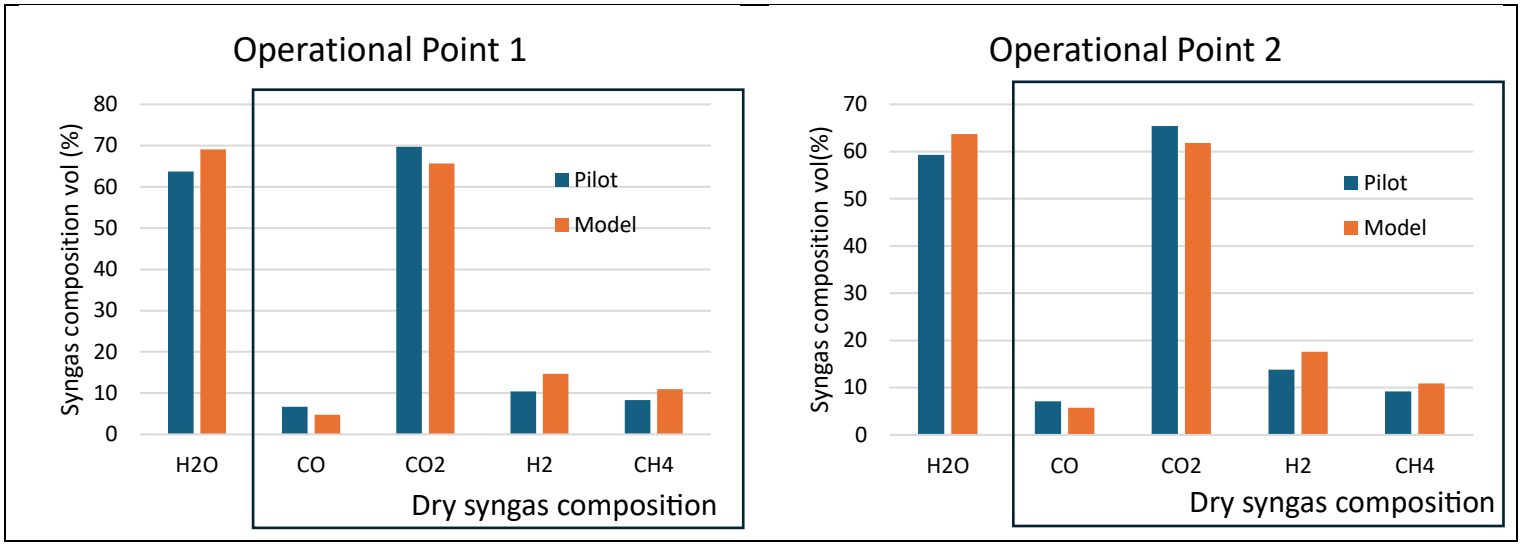

Figure AII 1: Comparison of major syngas species in the pilot tests at 1 MW_{th} and the model's predictions.

- **50 kW_{th} pilot plant** [109], [69]

The compared operational points from the 50 kW_{th} pilot plant are presented in Table AII 3.

Table AII 3: Operational points at the 50 kW_{th} scale with WSP and PFR.

	WSP			PFR	
OP	1	2	3	4	5
TFR	827	897	910	920	935
S/B	0.7	0.7	0.7	0.7	0.7
ER	0.34	0.29	0.3	0.44	0.24
Cc	0.879	0.925	93.3	0.917	0.811

The Wheat Straw Pellets (WSP) and Industrial Wood Pellets (IWP) composition used in the 50 kW_{th} pilot plant is shown in Table AII 4.

Table AII 4:Feedstock composition used in the 50 kW_{th} pilot tests.

WSP				PFR			
M	10.3	**ASH**	6.91	**M**	3.3	**ASH**	1.34
FC	15.27	**CARBON**	46.15	**FC**	18.82	**CARBON**	53.26
VM	77.82	**HYDROGEN**	5.8	**VM**	79.84	**HYDROGEN**	6
ASH	6.91	**NITROGEN**	0.45	**ASH**	1.34	**NITROGEN**	0.31
		CHLORINE	0.01			**CHLORINE**	0.01
		SULFUR	0.11			**SULFUR**	0.01
		OXYGEN	40.57			**OXYGEN**	39.07

The model predictions are shown in Figure AII 2.

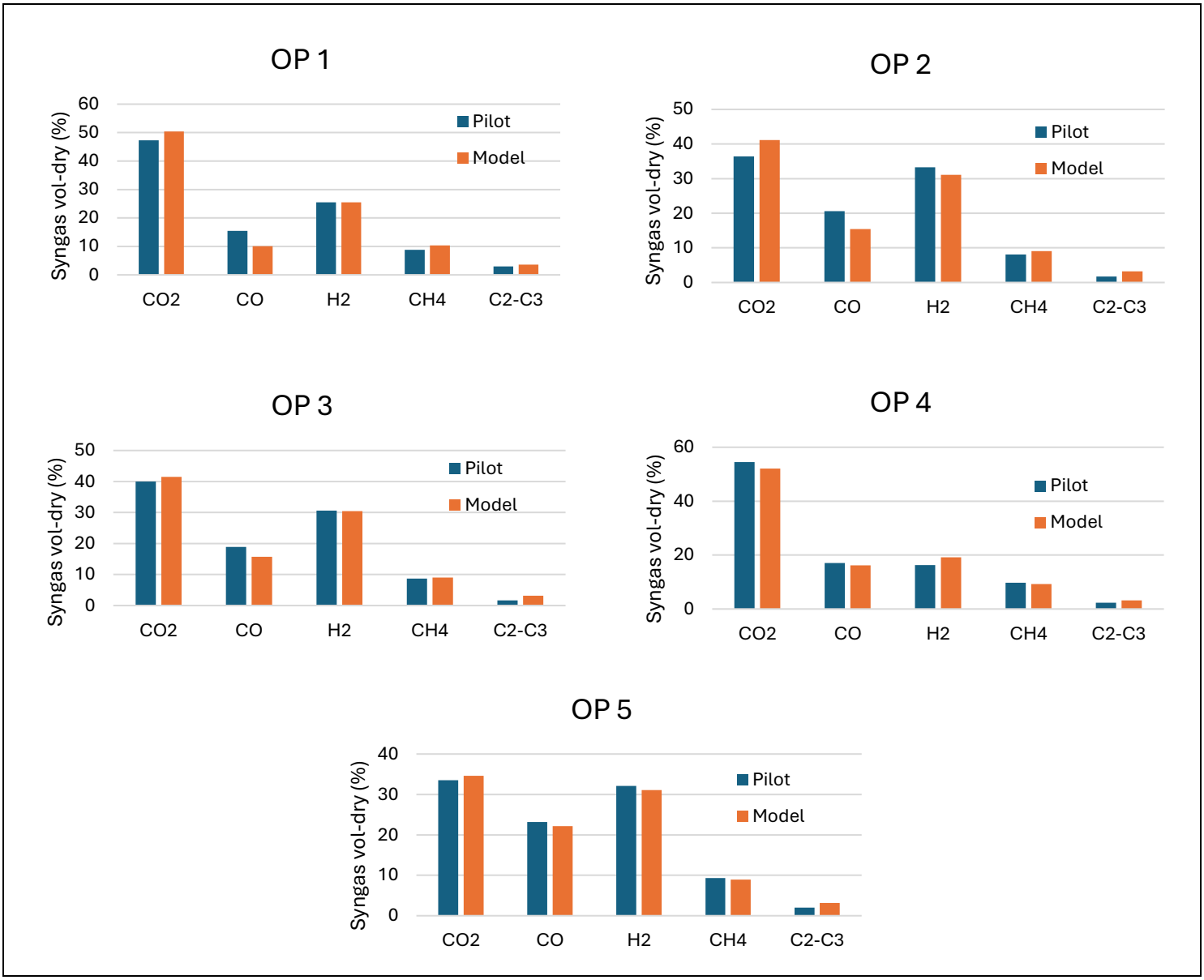

Figure AII 2: Comparison of major syngas species from pilot tests at 50 kW_{th} and model's predictions.

- **1.5 kW_{th} pilot plant** [110]

The compared operational points from the 1.5 kW_{th} pilot plant are presented in Table AII 5.

Table AII 5: Operational points at the 1.5 kWth scale with Pine Wood.

	Pine Wood		
OP	1	2	3
T_{FR}	880	880	940
S/B	0.6	0.9	0.6
ER	0.33	0.3	0.34
C_c	0.928	0.943	0.957

The Pine Wood composition used in the 1.5 kW_{th} pilot plant is shown in Table AII 6.

Table AII 6:Feedstock composition used in the 1.5 kWth pilot tests.

Pine Wood Composition			
M	5.6	**ASH**	0.636
FC	16.208	**CARBON**	52.648
VM	83.157	**HYDROGEN**	6.674
ASH	0.636	**NITROGEN**	0.106
		CHLORINE	0.011
		SULFUR	0.011
		OXYGEN	39.915

The model predictions are shown in Figure AII 3.

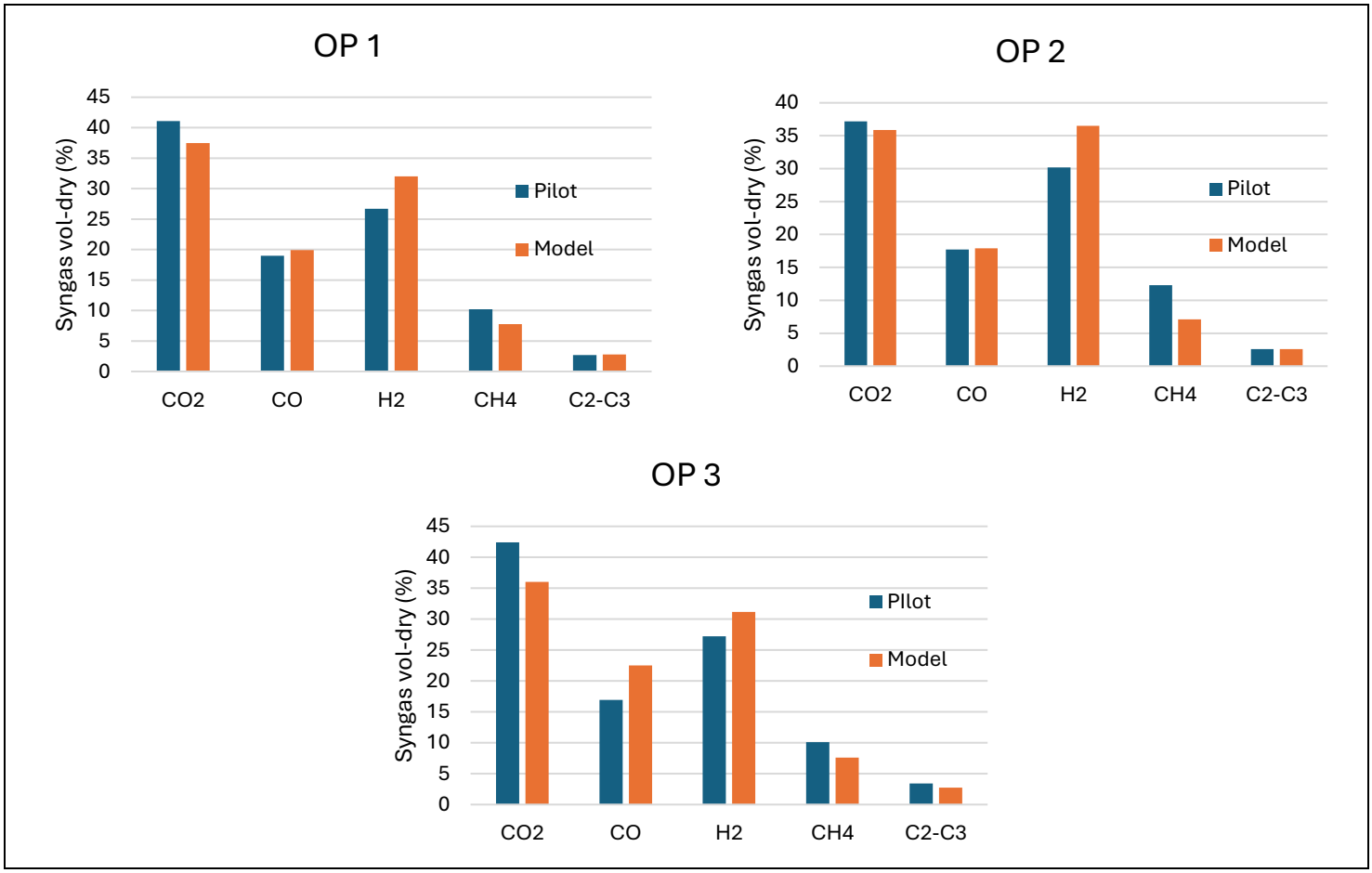

Figure AII 3: Comparison of major syngas species from pilot tests at 1.5 kW_{th} and model's predictions

- **CLARA point** [102]

The compared operational point from the model is shown in Table AII 7.

Table AII 7: Operational point in CLARA model with forest residue.

Forest Residues		
Input	200	MW
Fuel feed	10.93	kg/s
S/B	0.6	kg/kg
Air-in	19.3	kg/s
T_{AR}	1000	^{o}C
T_{FR}	900	^{o}C
C_c	0.891	

The Forest Residues composition used in the CLARA model is shown in Table AII 8.

Table AII 8: Feedstock composition for forest residue used in the CLARA model.

Forest Residues			
M	4.40	**ASH**	2.30
FC	17.40	**CARBON**	51.15
VM	80.30	**HYDROGEN**	6.07
ASH	2.30	**NITROGEN**	0.44
		CHLORINE	0.01
		SULFUR	0.02
		OXYGEN	40.01

The model predictions are shown in Figure AII 4.

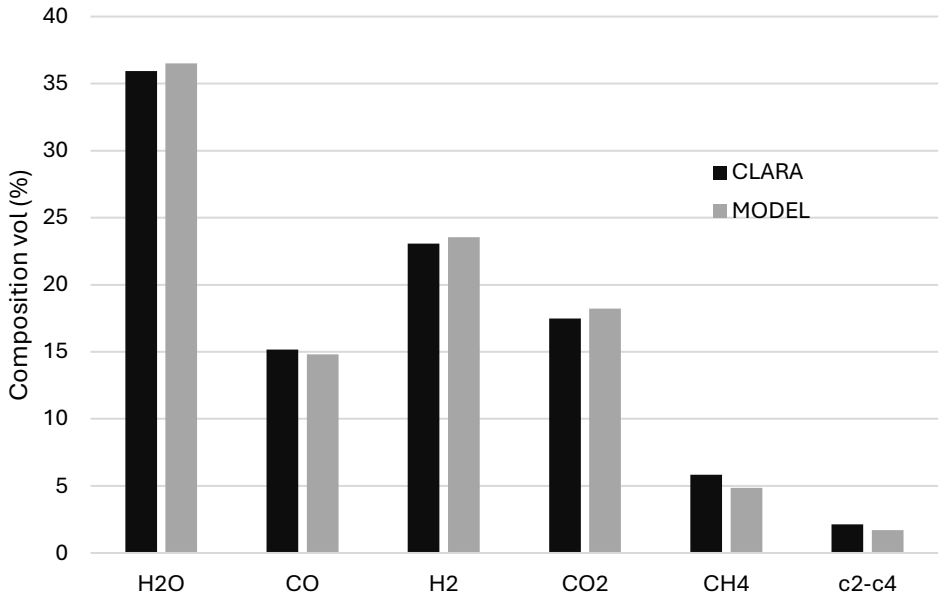

Figure AII 4: Comparison of major syngas species from the two model's predictions.

Annex III: Discounted Cash Flow Analysis

Table AIII 1: Discounted Cash Flow sheet for 2023 basis year.

Year	Others	Revenue	Op. Expenses	Depreciation	Profit (before tax)	Net profit	Net Cash flow
-2	2585129		18033859		-18033859	0	-20618987
-1			135253939		-135253939	0	-135253939
0			72135434		-72135434	0	-72135434
1	11271162	95590985	64076820	23008285	-2765282	-2765282	20243004
2		95590985	63721889	23008285	8860811	6911432	29919717
3		95590985	65590573	23008285	6992127	5453859	28462144
4		95590985	63721889	23008285	8860811	6911432	29919717
5		95590985	63721889	23008285	8860811	6911432	29919717
6		95590985	65784666	23008285	6798034	5302467	28310752
7		95590985	63721889	23008285	8860811	6911432	29919717
8		95590985	63721889	23008285	8860811	6911432	29919717
9		95590985	65590573	23008285	6992127	5453859	28462144
10		95590985	63721889	23008285	8860811	6911432	29919717
11		95590985	63721889		31869096	24857895	24857895
12		95590985	65784666		29806319	23248929	23248929
13		95590985	63721889		31869096	24857895	24857895
14		95590985	63721889		31869096	24857895	24857895
15		95590985	65590573		30000412	23400322	23400322
16		95590985	63721889		31869096	24857895	24857895
17		95590985	63721889		31869096	24857895	24857895
18		95590985	65784666		29806319	23248929	23248929
19		95590985	63721889		31869096	24857895	24857895
20		95590985	63721889		31869096	24857895	24857895
21		95590985	65590573		30000412	23400322	23400322
22		95590985	63721889		31869096	24857895	24857895
23		95590985	63721889		31869096	24857895	24857895
24		95590985	65784666		29806319	23248929	23248929
25	22542323	95590985	63721889		31869096	24857895	47400218

Table AIII 2: Discounted Cash Flow sheet for 2020 basis year.

Year	Others	Revenue	Op. Expenses	Depreciation	Profit (before tax)	Net profit	Net Cash flow
-2	1832336		12782377		-12782377	0	-14614713
-1			95867826		-95867826	0	-95867826
0			51129507		-51129507	0	-51129507
1	7988985	80917877	59481773	23008285	-9561167	-9561167	13447118
2		80917877	59070323	23008285	-1160731	-1160731	21847554
3		80917877	60554719	23008285	-2645128	-2645128	20363157
4		80917877	59070323	23008285	-1160731	-1160731	21847554
5		80917877	59070323	23008285	-1160731	-1160731	21847554
6		80917877	60692292	23008285	-2782701	-2782701	20225584
7		80917877	59070323	23008285	-1160731	-1160731	21847554
8		80917877	59070323	23008285	-1160731	-1160731	21847554
9		80917877	60554719	23008285	-2645128	-2645128	20363157
10		80917877	59070323	23008285	-1160731	-1160731	21847554
11		80917877	59070323		21847554	17041092	17041092
12		80917877	60692292		20225584	15775956	15775956
13		80917877	59070323		21847554	17041092	17041092
14		80917877	59070323		21847554	17041092	17041092
15		80917877	60554719		20363157	15883263	15883263
16		80917877	59070323		21847554	17041092	17041092
17		80917877	59070323		21847554	17041092	17041092
18		80917877	60692292		20225584	15775956	15775956
19		80917877	59070323		21847554	17041092	17041092
20		80917877	59070323		21847554	17041092	17041092
21		80917877	60554719		20363157	15883263	15883263
22		80917877	59070323		21847554	17041092	17041092
23		80917877	59070323		21847554	17041092	17041092
24		80917877	60692292		20225584	15775956	15775956
25	15977971	80917877	59070323		21847554	17041092	33019063